DESIGN AND DYNAMIC ANALYSIS OF THREE- LEGGED ARTICULATED SUPPORTING TOWER FOR OFFSHORE WIND TURBINE

Thesis

Submitted to University of Kerala for the award of the degree of Doctor of Philosophy in Civil Engineering under Faculty of Engineering and Technology

Chinsu Mereena Joy

Research Centre

UNIVERSITY OF KERALA

TKM COLLEGE OF ENGINEERING, KOLLAM

MAY 2021

DECLARATION

I hereby declare that the Ph.D. thesis entitled **"DESIGN AND DYNAMIC ANALYSIS OF THREE-LEGGED ARTICULATED SUPPORTING TOWER FOR OFFSHORE WIND TURBINE"** is an independent work carried out by me and it has not been submitted anywhere else for any other degree, diploma or title.

Place: Kollam

Date: 4-05-2021 **CHINSU MEREENA JOY**

CERTIFICATE

This is to certify that the work embodied in the thesis entitled **"DESIGN AND DYNAMIC ANALYSIS OF THREE-LEGGED ARTICULATED SUPPORTING TOWER FOR OFFSHORE WIND TURBINE"** has been carried out by **CHINSU MEREENA JOY** under our supervision and guidance.

Research Supervisor

Dr. ANITHA JOSEPH

(Former Professor,
Dept. of Civil Engineering,
T K M C E, Kollam)

Professor
Saintgits College of Engineering
Kottayam

Co- Supervisor

Dr. LALU MANGAL

(Former Professor,
Dept. of Civil Engineering,
T K M C E, Kollam)

Structural Consultant
Manibil
Thiruvananthapuram

DEDICATED
TO
MY BELOVED
MOTHER

ACKNOWLEDGEMENTS

The thesis is the outcome of five years of relentless work where many of my well-wishers have extended their supported to me. At the moment I take this opportunity to express my deep gratitude to all of them. I extend my sincere thanks to:

Prof. Anitha Joseph and **Prof. Lalu Mangal** under whose inspiring guidance and supervision this investigation was carried out. Their consistent support and timely advice have led to the successful completion of this work.

I place my sincere gratitude to **Prof. V. Anantha Subramanian**, Head of Department of Ocean Engineering, IIT Madras during the period of my experimental work in the wave flume of IIT Madras, for sparing the wave testing facilities.

Prof. V.G. Idichandy and Prof. Nilanjan Saha, Department of Ocean Engineering, IIT Madras for their fruitful suggestions.

My doctoral committee members, **Prof. M. Satyakumar** as subject expert**, Prof. R. Sathikumar,** and **Prof. S. Anil Lal,** both as Chairman of the doctoral committees held during these period for their critical evaluation and creative suggestions.

Dr. T. A. Shahul Hameed, Principal, and **Dr. M. Sirajuddin**, Head of the Department and the other fellow faculty of the Department of Civil Engineering, TKM College of Engineering, Kollam for the support received in completing this work.

All my fellow research scholars especially **Ms. Raji R.** for their excellent support and encouragement.

Mr. Senger Mayank, Mr. Anu S. Nair and Mr. Lal Krishnan MS. students, Department of Ocean Engineering, IIT Madras for rendering technical assistance during the experimental investigation.

Mr. K. Ramadoss, **Mr. Suresh** for their indispensable assistance in model fabrication and experiment set up.

My student **Mr. Vivek Philip** for his priceless help and companionship.

My parents-in-law **Mr. P. S. Mani** and **Mrs. M. C. Annamma** for their patience, prayers and understanding.

My loving father **Mr. Joy George** and my brother **Mr. Chintu Joy** for their affection and inspiration.

My precious daughters **Anna** and **Mariya** for cheerfully trying not to miss me.

My beloved husband **Mr. Promod P. Mani** for his sincere efforts that helped me stay afloat throughout my career.

Chinsu Mereena Joy

ABSTRACT

KEYWORDS: Offshore wind turbine, Three-legged articulated support, Response Amplitude Operator, Compliant offshore wind tower

Demand for renewable energy sources is rapidly increasing since they are able to replenish the depleting fossil fuels and their capacity to act as a carbon neutral energy source. A substantial amount of such clean, renewable and reliable energy potential exists in offshore winds. The major engineering challenge in establishing an offshore wind energy facility is the design of a reliable and financially viable offshore support for the wind turbine tower. An economically viable support for an offshore wind turbine is a compliant platform since it moves with wave forces and offer less resistance to them. Amongst the several compliant type offshore structures, articulated type is an innovative one. It is flexibly linked to the seafloor and can move along with the waves and restoring is achieved by the horizontal component of the large buoyancy force.

An innovative concept, three-legged articulated support for an offshore wind turbine is designed in this thesis. The platform is designed to support the National Renewable Energy Laboratory (NREL) 5 MW reference turbine in a water depth of 144 m. Experimental and numerical investigations are done on the designed three-legged articulated structure supporting the above 5 MW wind turbine. The experimental investigations are performed on a 1: 60 scaled model in a 4 m wide wave flume at the Department of Ocean Engineering, Indian Institute of Technology, Madras. The experimental investigation includes free oscillation study and motion response under regular waves. The tests are conducted for regular waves of various wave periods and wave heights and for different orientations of the platform. The motion responses are presented in the form of Response Amplitude Operators (RAO). The results from the experimental study revealed that the proposed articulated structure is technically feasible in supporting the offshore wind turbine because the natural frequencies are away from ocean wave frequencies which make the RAOs relatively small and the tower always remains vertical.

The numerical study is carried out using hydrodynamic software ANSYS AQWA. The natural periods computed and those obtained from free oscillation experiment are in good agreement, indicating that all principal effects are incorporated in the numerical model. The comparison of the experimental and numerical results for regular waves show that the surge

responses agreed well with the experiments conducted and is revealed through favourable comparison of Response Amplitude Operator in the predominant degree of freedom (surge).

Thereafter, to investigate the complete behaviour of this compliant support system under the actual ocean environment, a comprehensive numerical investigation on the various aspects of dynamic response of the three-legged articulated wind tower under different sea states are evaluated for several waves as well as combined wind and wave cases. The results show that this three-legged articulated support is a promising concept for supporting an offshore wind turbine.

TABLE OF CONTENTS

Table of Contents (continued) **Page**

Table of Contents (continued) **Page**

LIST OF TABLES

LIST OF FIGURES

List of Figures (contd.) **Page**

ABBREVIATIONS

OWT	Offshore Wind Tower
TLP	Tension Leg Platform
MW	Mega Watt
NIWE	National Institute of Wind Energy
SFOWT	Submerged Floating Offshore Wind Turbine
SDOF	Single Degree of Freedom
FOWT	Floating Offshore Wind Turbine
FAST	Fatigue, Aerodynamics, Structures and Turbulence
WAMIT	Wave Analysis by Massachusetts Institute of Technology
ADAMS	Automatic Dynamic Analysis of Mechanical Systems
CFD	Computational Fluid dynamics
NMRI	National Maritime Research Institute
MARIN	Maritime Research Institute Netherlands
NREL	National Renewable Energy Laboratory
RAO	Response Amplitude Operator
AQWA	Advanced Quantitative Wave Analysis
PSD	Power Spectral Density
B.F	Buoyancy Force
W	Weight
RM	Restoring Moment
OM	Overturning Moment
HBM	Holtinger Baldwin Messtechnik

NOTATIONS

P	power
ρ	density of air
A	area swept by rotor
R	radius of the circle swept by the rotor
V	wind velocity
F_b	buoyancy force
C_b	distance from hinge to centre of buoyancy
Cg	distance from hinge to centre of gravity
D	characteristic diameter
L	wave length
λ	scale factor
C_m	inertia coefficients
C_d	quadratic drag coefficients
ρ	mass density of sea water
u_f	transverse directional fluid particle velocity,
u_s	transverse directional structure velocity,
$\dot{u}_f$	transverse directional fluid particle acceleration,
$\dot{u}_s$	transverse directional structure acceleration
A	cross-sectional area
u	velocity
g	acceleration due to gravity
l	characteristic dimension
Fr	Froude number
$[M]$	total mass of the three legged articulated platform
$[C]$	damping stiffness matrix of the three legged articulated platform
[K]	hydrostatic stiffness matrix of the three legged articulated platform
F	wave force

$\{\ddot{X}\}$ acceleration vector

$\{\dot{X}\}$ velocity vector

$\{X\}$ displacement vector

Kxx, Kyy, and Kzz. radius of gyration about x, y and z axes respectively

Ixx, Iyy, and Izz mass moment of inertia about x, y and z axes respectively

S(ω) spectral ordinate at a frequency

ω_p the peak frequency

γ peak enhancement factor

α constant

P_H mean pressure on rotor swept area

ρ_a air density

C_{FB} coefficient based upon the Betz momentum theory

F_H mean wind force on the top of tower

A area swept by rotor

D blade diameter

C_{DD} damping coefficient

S sum of the area of all blades

H_s significant wave height

T_z zero crossing period

$u(z)$ wind velocity

CHAPTER 1

INTRODUCTION

1.1 GENERAL

Sources of energy can be categorized as renewable and nonrenewable. Nonrenewable sources of energy are consumed at a rate, which is faster than nature can replenish. Our planet, earth is currently experiencing rapid climate change due to the consequences of global warming resulting from massive fossil fuel production and use. The consequences of global warming and climate change are affecting the survival of biomass existing on the earth so much that reaching out renewable, energy-efficient and eco-friendly resources have become inevitable. The various forms of renewable energy resources are depicted in Fig. 1.1.

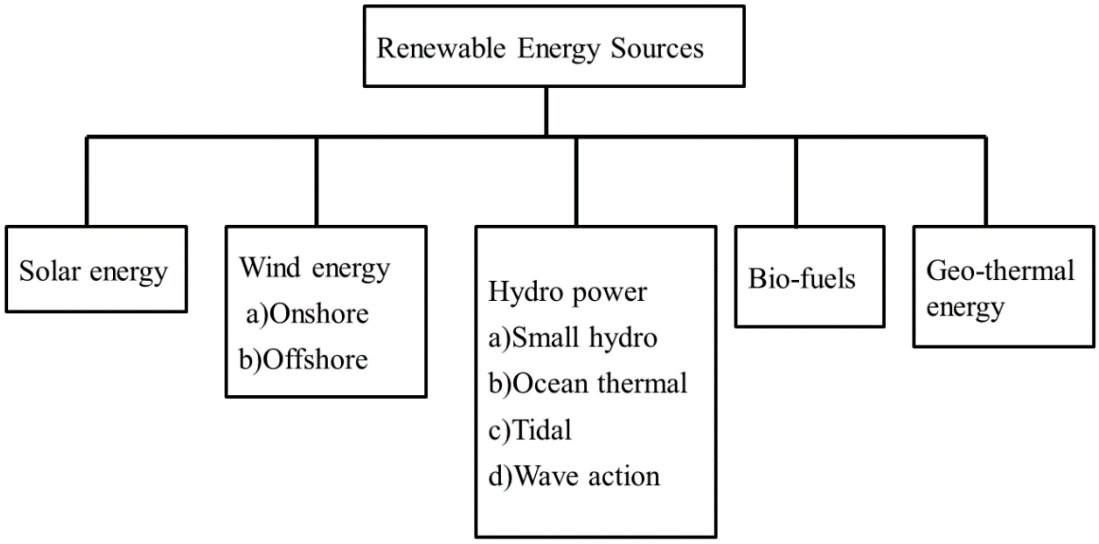

Fig.1.1 Different forms of renewable energy sources

Among the different renewable energy sources such as solar, geothermal, ocean and tidal energy, exploiting wind energy is proved to be promising. Significant reduction in CO_2 emissions can be accomplished by using wind power and is depicted in Fig. 1.2 (Guerrero-Lemus and Martínez-Duart, 2013)

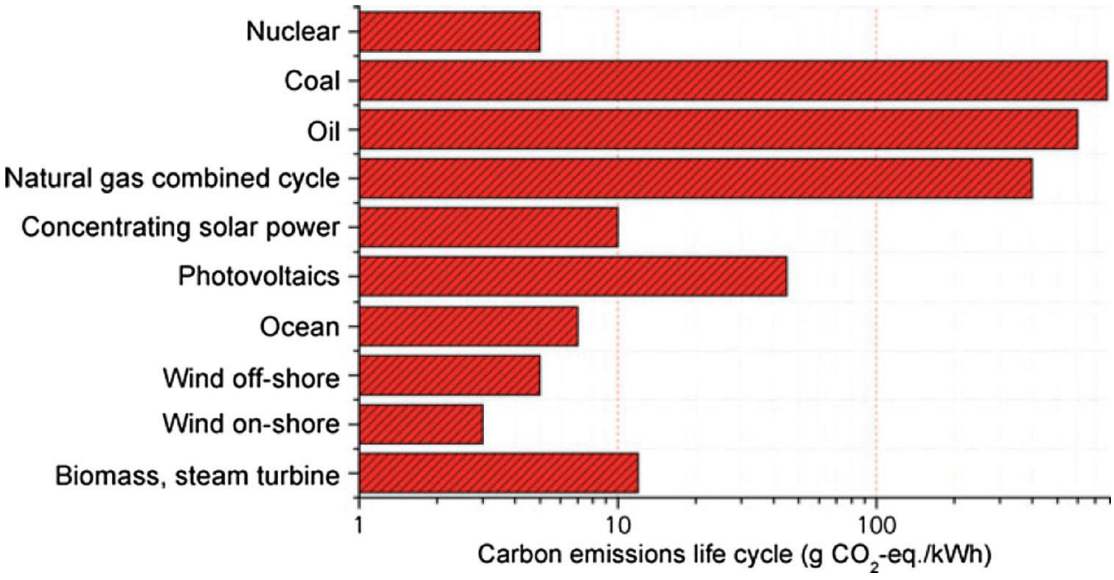

Fig. 1.2 CO_2 emissions per kWh of electricity produced (Guerrero-Lemus and Martínez-Duart, 2013)

1.2 WIND ENERGY

Amid the renewable energy sources, wind energy is proved to be the utmost promising source and popular worldwide for clean and healthy electricity production. The economically viable capacity of Earth's wind power is projected to be 72 TW which is four times greater than the global total energy demand. Wind is caused due to pressure difference created by the uneven heating of Earth's atmosphere by solar radiation. Wind turbine converts kinetic energy of wind into mechanical energy which in-turn is transformed into electrical energy. The subsystems of a wind turbine are nacelle, blades, generator, rotor, controller, tower, and supporting structure. Nacelle is the part that encloses the gearbox, generator, and blade hub and the electronic components (Fig. 1.3.). When the wind blows through the aerofoil shaped blades, it will rotate the rotor, which turns the drive shaft of the electric generator. The main factors that influence the amount of energy that a turbine can harvest from the wind are wind velocity, air density and swept area. Power in the wind is given by:

$$P = \frac{1}{2}\rho A V^3 \quad \text{.....1.1}$$

Where, P= Power (W), ρ = Density of air (kg/m^3), Area swept by rotor (A) = πR^2 (m^2), R = radius of the circle swept by the rotor, V = Wind Velocity (m/s)

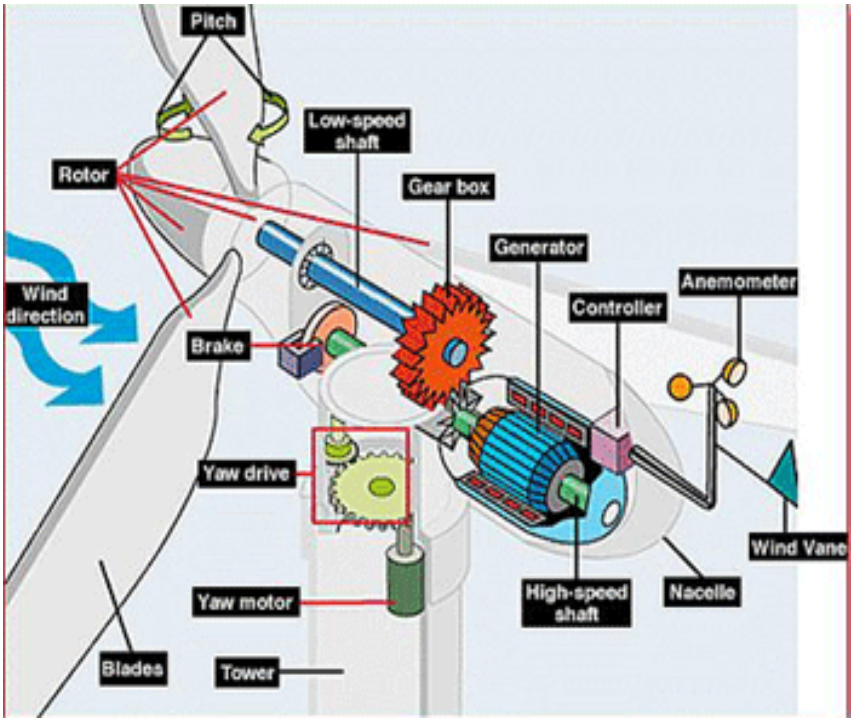

Fig. 1.3 Wind Turbine Nacelle Schematic (Credit: NREL)

Based on the direction of axis, wind turbines are classified as the horizontal-axis and the vertical-axis wind turbines (Fig. 1.4). Horizontal-axis wind turbines generally consist of two or three blades, which are operated "upwind," with the blades facing towards the wind.

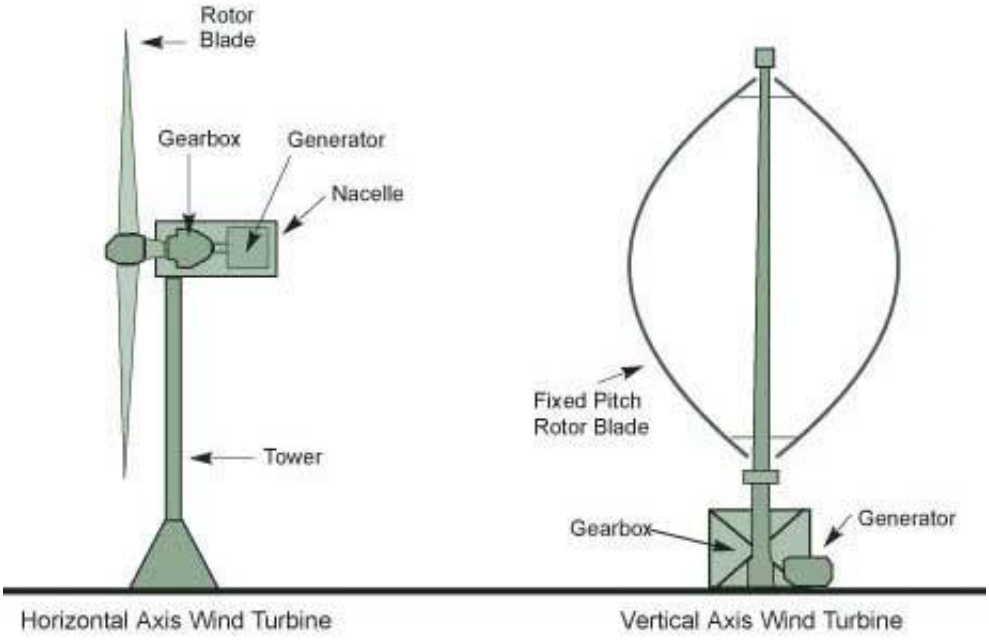

Fig. 1.4 Horizontal axis and vertical axis wind turbine (Purohit. and Michaelowa, 2007)

The installed capacity of wind energy generation has increased 22-fold during the period from 2001 to 2017 and is depicted in Fig. 1.5

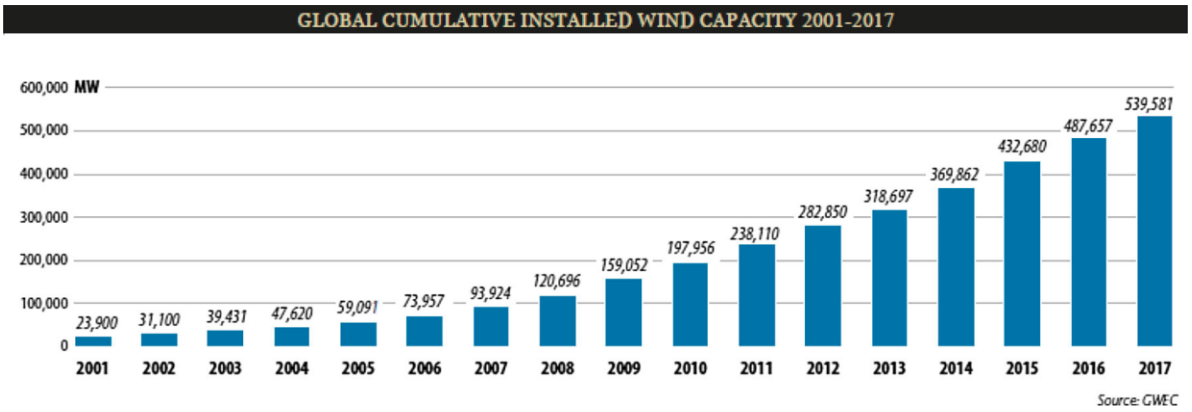

Fig. 1 5 Global cumulative installed wind capacity 2001–2017 (Global Wind Energy Report, 2018)

Offshore wind energy is gaining more importance than onshore wind energy due to its several advantages. It avoids noise and visual conflicts; vast offshore areas can be utilized, with consistent wind conditions, less turbulence and boundary layer effects and better capacity factor. Moreover, the magnitude of the untapped potential for the offshore wind energy is enormous as compared to any other renewable and clean energy source.

1.3 OFFSHORE WIND ENERGY-STATISTICS

Our future promise of energy can be offshore wind energy owing to the rapid development in offshore wind industry (Kota *et al.* 2015). This is evident from the fact that the installed capacity has increased almost fivefold during the period from 2011 to 2017 (Fig.1.6). Globally, offshore wind energy installations are coming up in a big way. In Europe, at present, the total installed offshore capacity of wind energy installation has reached 15,780 MW. UK ranks first with 6836 MW, followed by Germany 5355 MW and Denmark 1271 MW. It is expected that the offshore wind energy installations may exceed 500 MW a year by 2026 at an incremental rate about 1 GW a year by 2030 and is shown in Fig. 1.7.

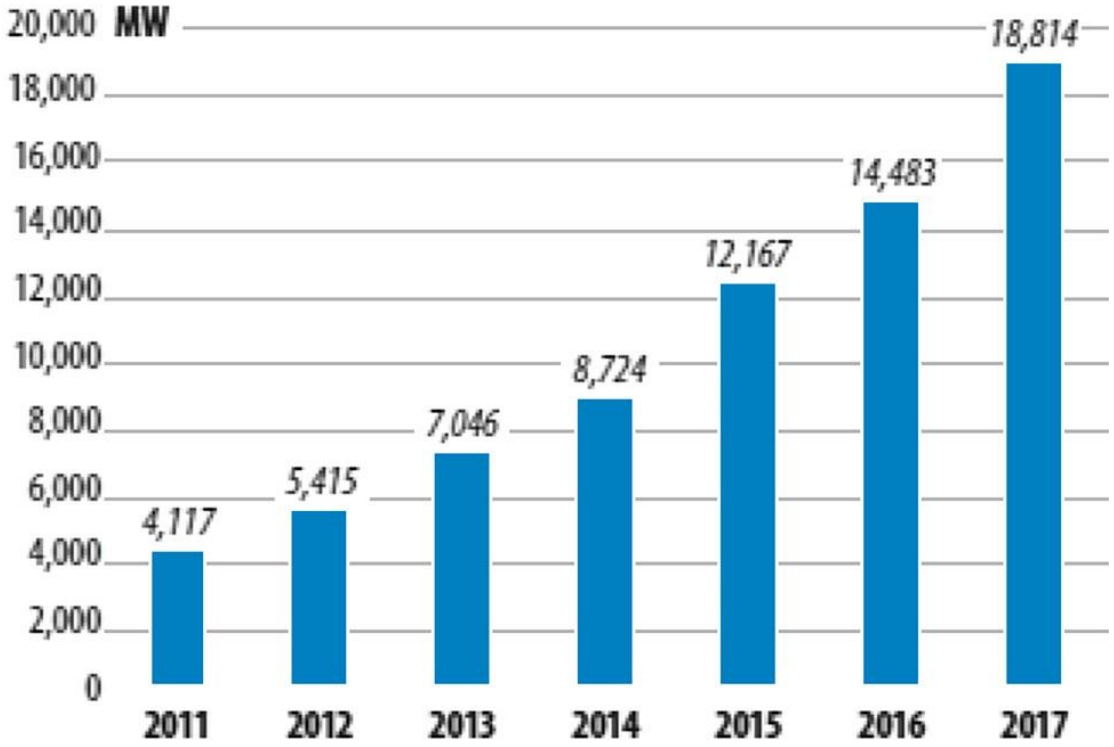

Fig. 1.6 Annual cumulative offshore wind capacity (2011–2017) (Global Wind Energy Report, 2018)

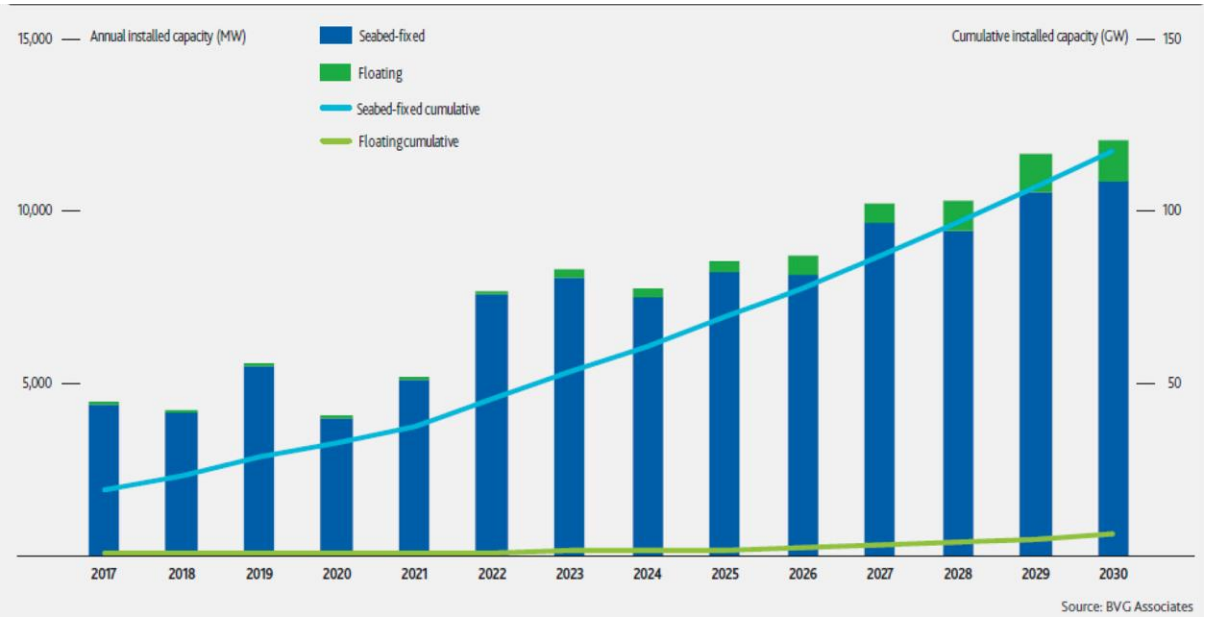

Fig. 1.7 Projections for offshore wind development globally out of 2030 (Global Wind Energy Report, 2018)

1.4 OFFSHORE WIND SCENARIO IN INDIA

Though India is the fourth largest onshore wind market in the world, there is severe need for green clean alternate energy. India, with long coastline of over 7600 km, has promising offshore wind potential awaiting exploitation. Offshore wind power could lead an important role since India has fairly large wind resources. In India, initial assessments along the coastline have reported good prospects towards the installation of offshore wind energy. Rameshwaram–Kanyakumari sector in Tamil Nadu and Gujarat coast have potential for the development of economically viable offshore wind projects. Coastline of Tamil Nadu itself has reported to have a potential of 1 GW capacity for the offshore wind turbine (National Offshore Wind Energy Policy, Government of India, 2015). National Institute of Wind Energy (NIWE) has initiated steps to set up a 1GW offshore wind farm in the Gulf of Khambat, Gujarat.

Availability of wind power at a specific location is often assigned a wind power class. The Fig. 1.8 shows some potential sites in the Gulf of Kutch and the region between Tamil Nadu and SriLanka

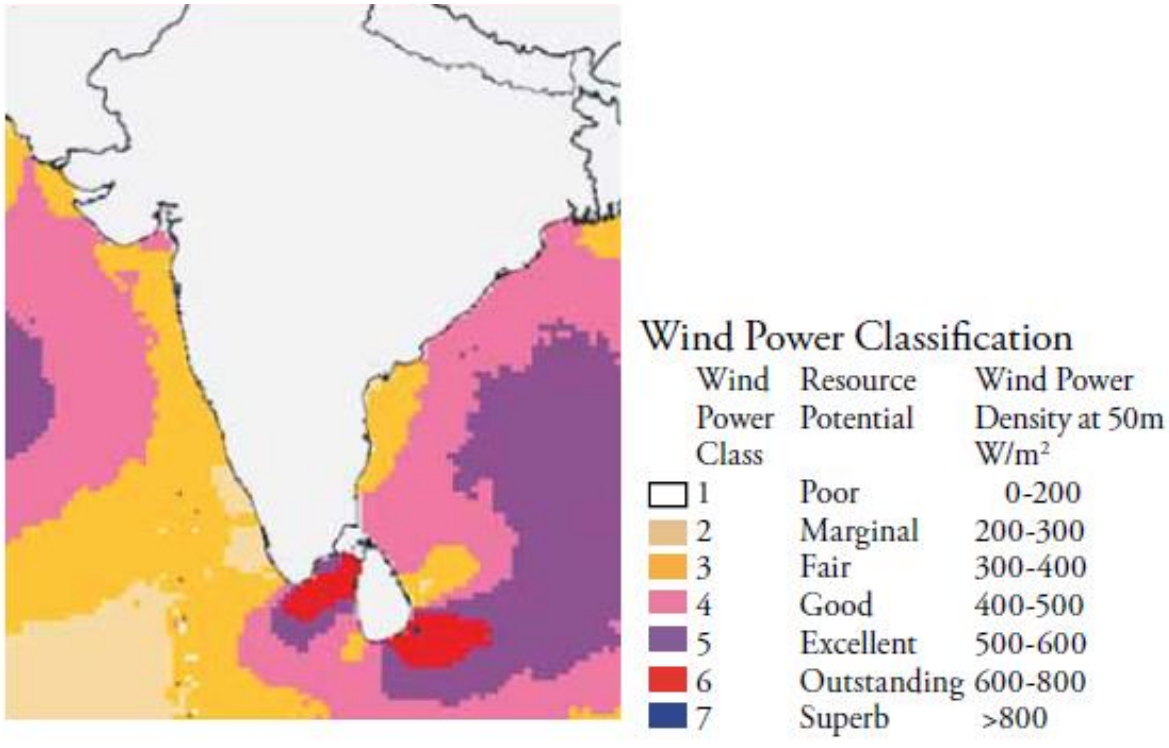

.

Fig.1.8 Map showing wind power potential

1.5 SUPPORT STRUCTURES FOR OFFSHORE WIND TURBINE

The biggest challenge in the design of dynamic Offshore Wind Tower (OWT) is the design of a suitable platform to support the wind turbine under various conditions of varying ocean depth, wind intensity, tide, etc. Designing of the support structure for offshore wind turbine is more intricate and expensive when compared to the onshore wind turbines (Fig. 1.9).

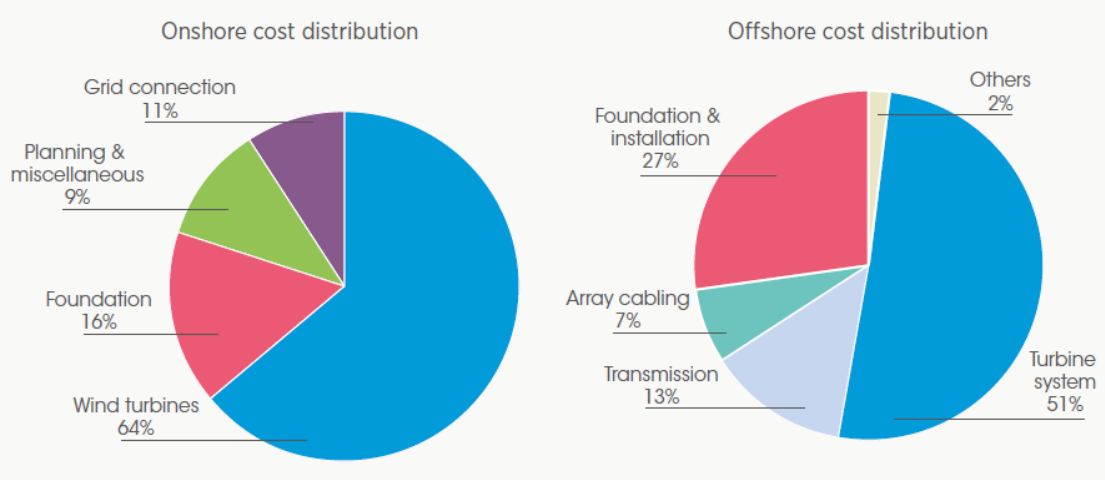

Fig. 1.9. Cost distribution of onshore and offshore wind power projects (Taylor, 2012)

Even though the issues that govern static offshore oil and gas rigs and its design considerations can be adopted for offshore wind platforms, the significance of each parameter has to be considered differently in the design. Design parameters related to OWT include the aerodynamics, dynamics of waves and ocean current, hydrodynamics and dynamics of foundation. Tuning of the tower's structural dynamics to avoid interactions with the rotating turbine is also critically important in the design of OWT. The challenge of supporting an above-waterline structure with high centre of gravity distinguishes floating wind tower from other offshore structures. The technology for the design and installations of offshore wind platforms has been established as a proven one several decades back. Further to that, the concept of large offshore floating turbine platform was introduced by Professor W. E. Heronemous in 1972 . However, it was only in 1991 that the first commercially viable wind farm was established for the first time in Denmark, that too in shallow water (2–6 m deep) and 1.5–3 km from the shore. The capacity of this single wind turbine is only 450 kW (Kaldellis and Kapsali, 2013). In order

to establish economically viable offshore wind turbines, it is required to move to higher capacities and locations where the wind is stronger and consistent. Such locations in the ocean are characterized by greater depths and higher wind speed. Also at such sites, wind speed is consistent and with lower turbulence resulting in higher energy. However, many of these wind potential areas reside in water depths more than 60 m where existing technology for supports of wind turbines fixed at the seabed is not economical. The latest technologies in OWT are: (1) Hywind (spar buoy) developed by 'Statoil', (2) PelaStar (TLP) developed by Glosten and (3) the semisubmersible developed by Principle Power and the damped floater developed by Ideol. The first full-scale floater prototype deployed is a spar buoy in Norway in 2009, followed by a semisubmersible installation in Portugal in 2011 and three installations in Japan (spar and semisubmersible) between 2011 and 2015 (World Energy Resources—Wind, 2016)

1.6 CLASSIFICATION OF OFFSHORE WIND TURBINE SUPPORTS

OWTs are classified on the basis of following criteria:

1. Method of supporting the wind turbine tower - OWTs are classified as fixed and floating types. The common fixed supports utilised for existing offshore wind turbines includes gravity based, tripod, monopile, suction bucket and jacket structures. The different types of fixed supports for offshore wind turbines are depicted in Fig.1.10. A fixed platform comprises of a rigid jacket which is a vertical tubular section made of steel members supported by piles driven into the seabed. The main legs in jacket platforms are connected by bracings. Differing from the fixed platform; the compliant towers flex with the waves rather than resist them. When the installations of the wind turbines are in deep waters, floating platforms are required to be used as support structures. For offshore wind turbines, various floating support platform configurations are feasible considering the various mooring systems, buoyancy chambers, and ballast chambers employed in the oil and gas industry (Fig. 1.11).

2. Based on water depth—classified as shallow water towers, transitional water towers and deep-water towers. Shallow water towers are suction bucket structure, gravity base structure and monopile structure which generally are used in water depths 5–30 m. Transitional water towers are jacket, tripod tower, submerged jacket with tower and guyed monopole which are suitable for

30–60 m water depths. Deep-water towers are spar, pontoon, semisubmersible and Tension Leg Platform (TLP) types which are suitable for 60 m and deeper (Fig. 1.12).

3. Method by which floating platforms achieve static stability. A barge, accomplishing pitch restoring by means of waterplane area moment; a spar buoy with pitch restoring is accomplished by providing ballast; and a TLP for which pitch restoring is accomplished by the taut mooring lines. Fig. 1.13 represents the structures and their restoring mechanism.

4. Method of mooring—classified as catenary and vertical mooring. Vertical mooring structures need expensive anchors but the dynamics is simple, whereas catenary mooring structures require low-cost anchors but the dynamics is complex.

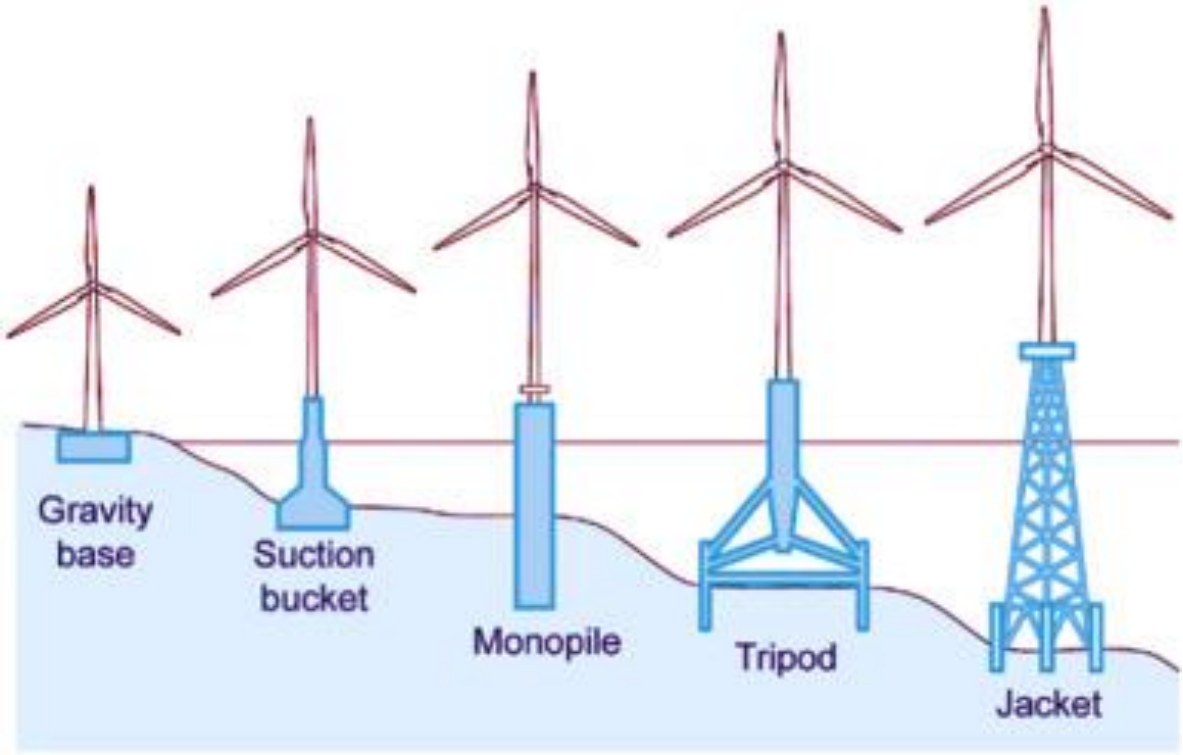

Fig. 1.10 Fixed supports used in the offshore wind industry (Moulas *et al.* 2017)

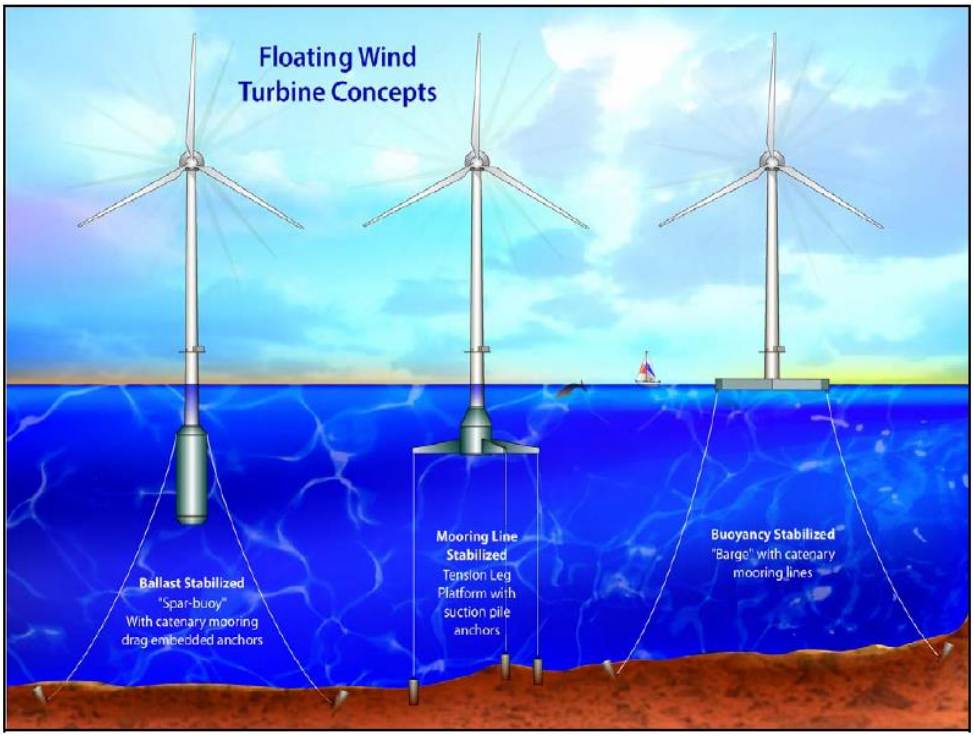

Fig. 1.11 Floating supports for offshore wind turbines (Jonkman and Bhul, 2007)

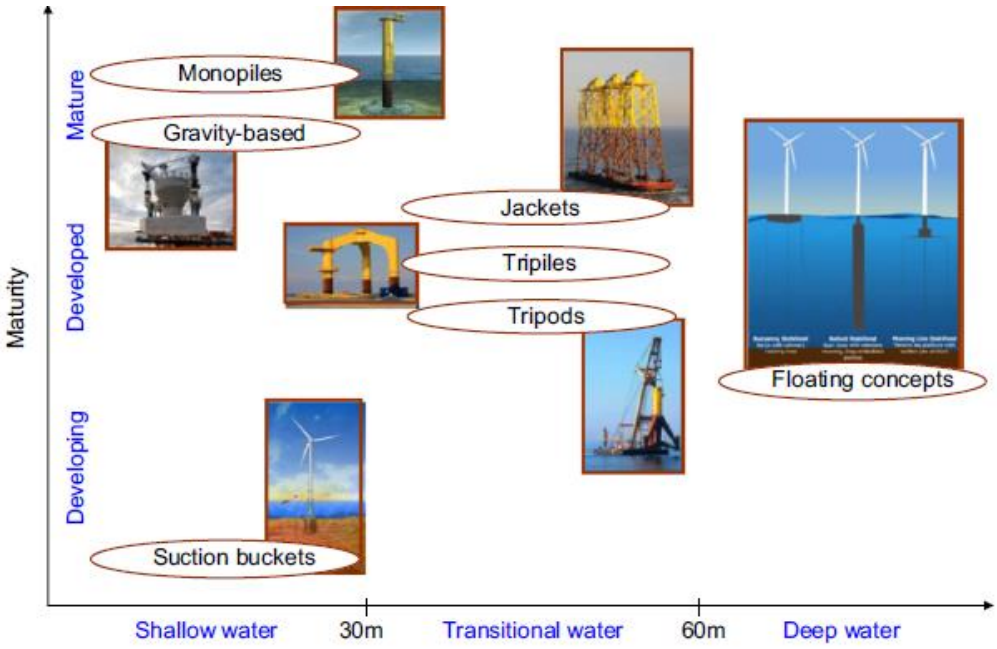

Fig.1.12 Support structure technology with respect to water depth
(Kaldellis and Kapsali, 2013)

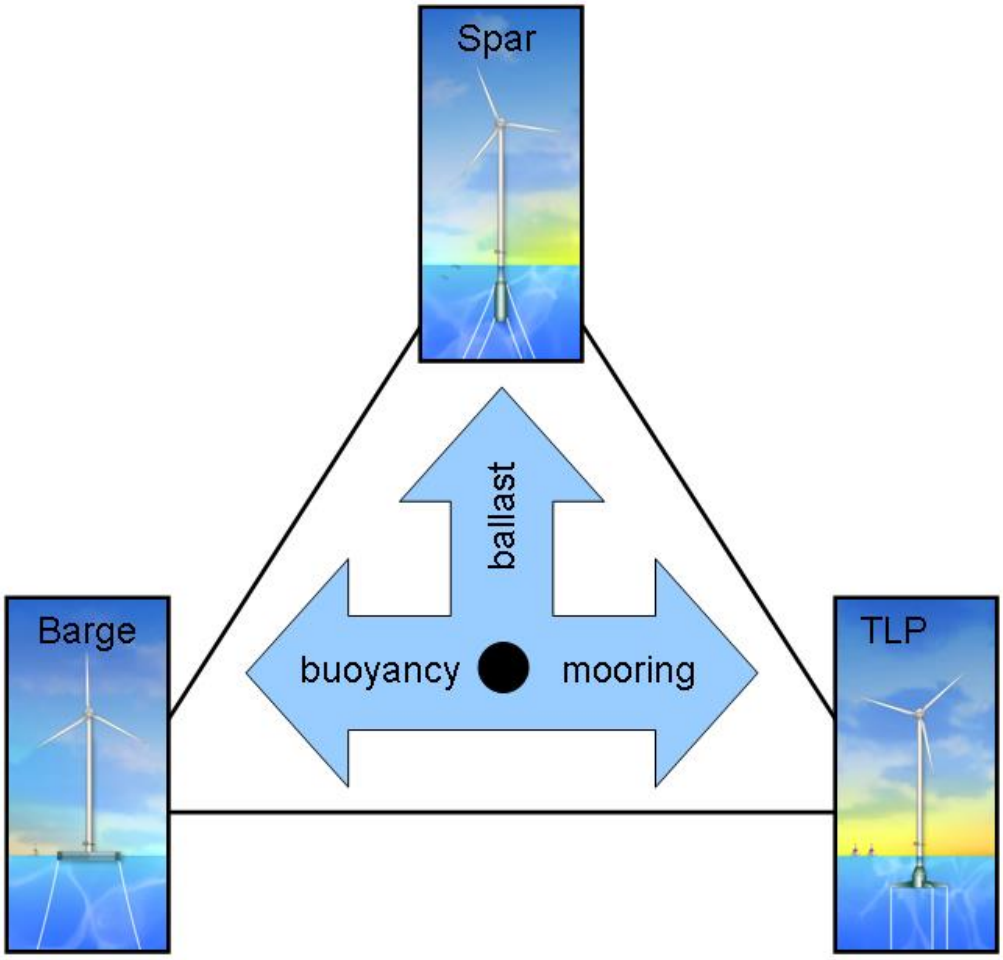

Fig. 1.13 Stability triangle (Matha, 2010)

The selection of support platforms for the offshore wind turbine mostly depends on the location where it will be installed. This work focuses on designing an articulated platform for installing an offshore wind turbine. Articulated tower is a compliant structure, flexibly connected to sea bed, so that it can move along with the waves and restoring is achieved by buoyancy force. The literal meaning of the term compliant is 'to agree with, to a greater degree'. As name implies, this structure displaces with lateral forces and offer less resistance to them. For installing wind turbines in deeper water with severe weather conditions, conventional fixed structures need large physical dimensions to obtain the required strength and stiffness. So a compliant type of support can be considered as an economically viable solution. This study proposes a three legged articulated offshore wind turbine support and evaluates its performance.

1.7 ORGANISATION OF THESIS

The flow of chapters of the thesis is as follows:

Chapter 1 Introduction: The chapter briefly presents an introduction about different types of energy resources available in the world. Further it discusses about the different types of offshore wind turbine supporting structures.

Chapter 2 Literature review: The chapter presents a comprehensive review of the connected literature. The scope and objectives of the work are then presented.

Chapter 3 Design of the articulated platform: The chapter describes the design of the proposed articulated platform. The design details of the scaled model are also presented.

Chapter 4 Experimental Investigation: The chapter explains the fabrication details of the model and the instruments used for the experimental study. Different cases for the experimental investigation are also elucidated.

Chapter 5 Numerical investigation on the scaled model: The chapter describes numerical analysis carried out on the scaled model by the hydrodynamic software ANSYS AQWA. The experimental and numerical results are also compared here.

Chapter 6 Numerical investigation on the prototype: The chapter details the numerical investigation done on the prototype, in order to obtain the response of the articulated tower under regular and random waves for wave induced as well as wind-wave induced cases.

Chapter 7 Summary and Conclusions: The chapter summarises the thesis and highlight the major conclusions along with the scope of further investigation in this area.

CHAPTER 2

LITERATURE REVIEW

2.1 GENERAL

The thesis deals with design of an innovative structural configuration of three-legged articulated platform to support a 5 MW offshore wind turbine by experimental and numerical investigations. A comprehensive review of the related literature is revealed in this section. The need for the research work is identified based on the assessment of literature, and the scope and objective of the present research is defined and presented here. The review is categorized under five themes:

- Offshore wind turbine support concepts
- Articulated supports
- Coupled dynamics
- Experimental studies on articulated supports
- Experimental studies on offshore wind turbines

2.2 OFFSHORE WIND TURBINE SUPPORT CONCEPTS

Several concepts are discussed in various literatures. Some of them are discussed in this section.

Tong (1998) developed FLOAT, a conceptual design for an OWT which supports a three-bladed 1.4 MW turbine for 100 to 300 m water depth. The turbine is three bladed which is supported on steel space frame tower 45m high. FLOAT consists of a concrete cylindrical buoy hull with a bottom disc and it is moored to the seabed by eight lines. An investigation on the dynamic behaviour in operating conditions and extreme environments has been carried out. The results revealed that the effect of wave impact of the platform on the fatigue of the rotor is not significant.

Musial *et al.* (2004) presented a description of different kinds of floating foundations for offshore wind turbines. The merits and demerits of platforms with catenary mooring systems and vertical mooring systems are detailed. An economic feasibility study for Dutch tri floater

and monocolumn TLP (Fig.2.1) for 5MW wind turbine is done and recommended that the tri floater is seen to be costlier than TLP.

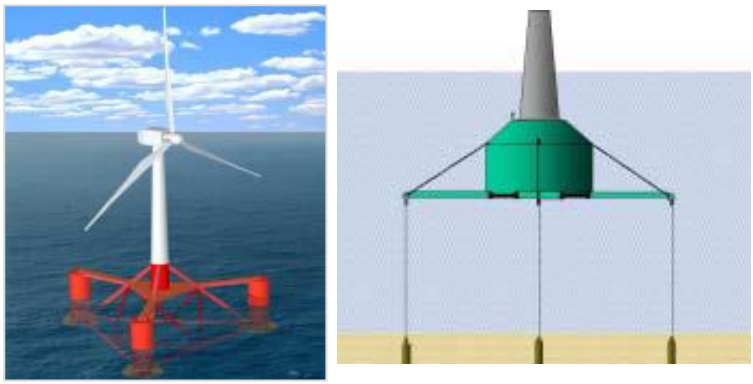

Fig. 2.1. Dutch Tri-floater and NREL TLP concept (Musial *et al.*, 2003)

Lee (2005) presented the technical description of two floating offshore wind turbine design concepts (TLP and Spar Buoy). Frequency domain analysis of these floating wind turbines are conducted in order to compare their performances and found the TLP concept to be relatively stiff in the rotational modes but soft in surge and sway modes while the spar concept was soft in rotational modes but stiff in surge and sway modes.

Fulton *et al.* (2005) introduced a new concept of submerged triangular Tension Leg Platform (Fig.2.2), for supporting a 5 MW wind turbine, in water depth of 61m. Analysis in time and frequency domain is done to find the response to first and second order forces and extreme conditions. It is established that the triangular TLP is suitable for installation in deep water.

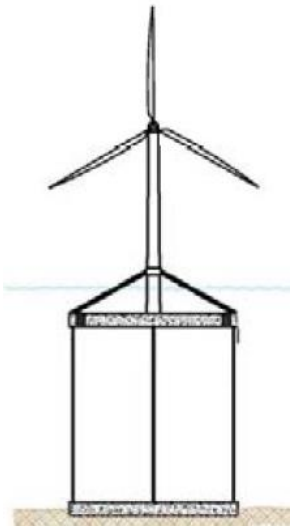

Fig. 2.2. Semi-submerged triangular platform (Fulton *et al.*, 2005)

Butterfield *et al.* (2005) revealed the appropriate characteristics of a floating wind turbine platform and categorized the floating structures on the basis of their principle of static stability like buoyancy, mooring lines and ballast (Fig. 2.3). The pros and cons of the various platform stability concepts depending on the technical challenges are also discussed. The challenges and recommended goals that lead to economical floating systems are also highlighted.

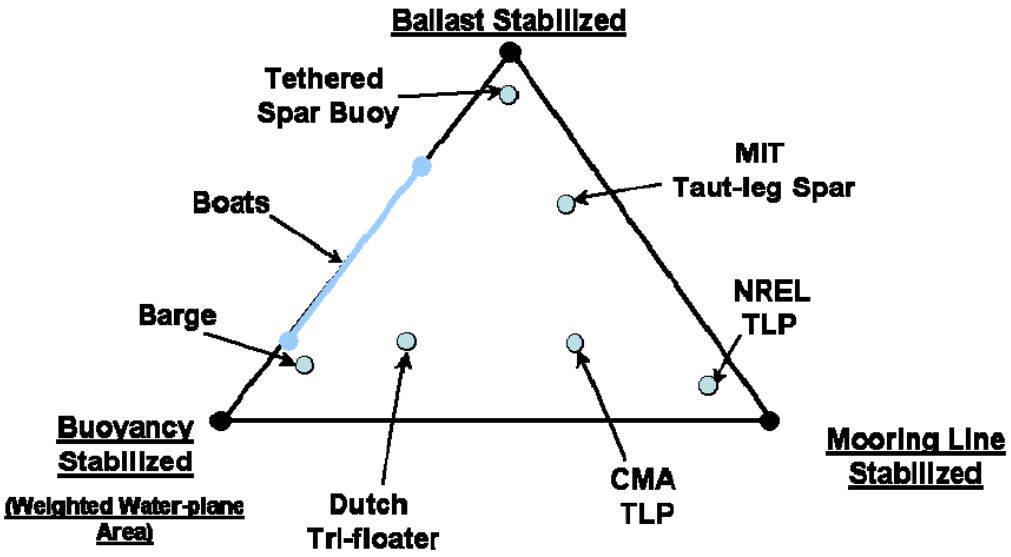

Fig.2.3 Stability triangle for floating platform (Butterfield *et al*., 2005)

Withee (2006) designed a Tension Leg Spar buoy for supporting 1.5 MW wind turbine. The tethers are connected to the radiated spokes with the intention that the system is stiff in pitch and roll modes. For the purpose of determining the extreme wind and wave event response analysis are done and found that the system is capable for supporting an offshore wind turbine.

Jonkmann and Buhl (2007) conducted fully coupled aero-hydro-servo-elastic analysis on the ITI Energy barge platform with catenary moorings (Fig.2.4) and found that the barge concept is vulnerable to excessive pitching. Necessary alterations to the design for reducing the barge motion and to remove the instabilities are done.

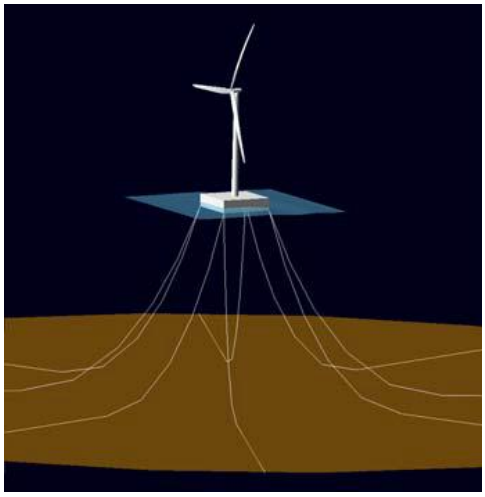

Fig.2.4 ITI Energy barge (Jonkmann and Buhl, 2007)

Roddier *et al.* (2009) designed WindFloat, a 3-legged floating foundation (Fig. 2.5) for a 5 MW wind turbine. It comprises of a column-stabilized offshore platform with an asymmetric mooring system and water-entrapment plates. The wind turbine tower is placed directly on top of one of the stabilizing columns. The researchers addressed the constraints in fabrication right from the early stages of design to avoid complexities and related cost overrun.

Fig.2.5 WindFloat Concept (Roddier *et al*., 2009)

Weinzettel *et al.* (2009) presented the life cycle assessment of TLP (developed by Sway Company) which supports offshore wind turbine. The assessment emphasized the environmental effect of the floating offshore wind turbine and showed the significance of using recycled materials to mitigate adverse environmental effects.

Matha (2010) analysed three floating-platform concepts (TLP, barge and spar buoy) supporting same 5-MW turbine. The results of the analysis showed the advantages and disadvantages of these floating concepts and to enhance the design of the floating offshore wind turbine platforms.

Sclavounos *et al.* (2010) presented two stiff floating wind turbine concepts having low weight (Tension Leg Platform with vertical tethers and Taut Leg Buoy with taut mooring lines) supporting 3 to 5 MW, suitable for water depths varying from 30 to several hundred meters in various seastates for wave heights up to 30 m.

Lefebvre and Collu, (2012) developed the tri-floater configuration (Fig.2.6) for supporting 5 MW wind turbine by comparing seven preliminary concepts using a techno-economic analysis. An analysis is also carried out to assess the structural strength of the platform.

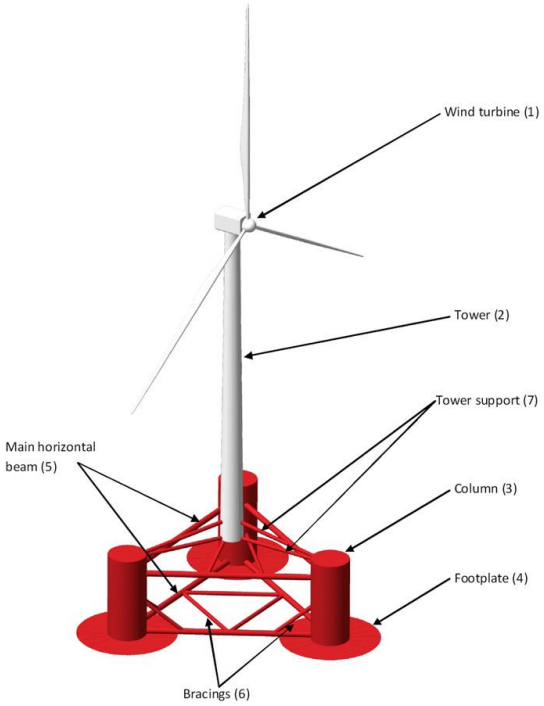

Fig.2.6 Tri-floater configuration (Lefebvre and Collu, 2012)

Zhang *et al.* (2013) considered the feasibility of a semisubmersible foundation (Fig.2.7) to support a 600kW turbine in 60 m water depth. The stability of the supporting structure is improved by lowering the centre of gravity by providing watertight ballast tank under the column symmetrically.

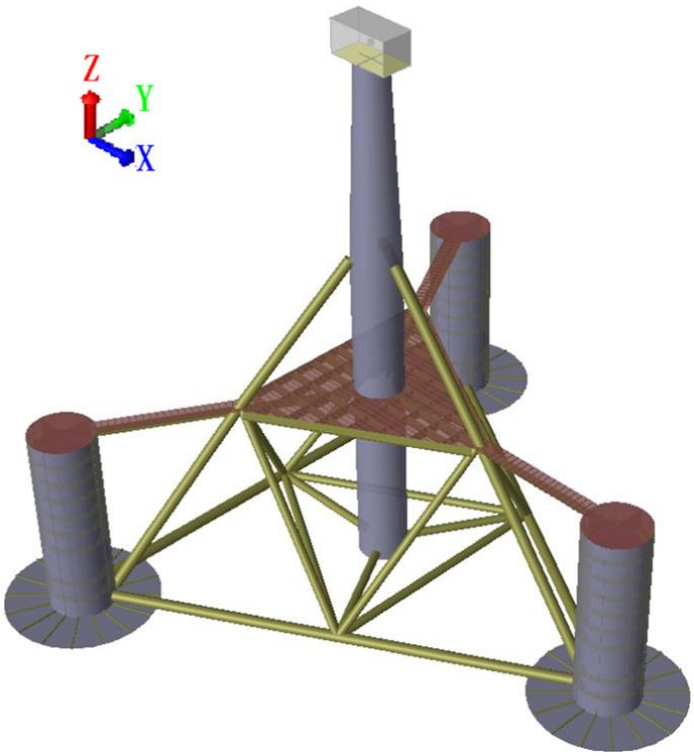

Fig.2.7 Semisubmersible foundation (Zhang *et al*., 2013)

Myhr *et al.* (2014) compared the marginal cost of energy for different concepts of floating offshore wind turbine such as Spar-Buoy, Tension-Leg-Spar, Semi-Submersible, Tension-Leg-Wind-Turbine and Tension-Leg-Buoy and found that levelised cost of energy values depends on water depth due to mooring costs and distance from the shore due to increased cable length.

Cheema *et al.* (2014) established a conceptual design of floating wind turbine suitable for Bass Strait region. The response of the new platform in frequency and time domain is investigated using ANSYS AQWA. It is found that the new floating wind turbine can safely produce power for a significant wave height up to 4 m.

Karimirad and Michailides (2015) presented the design features of a floating V-shaped semisubmersible wind turbine (Fig. 2.8) for a water depth of 100 m. The static and dynamic response analyses of the semisubmersible platform due to the actions of wind and wave forces are also presented.

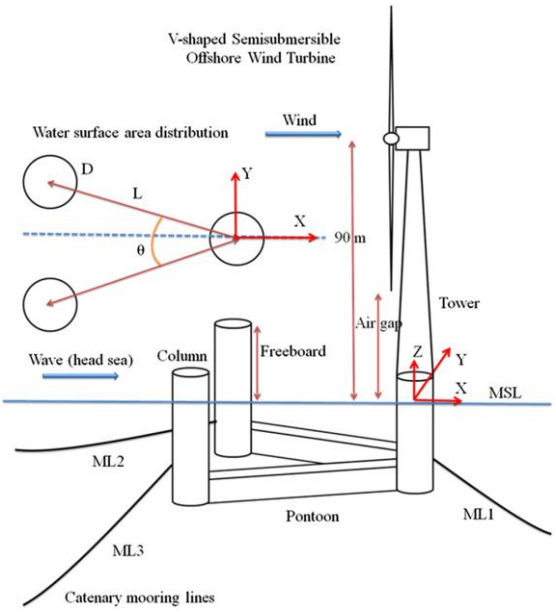

Fig.2.8 V-shaped semisubmersible platform for offshore wind turbine, (Karimirad and Michailides 2015)

Nejad *et al*. (2015) analysed the damage that has occurred due to fatigue of mechanical parts in the gear box on a land based tower and four different floating structures viz spar, TLP and two semisubmersibles (Fig. 2.9), and seen that the more damage occurred in the main bearing of wind turbine on spar platform.

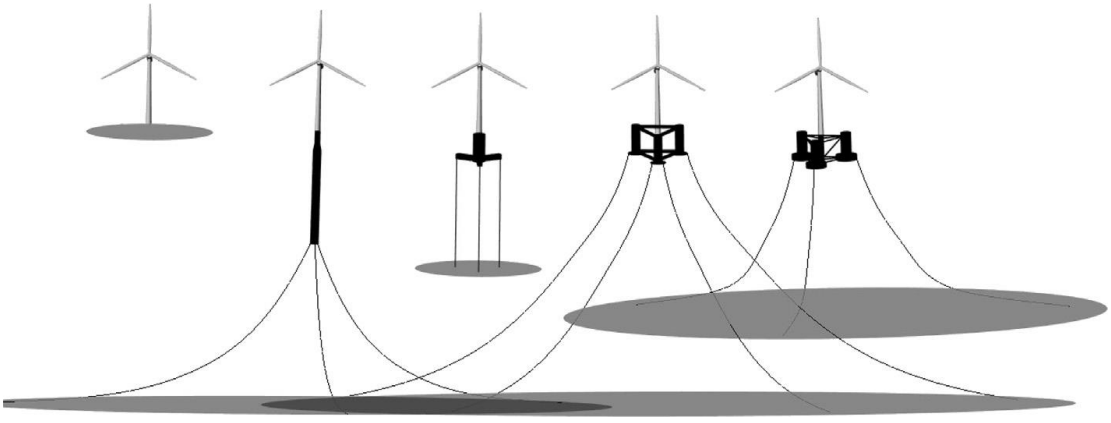

Fig. 2.9 Land-based, spar, TLP, semi-submersible (with offset turbine), and semisubmersible (with turbine in middle). (Nejad *et al*., 2015)

Kausche *et al.* 2018 conducted the economic feasibility study of a TLP designed by GICON company (Fig. 2.10). The unique characteristics of the chosen TLP, towing of the assembled TLP to the wind farm and the usage of heavyweight anchor reduces levelised cost of energy.

Accumulative energy demand and analysis of CO_2 emissions for the platform is also presented.

Fig.2.10 TLP designed by GICON (Kausche et al. 2018)

Le *et al.* (2019) proposed a submerged floating offshore wind turbine (SFOWT, Fig. 2.11) for a water depth of 50 to 200 m. The effects of variation in tether length and pretension on the performance of SFOWT are investigated. The effect of the tether failure is also investigated and found that the system has a better performance during the operational condition with a broken tether.

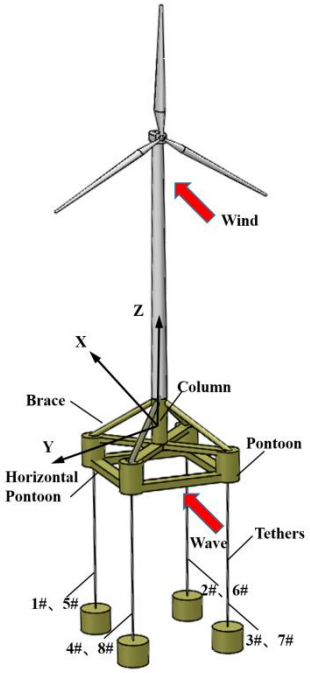

Fig.2.11 Submerged floating offshore wind turbine (Le et al., 2019)

2.3 ARTICULATED SUPPORTS

Articulated towers are compliant structures which are economically suited for deepwater seas due to their lower structural weight when compared to the conventional fixed structures. Restoring moments in these structures are provided by buoyancy force and the foundations of these structures do not resist any lateral force due to environmental loads like wind, wave etc. A detailed review of response of compliant structures due to wind, wave and current with emphasis on modeling techniques and solution methods is given by (Adrezin *et al.,* 1996). Following are the studies reported on the articulated offshore structures.

Bar-Avi and Benaroya, (1997) investigated the response of an articulated tower under deterministic and random wave. The articulated tower is modeled as an upright pendulum with a mass at the top. Geometrical non-linearities along with non-linearities caused by wave drag force, are considered in the analysis.

Datta and Jain (1990) presented an iterative method in frequency domain for finding the response due to random wind and wave forces. The response of a articulated tower under random wind load alone and due to the combined wind, wave and current loads was investigated and concluded that the effect of different nonlinearities do not affect the response due to wind load alone.

Banik and Datta (2003) presented a procedure for determining the stochastic response and stability of an articulated platform under random sea state. It is concluded that the articulated tower was asymptotically stable in the parametric excitation caused by hydrodynamic damping.

Banik and Datta (2008) investigated the response of an articulated platform due to regular wave. The articulated platform is modeled as a SDOF nonlinear oscillator. The dynamic response of the platform is determined by means of incremental harmonic balance method using arc-length continuation technique.

Murtedjo *et al.* (2005) analysed the effects of variations in buoyancy parameter (diameter, length and position of the buoyancy chamber) on articulated tower under regular and random waves. It is established that the platform is feasible for the South East Asia region because of the lower value of maximum Response Amplitude Operator and natural frequency.

Islam *et al.* (2009) explained the comparison of the responses of single and double hinged articulated towers in several ocean environments. The sea state is represented by Pierson–Moskowitz spectrum and the wind by Simiu's spectrum. Analyses are conducted in time domain and compared. The results revealed that the second articulation causes a decrease in RMS bending moment and an increase in central hinge shear.

Hasan *et al.* (2011) studied the response of a multi-hinged articulated platform under random waves subjected to different seismic excitations. Time histories and spectral densities of the responses are presented. It is found that the axial force at the base increases with the vertical ground motions.

Zaheer and Islam (2012) investigated the tower responses due to effect of wave, wind and the combined effect of wind and waves. For comparative analyses of the responses of the tower, different spectra are employed and concluded that lower response is shown for the Davenport spectrum than those for API RP 2A, Kareem and Simiu spectra because of greater energy offered in these spectra at low frequencies. It is also concluded that the central hinge design is more critical because of the large fluctuations in shear.

Atreya *et al.* (2014) conducted a nonlinear analysis of the articulated offshore tower under waves and earthquake. Time domain responses are obtained using Langrangian approach. The joint is modeled as mass-less rotational spring having zero stiffness. The dynamic stability is evaluated using two dimensional phase plots.

Zaheer and Islam (2017) studied the behaviour of double hinged articulated platforms due to interrelated wind and waves for different sea states under actual ocean environments. It is found that simultaneous wind and wave studies was very vital for double hinged articulated platforms for surviving in the extreme environment, since response is different in the presence of waves along with wind than due to wave alone.

2.4 COUPLED DYNAMICS

Hydrodynamic analysis consists of modeling the wave parameters and evaluating the dynamic response of the structure. Aero-elastic analysis includes time-variant aerodynamic loading and evaluating the dynamic response of the structure. Coupled analysis is a combination of hydrodynamic and aero-elastic analysis. The most notable design challenge inherent with any floating turbine system is the computation and coupling of the

hydrodynamic loads and aero-servo-elastic loads (loads from aerodynamics, control systems, structural dynamics) (Moon and Nordstrom, 2010). Predicting the loads and resulting coupled dynamic responses of turbine and platform is the key to the design of support structure. The FAST (fatigue, aerodynamics, structures and turbulence) by NREL is an aero-elastic code capable of handling two- and three-bladed horizontal axis wind turbines. FAST user's guide gives the details. FAST couples hydrodynamics models for offshore structures, aerodynamics models, control and electrical system (servo) dynamics models and structural (elastic) dynamics models to enable time domain coupled nonlinear aero-hydro-servo-elastic simulation (Jonkman and Buhl, 2005). Following are the numerical studies reported on the coupled dynamic analysis of offshore wind towers:

Bulder *et al.* (2002) found the Response Amplitude Operators and standard deviations of the motion response in all modes for the tri-floater design platform supporting a 5 MW wind turbine using linear frequency-domain hydrodynamics techniques.

Withee (2004) presented a fully coupled dynamic analysis tool forecast the response of a floating platform with an offshore wind turbine under stochastic wind and wave. The tool combines both wave forces on the floating platform and the aerodynamic forces on the wind turbine. Tools - FAST (Fatigue, Aerodynamics, Structures, and Turbulence) and ADAMS (Automatic Dynamic Analysis of Mechanical Systems) are utilised for the modeling and dynamic analysis.

Fulton *et al.* (2005) employed OrcaFlex code and Bladed software to study the performance of a semisubmersible structure for a deep-sea installation. OrcaFlex code is used to model the structure, mooring lines and wind turbine. The wave loading is incorporated by altering the Bladed software which is designed to model the wind turbine aerodynamics. The two codes are successfully interfaced for obtaining the results.

Wayman (2006) proposed few novel and economic floating platforms for supporting a 5MW turbine suitable for water depths of 30-300m. A numerical method for frequency domain analysis in coupled structural, hydrodynamic and aerodynamic analysis of floating wind turbine platforms is presented. The codes used for analyses were FAST, WAMIT and LINES module. This tool computes the influence of the gyroscopic loads of the rotor of wind turbine on the tower as well as the platform, the aerodynamic damping of the rotor, the added mass

and damping of wave-body interactions, and the hydrodynamic loads produced by wave forces.

Jonkman and Sclavounos (2006) developed a numerical method by interfacing FAST and ADAMS with LINES which could couple aerodynamics, structural dynamics and mooring line forces. The sea current effects, vortex-induced vibrations and sea ice loading are not included in the study.

Zambrano *et al.* (2006) studied the motion response of a moored floating structure fixed with three wind turbines by applying a Fourier spectrum model of storm conditions of Gulf of Mexico. The wave forces on the platform are developed by the WAMIT program and the wind turbine load was estimated by using a constant force coefficient. The motion of the platform due to the various forces and inertia of the system are calculated using a computer code TIMEFLOAT.

Jonkmann and Buhl (2007) developed a fully coupled aero-hydro-servo-elastic numerical analysis tool to carry out a load analysis of a 5-MW offshore wind turbine supported on a barge platform with catenary moorings. Generation of large loads on the system is found due to the coupling among the response of turbine and the motion of the barge.

Van and Ishihara (2007) developed a FEM code to predict the behaviours of elastic floating offshore wind turbine platforms in the time domain. The elastic responses of the platform are investigated, and the peak responses are observed at resonant points.

Skaare *et al.* (2007) presented the integration of two codes namely SIMO/RIFLEX from MARINTEK and HAWC2 from Risø National Laboratory. The aim of this integrated program is to obtain the structural response of a wind turbine under aerodynamic loading and control actions. This simulation tool developed for floating wind turbine has shown successful results.

Sclavounos *et al.* (2008) presented a parametric design study of floating wind turbine concepts which supports a 5 MW wind turbine by conducting fully coupled dynamic analysis. The coupled frequency domain analysis is done by coupling the LINES, WAMIT and FAST codes. Pareto optimal designs are also presented that possesses a good combination of nacelle acceleration, mooring tension and displacement of the floating system.

Matsukuma and Utsunomiya (2008) studied the motion response analysis of an offshore wind turbine supported on a spar considering rotor-rotation due to steady wind. The blade element momentum theory is employed for the calculation of wind forces on the rotor blades. Due to the gyroscopic effect due to rotation of rotor, the yaw, sway and roll motions are generated. The importance of including effects of rotor rotation in the dynamic analysis is highlighted.

Cermelli *et al.* (2009) developed a coupled aeroelastic-hydrodynamic model which provides better accuracy of wind turbine loads and the turbine control system effects. This tool evaluates the effect of blade pitching on the platform and also provides precise calculation of the loads caused by the wind turbine on floating platform by interfacing FAST with TimeFloat.

Jonkman (2009) developed a simulation tool for coupled analysis in time domain. The tool is able to perform analysis for a range of support platforms, rotor–nacelle assembly, tower and mooring system configurations. The same tool could be employed to model onshore wind turbines by inactivating the mooring system and hydrodynamic modules. The effectiveness of the tool is verified by comparison with results of other numerical models.

Iijima *et al.* (2010) developed a method for the fully coupled aerodynamic and hydroelastic time-domain analysis of an offshore wind turbine supported on floating platform. This procedure employs FAST for aerodynamic analysis and Shell-Stress Oriented Dynamic Analysis Code for time-domain hydroelasticity response analysis. This procedure includes dynamics of blades of rotor, dynamic motions and flexible structural system deflections.

Matha (2010) conducted a fully coupled time domain analysis of a 5 MW wind turbine on a floating offshore TLP by FAST with AeroDyn and HydroDyn. Responses are compared with a land-based turbine and two other platforms, ITI Energy barge and OC3 Hywind spar buoy. Greater loads are observed on turbine components in floating platform than on land-based structure. Significant roll and pitch motions are exhibited by barge and pitch, and roll motions of spar are greater than for the TLP.

Collu *et al.* (2010) performed two preliminary designs, one fixed and one floating, of a support platform for a 5 MW offshore wind turbine. The hydrostatic analysis is done using HydroD program and hydrodynamic analysis using Wadam program of Seasam software. It was concluded that in water depths between 80 m and 100 m the semisubmersible platform becomes more economic than the jacket platform.

Babanci *et al.* (2011) carried out coupled analysis of spar platform supporting a 5 MW turbine in frequency domain. Hydrodynamic analysis is done using WAMIT. The coupled model is obtained by combining WAMIT with FAST. The results obtained are validated with that for OC3 Hywind. The spar platform exhibited same moment rotation but low hydrodynamic damping for force translation compared to OC3 Hywind.

Karimirad and Moan (2012) developed a simplified numerical tool based on the coupled Simo-Riflex-Thrust-Dynamic-Horizontal-Mill to determine the responses of floating wind turbines. The aerodynamic loads at the rotor hub were given as a time varying force. This tool is compared with HAWC2 code. Comparison between the codes for two spar-type wind turbines showed that the simplified approach was very fast with acceptable accuracy.

Karimirad and Moan (2012) conducted a feasibility study of a spar-type wind turbine at a moderate water depth and compared the responses of the ShortSpar and DeepSpar supporting wind turbine. The coupled aero-hydro-servo-elastic analyses is done using HAWC2 code in different environmental conditions

Stewart *et al.* (2012) presented a calibrated FAST model made for representing a scaled model of a TLP supporting an offshore wind turbine. Validation study of this model is also presented. For validation of the FAST model, the coupled hydrodynamic and aerodynamic performance is compared with the combined wind and wave tests

Bachynski and Moan (2012) analysed a TLP supporting wind turbine for a wide variety of parametric single-column TLP designs. The motions of the platform and structural forces on the components of turbine and tendons in various wind-wave environments are evaluated by the Simo, Riflex, and AeroDyn tools in a coupled analysis. It is concluded that performance of TLPs can be improved by selecting the natural period, dimension of platform at the water surface, ballast, pontoon radius and pretension carefully.

Bae and Kim (2013) developed a numerical simulation for the time domain rotor-floater-tether fully-coupled analysis of FOWTs along with dynamics and control of aero-blade-tower, dynamics of mooring lines and motions of the platform. The influences of second-order sum–frequency wave forces on the coupled dynamic analysis are also presented.

Philippe *et al.* (2013) studied the influence of wave direction with respect to wind on the floating wind turbine system by performing a coupled dynamic analysis. Natural frequencies

and natural modes of the system under various wave directions are calculated by modal analysis method and concluded that natural modes varied with the direction of wave.

Jeon *et al.* (2013) numerically investigated the dynamic analysis of a spar platform supporting a wind turbine. Three catenary cables were used for mooring the platform. The structure is analysed by simplifying the upper part of the OWT above the wind tower as a lumped mass. Coupled iterative BEM–FEM methods are used to simulate wave floating substructure and wave-mooring cable interactions. The responses of the floating structure were parametrically investigated relating to the connection position of catenary cables. It is concluded that by connecting the catenary cables above the centre of buoyancy or at the centre of buoyancy, the surge and pitch motions could be minimized.

Zhang *et al.* (2013) studied the dynamic behaviour of a semisubmersible floating foundation for 600 kW wind turbine. The coupled dynamic analysis under the various combinations of wind and waves is carried out using SESAM software. The response is calculated for wave loads in frequency domain and for various combinations of turbulent wind, constant current and irregular wave in time domain and concluded that for the safe operation of the floating wind power generation system, the significant wave height shall be less than 4 m.

Viré et al. (2013) presented a novel tool for modeling the interactions among fluids and floating solids. This numerical tool had equivalent capabilities of existing tools to model the floating wind turbines. This study provides a first-step for the fully coupled simulation of spar type floating wind turbine.

Gutierrez *et al.* (2013). presented FASTLognoter software which is the integration of two tools, FAST (aeroelastic simulator tool for wind turbines) and Lognoter (software to manage and create engineering forms). It offers a graphical user interface for FAST also provides parameterized studies and design optimization of offshore wind turbine platform.

Yu *et al.* (2014) studied and reported the dynamic response of OC3 Hywind spar supporting a wind turbine. The numerical simulation of wind-wave-induced motion is conducted using FAST code in time domain and frequency analysis using FFT. A concept of “effective RAOs” is implemented to calculate the platform’s frequency response. Multiple excitation frequency response is exhibited by the system caused by gyroscopic effect of the rotor and instability induced by blade–pitch–controller. Responses of the system in various sea states

are computed and the results helped to understand the behaviour of the floating platform under actual ocean environment.

Bae and Kim (2014) presented a numerical simulation method for the coupled dynamic analysis of multiple turbines supported on a single floater. The aero-blade-tower dynamics and control of multiple-turbine, dynamics of mooring lines, and motions of platform are also included in the time domain analysis. The analysis showed that damage-induced excitations from one turbine cause considerable variations in the performance of other turbines.

Shi *et al.* (2015) compared the dynamic responses of various types of supporting structures like the monopile, jacket and multipile. The feasibility of these platforms in Korean offshore wind farm is also evaluated. The coupled aero-hydro-servo-elastic analysis is conducted in the time domain with Bladed V4.3.

Lee and Kim (2015) presented a method for seismic fragility analysis of offshore wind turbines. Nonlinear spring element was used to model the interface between underground soils and piles. It is concluded that to obtain seismic response of offshore wind turbine, layer by layer ground motions from free field analysis is required.

Abhinav and Saha (2015) compared the response of an offshore wind turbine fixedcon a jacket under wave loading, with and without considering soil–structure interaction. The jacket structure is analysed in time domain using the hydrodynamic and geotechnical software USFOS along with the aerodynamic load at the hub. Aerodynamic load is calculated using the software FAST and given as a point force at the hub.

Wang *et al.* (2016) explained a frequency domain approach to forecast the coupled response of an offshore wind turbine on a floating platform using ANSYS AQWA. The new approach is validated by comparing the results with the experiment of DeepCwind floating wind turbine. The influence of damping caused by wind, current and mooring lines on the response of floating wind turbine is also investigated.

Liu *et al.* (2017) established an OpenFOAM based for CFD modelling of the FOWT. The coupled dynamic responses of the OC4 semi-submersible FOWT in various operating conditions are investigated.

Le *et al.* (2019) presented the coupled dynamic responses of a submerged floating wind turbine in various mooring conditions. The fully coupled time-domain aero-hydro-servo-elastic analysis of the platform is performed using the tool FAST. Time domain analysis is performed to investigate the influence of variation in tether length on the performance of the submerged floating wind turbine. The influence of failure of tether is also investigated and found that tether failure increases the pitch response. Submerged floating wind turbine with a broken tether still shows better performance in the operational condition.

Xin-liang *et al.* (2020) proposed a new analysis procedure based on the theorem of moment of momentum and the Newton's second law for the dynamic behaviour of offshore wind turbine on a spar-type floating platform. To implement the proposed method, a code is developed and verified by comparing the results with those computed by FAST.

Huang *et al.* (2020) investigated coupled aero-hydrodynamic performance of a spar-type FOWT supporting NREL 5-MW wind turbine under combined wind-wave action to study the interference effects between the aerodynamic characteristics of wind turbine and the motion responses of the platform. The tool used for the analysis was FOWT-UALM-SJTU. It was concluded that surge and pitch motion of the platform considerably change the local attack angle and wind speed of the rotating blades is affected only by the pitch motion.

2.5 EXPERIMENTAL STUDIES ON ARTICULATED SUPPORTS

Nagamani and Ganapathy (2000) studied both analytically and experimentally, the influence of mass distributions on the variations of the bending moment and the deck accelerations of the model of a three-leg articulated tower (Fig. 2.12). The experiments on the model of a three-leg articulated tower are conducted for a range of wave frequencies and wave heights in a 2m flume and observed that the bending moment increases with wave height for all the legs.

Chandrasekaran *et al.* (2010) investigated experimentally the dynamic response characteristics such as the displacement and bending stress variations of a Multi-Legged Articulated Tower (Fig. 2.13) with and without tuned mass damper. It is found that the bending moment of the platform decreases with increase in the mass of tuned mass damper.

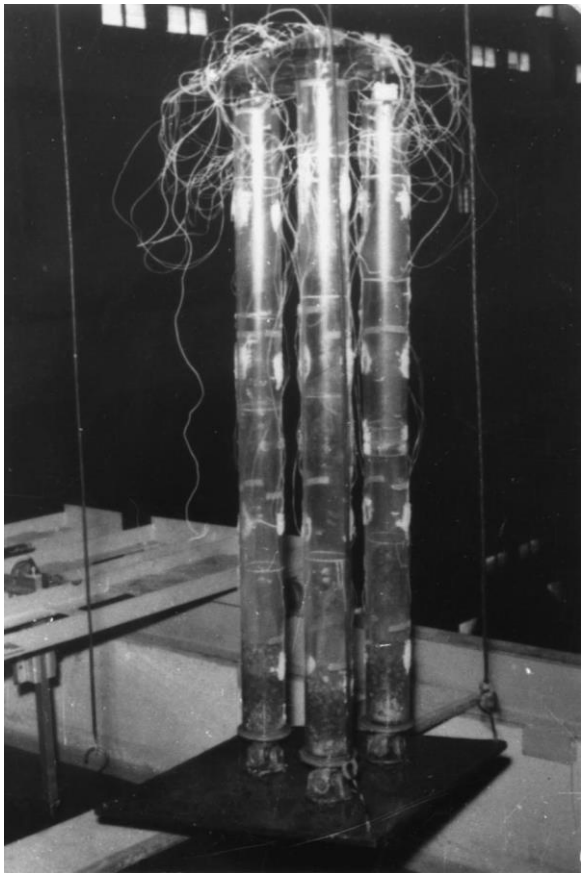

Fig.2.12 Model of three-leg articulated tower (Nagamani and Ganapathy 2000)

Fig. 2.13 Multi-Legged Articulated Tower (Chandrasekaran *et al*., 2010)

2.6 EXPERIMENTAL STUDIES ON WIND TURBINES

Testing in wave tank and numerical modelling should go hand in hand. For reproducing realistic behaviour particularly for complex systems like wind turbines characterized by static and dynamic coupling effects, experimental testing through physical scale models in a wave basin is usually conducted. The details of model tests from the literature in this area are given below.

Tong (1998) tested a 1:48 scale FLOAT model in BMT's towing tank, in collinear waves and winds to validate the design and theoretical models. Simulation of wind condition to satisfactory level was proved to be difficult due to scaling issues.

Skaare *et al.* (2007) carried out 1:47 scale model test at the Ocean Basin Laboratory at MARINTEK in Trondheim (Fig. 2.14), for the validation of the motion response of the Hywind concept to coupled wind and wave loads. Froude scaling was employed and the test was done with a variety of sea states and various parameters were measured. Strong correlation between experimental results and numerical simulations using SIMO/RIFLEX/HAWC2 program was demonstrated.

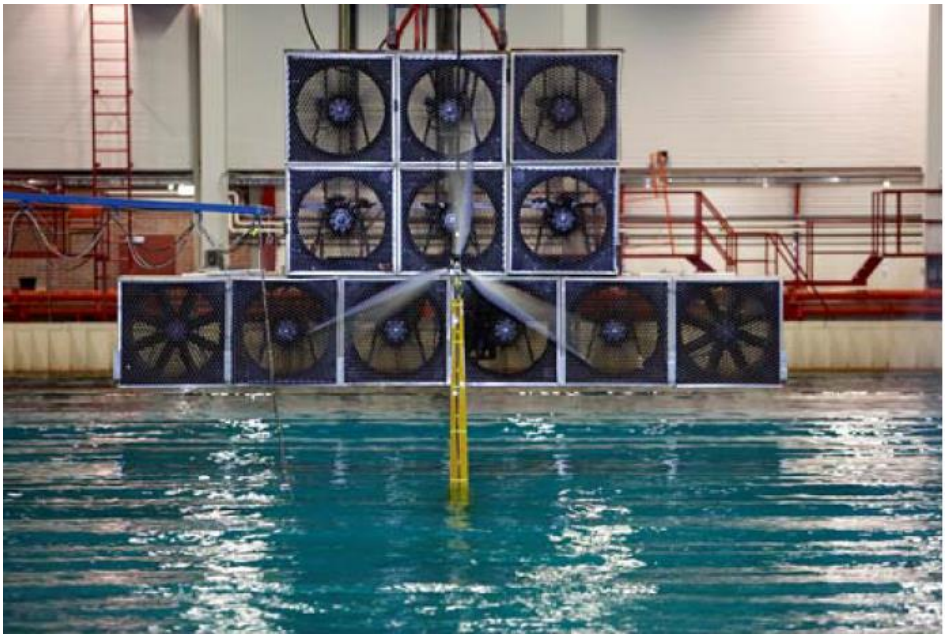

Fig. 2.14 Scale model test of Hywind concept (Skaare et al., 2007)

Ishihara *et al.* (2007) carried out 1:150 scale model tests on semi-submersible floating structure (Fig.2.15) which supports three wind turbine towers in a water tank.. The tests are

conducted in a water tank with wind tunnel at National Maritime Research Institute, Japan. The effect of the wind is incorporated by means of a rotor for operating and survival cases

Fig. 2.15 Model of semi-submersible platform for three wind turbine towers (Ishihara et al. 2007)

Utsunomiya *et al.* (2009) conducted a 1/22.5 scale experiment of a spar buoy platform (Fig. 2.16) at the National Maritime Research Institute (NMRI) in Tokyo, Japan. Tests conducted include free vibration, regular wave and irregular wave tests. Aerodynamic interactions are not considered, the effect of wind is given as a steady force on the top of the tower.

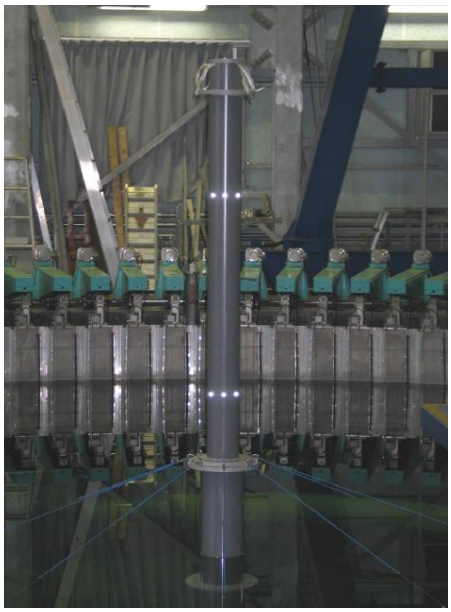

Fig.2.16 Scale model of SPAR-type platform at NMRI (Utsunomiya et al. 2009)

Cermelli *et al.* (2009) conducted a 1:105 scale model test of WindFloat, at the UC Berkeley ship model testing facility (Fig. 2.17). The gyroscopic effect was simulated with the help of an electric motor attached to the tower top. Wind loads were simulated with the help of fans and a foam disc fixed on the model. The experimental setup was capable of measuring surge, heave and pitch measurements using a video camera with a photo-tracking system. Effect of waves for 100-year-long period on the platform was simulated and realized in a 3-h-long test period. The results obtained agreed with the numerical simulations using TimeFloat.

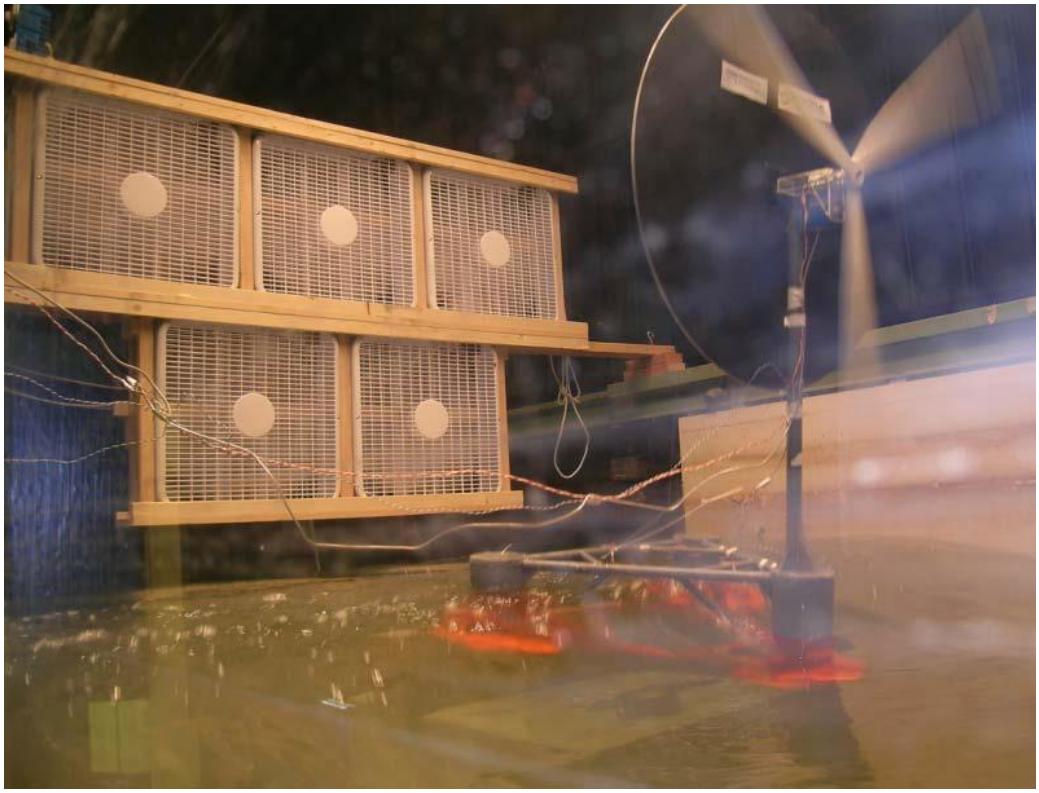

Fig. 2.17 Scale model of WindFloat (Cermelli *et al*., 2009)

Murai and Nishimura (2010) conducted an experiment in a water tank and also numerical simulation to study the influence of the gyro moment of the disk to the motion of the SPAR type floating platform (Fig. 2.18). Experiments are conducted to investigate the effect of disk rotation on the natural periods of different motions and on the harmonic motions under regular waves. It is found that natural period changed and roll and yaw occurred due to the gyro moment of the rotation.

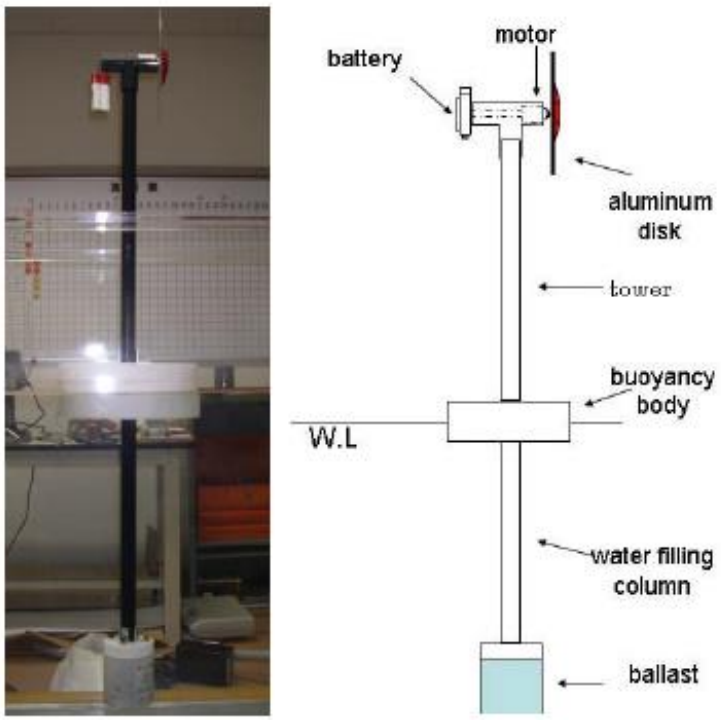

Fig. 2.18 Picture and sketch of the experimental model (Murai and Nishimura, 2010)

Martin (2011) developed a 1:50 functional scale model of 5 MW wind turbine for wind and wave basin model testing of floating wind turbine platforms. The model can generate thrust and torque from wind forces, control rotor speed, pitch blades remotely and obtain essential sensor data for the experimental program. The design is based on NREL 5 MW wind turbine. This model is useful to validate different floating wind turbine simulation codes.

Mostafa *et al.* (2012) carried out 1:360 scale model test of a prototype floating offshore wind turbine (FOWT) in a water tank. The study parameters are gyroscopic moment on the FOWT and dynamic motion of the spar-type FOWT. The effects of rotor are simulated using a flat blade with two small weights placed on it and a motor placed at the top of the tower to create the gyroscopic effect. Experimental and numerical results confirmed that the yaw motion is affected by the gyro moment produced by the rotation of blades.

Shin *et al.* (2013) investigated 1:128 scale models of three new spar platforms by changing the shape of OC3 Hywind spar which supports a 5 MW wind turbine. The tests are conducted at the Ocean Engineering Wide Tank of University of Ulsan. The volume and mass of these models are kept same but having different hydrodynamic and hydrostatic loads. In the scale model tests, wind generator comprising of eighteen fans is used to produce wind load. It is

concluded that the motion characteristics of the new modified platforms are better than original OC3 Hywind.

Sethuraman and Venugopal (2013) investigated the hydrodynamic responses of a stepped-spar floating wind turbine (Fig. 2.19) by conducting scale model test in the curved wave tank at the University of Edinburgh. In this 1:100 scale model, an optical tracking system is used to measure surge, pitch and heave motions at two locations, the centre of mass and the nacelle point. Numerical results simulated using OrcaFlex software is similar to the experimental results.

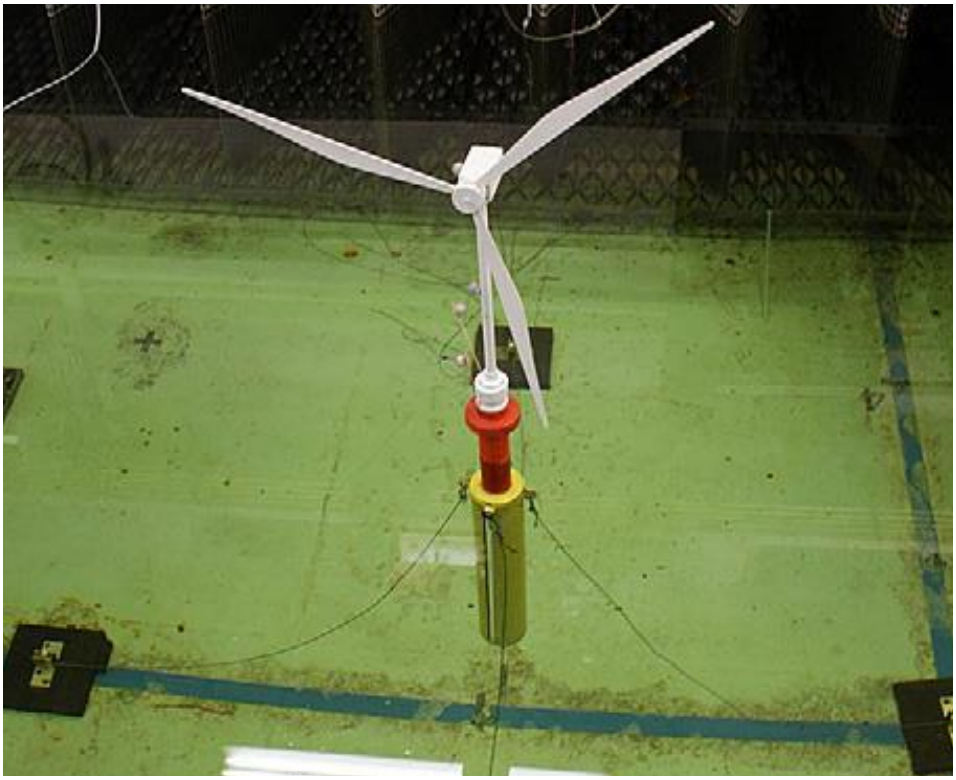

Fig.2.19 Stepped-spar floating wind turbine (Sethuraman and Venugopal, 2013)

Goupee *et al.* (2014) tested a TLP, a spar buoy and a semisubmersible (Fig. 2.20), each supporting the same horizontal axis NREL 5 MW reference wind turbine in wind-wave basin at the Maritime Research Institute Netherlands to compare the performance of these floating concepts. The model scale is 1:50. Free floating motion as well as dynamic behaviour in irregular sea states with dynamic wind is studied. It is concluded that the spar-buoy exhibits the lowest surge response under irregular seas whereas the TLP shows the lowest pitch response.

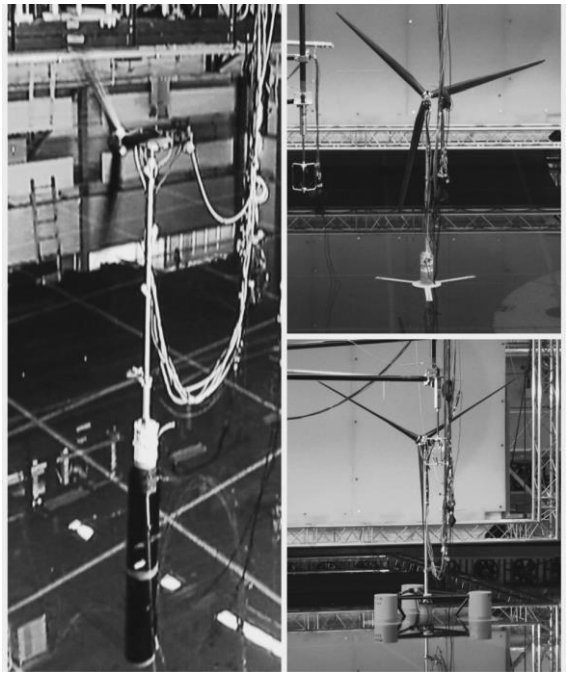

Fig. 2.20 TLP, spar buoy and semisubmersible platform (Goupee *et al.*, 2014)

Martin *et al.* (2014) presented a methodology for scale model testing of floating wind turbines in Froude scale conditions. For all the field variables of scale model testing like the wind turbine design, operation, and associated wind condition, scaling relationships are established.

Koo *et al.* (2014) described the instrumentation used, the wave and wind environments and the results of the tests for system identification carried out on 1:50 scaled model wind turbine on three floating platforms. The tests are conducted at MARIN (Maritime Research Institute Netherlands).

Myhr and Nygaard (2014) conducted 1:40 scale model tests on three different Tension-Leg-Buoy systems. Tests are done at the Deep Wave Basin at the IFREMER. Free oscillation tests as well as tests in regular and irregular waves are conducted and the results are presented in the form of Response Amplitudes Operators.

Duan *et al.* (2016) investigated the motion behaviour of 1:50 scale model of OC3 spar platform supporting wind turbine suitable for 200m water depth. In place of motor drive, the spinning of rotor is physically simulated by wind forces. The system is investigated under different load cases of wind and irregular wave to study its coupled response behaviour and found that wind load effect the surge, heave and pitch behaviour.

Ruzzo *et al.* (2016) conducted a small-scale field experiment on a 1:30 model of spar supporting offshore wind turbine. The test is carried out in sea water at the Natural Ocean Engineering Laboratory of Reggio Calabria. In this study only hydrodynamics is considered, and the turbine is considered as a lumped mass at the tower top.

Oguz *et al.* (2018) presented an experimental as well as numerical study of the Iberdrola TLP wind turbine concept (Fig. 2.21) under realistic wind and wave environments. The scale model experiments are conducted in the Kelvin Hydrodynamics Laboratory. The experimental investigation includes free decay tests, tests under regular and irregular waves and simulated wind environments. To incorporate the time-varying aerodynamic loads produced by the turbine during the tests, a Software-in-the-loop approach is used. It is found that the effect of wind have a significant effect on the response of the TLP platform compared to variation in wave condition.

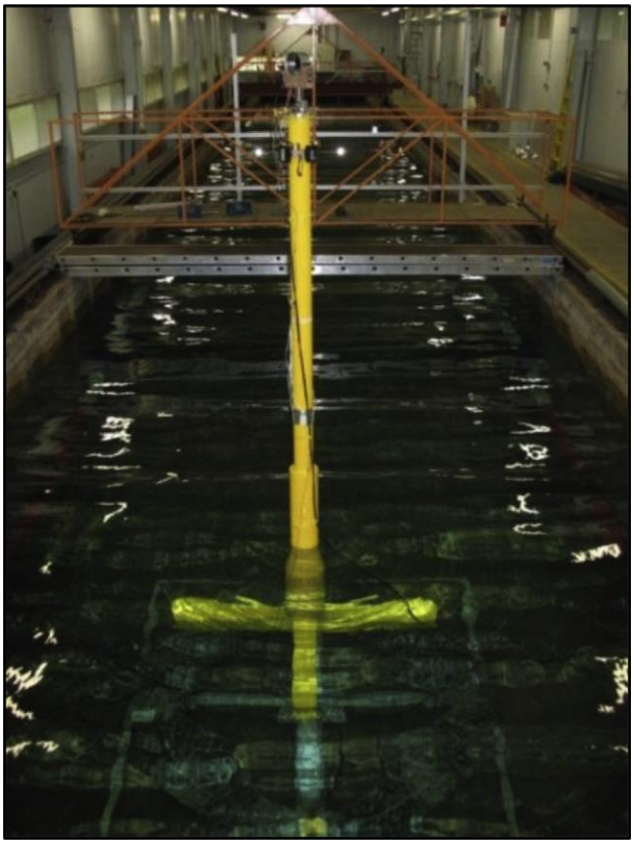

Fig. 2.21 Scale model of Iberdrola TLP wind turbine concept (Oguz *et al*., 2018)

Several researchers have proposed different conceptual designs such as mono column tension leg platform, spar buoy with catenary moorings, tension leg spar buoy, semisubmersible, four legged taut leg moored system. Technical and economic feasibility of these conceptual

designs were studied. The offshore wind turbines installed to date are on fixed structures. At deeper water depth, compliant platforms will be the most economical type. Articulated type supporting structure for wind turbine has not been investigated by any of the researchers. Hence it is worthwhile to study the complete coupled dynamics of wind turbine supported over articulated legs. A thorough experimental and numerical investigation is needed for the practical implementation of the system. Towards this objective, the present study attempts to design an articulated type of support for an offshore wind turbine.

2.7 OBJECTIVES AND SCOPE OF THE PRESENT WORK

Based on the assessment of the literature and the motivation outlined above, the objectives and scope of the study are as follows:

Objectives

- Propose an articulated type supporting structure for an offshore wind turbine
- Study on different configurations of proposed articulated support for 5 MW offshore wind turbine to evolve a feasible model
- Experimental investigation on a scaled model of the proposed articulated type supporting structure
- Investigations on the dynamic response characteristics of the proposed articulated type supporting structure for wind turbine in regular and random waves

Scope

- Propose the configuration of an articulated platform support for 5MW NREL offshore wind turbine
- Experimental investigation on the scaled physical model of the proposed structure in regular waves in the wave flume
- Theoretical validation of the experimental results
- Further analytical studies to evaluate the performance of the proposed structure

CHAPTER 3

DESIGN OF THE ARTICULATED PLATFORM

3.1 GENERAL

Ocean wind energy production is characterised by factors such as open space installation in the sea where there is absolutely no obstruction, thereby allowing visibility hindrance free and significantly minimising the effect of noise and electromagnetic interference as compared to installations on land. The mean speed of the wind is 90% greater than that on the land which is another added advantage. Presently the fixed bottom supports for offshore wind turbines that are in existence generally include single piles, tripods, and jackets. These support structures are required to react to all the environmental forces for the required stability. In order to achieve stiffness and strength needed they require excessive physical dimension hence are very costly. Also, greater the water depth (when exceeds 50 m), the construction cost of offshore wind turbines with fixed foundations increases considerably. The compliant platform serves as a foundation for mounting offshore wind turbines. The introduction of complaint mechanism into a platform provides the structure with a degree of mobility. Compliant platform has been proposed for the wind turbine because of the advantage of the survival competency. The compliance guarantees a simple and inexpensive structure which yields to the wave induced motions. The compliant structure utilizes buoyancy to support the payload.

3.2 ARTICULATED PLATFORM CONCEPT

Articulated towers are a compliant type of support suitable for deep waters. The major parts of an articulated tower are shown in Fig. 3.1. The articulated tower comprises of a vertical tubular column to which a buoyancy chamber is placed near the water surface and ballast is attached near the bottom of the column. The compliance is introduced by the utilisation of articulated (universal) joints permitting one portion of a structure to rotate relative to another. The vertical tubular column is linked to the sea floor using a universal joint attached to the base. The reasons for choosing the articulated platform are simplicity of design, its better under water reliability and beneficial motion responses (i.e. minimum surge response). Multi-leg articulated towers having minimum three legs developed from the conventional single leg platform have minimal movements in horizontal direction (Nagamani and Ganapathi, 2000).

The legs are connected by universal joints both to the beam and to the base. The utilisation of articulated joints guarantees that the parallel position of legs remains unchanged and deck remains horizontally by itself. A single leg, a multi-hinged and a multi-leg articulated tower are shown in Fig. 3.2.

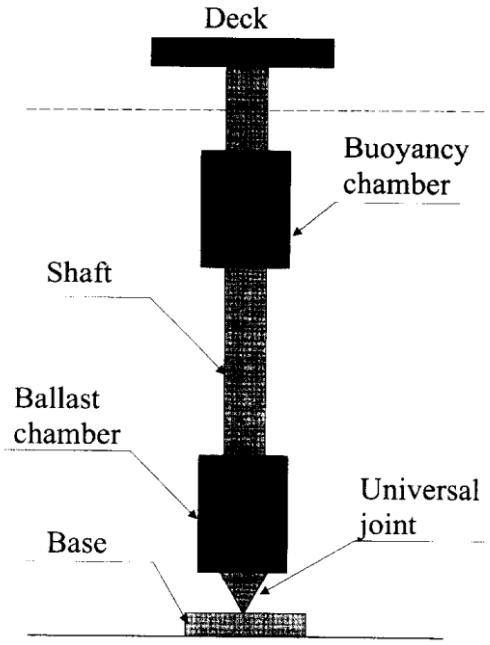

Fig. 3.1 Articulated tower (Adrezin et al.,1996)

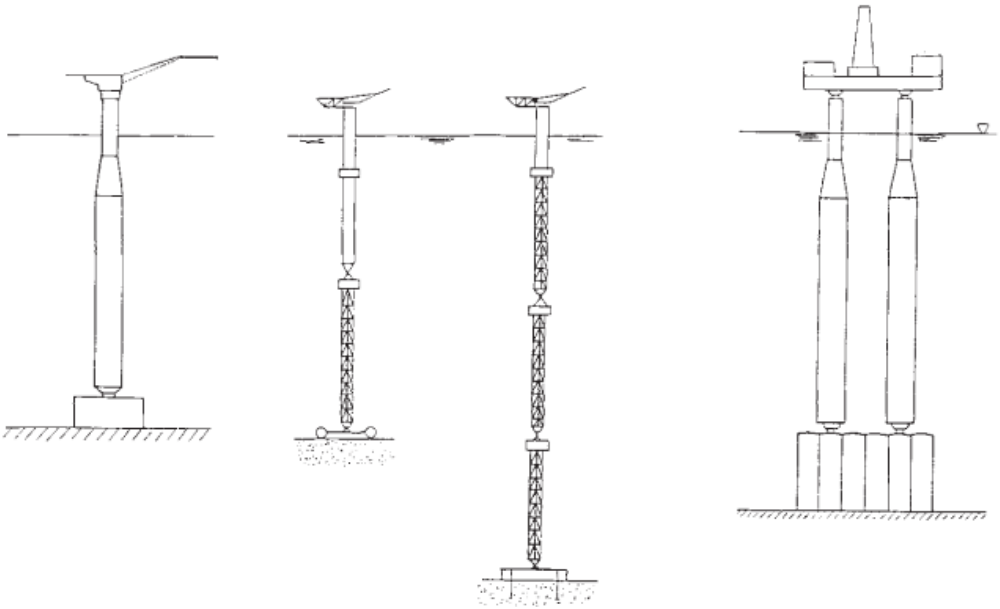

Fig. 3.2 A single leg articulated tower, a multi-hinged articulated towers and a multi-leg articulated tower (Nagamani and Ganapathi, 2000)

3.3 DESIGN OF THE THREE-LEGGED ARTICULATED PLATFORM

The design is an iterative procedure. The general design principles for compliant platform are that (i) must support the wind turbine which has significant mass of nacelle and rotor and is nearly at 90-100 m from the still water level, (ii) the natural frequency of the platform should not coincide with the frequency of dynamic loading and (iii) must survive extreme wave, wind and current environments throughout its design life.

A unique platform is conceived after taking into cognizance of the information gathered from various related literature. The basic form of the supporting structure for wind turbine proposed for investigation is shown in Fig. 3.3.

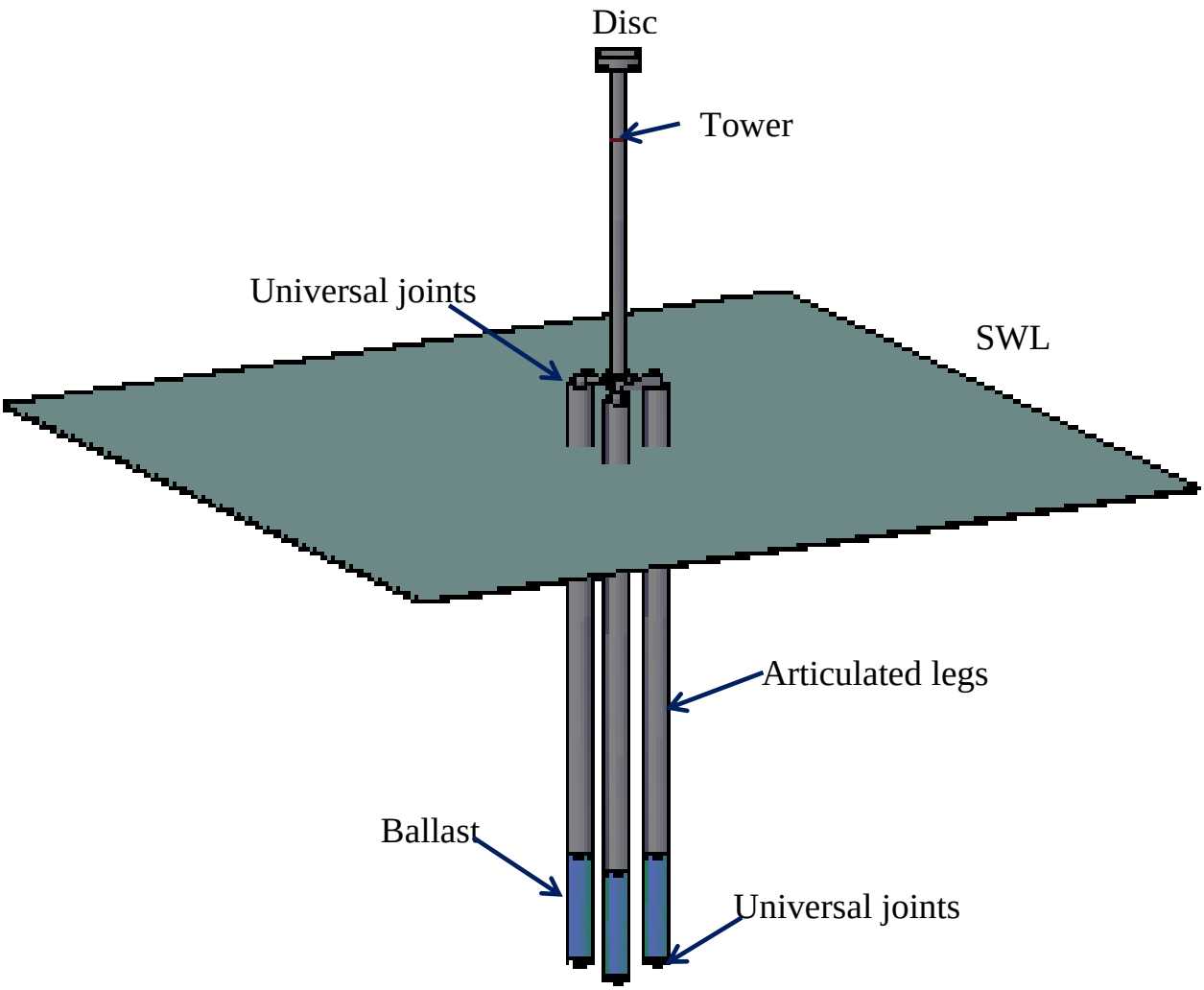

Fig. 3.3 Basic form of the proposed platform

This basic form of the proposed three-legged articulated support consists of three separate vertical tubular legs to which ballast is attached near the bottom on each leg. Uniqueness of the platform, as compared to those developed for similar studies, is that it consists of three tubular columns connected to the sea bed through articulated joints for each leg The utilisation of this joint will allow the overall system deflection in rotational mode and also release the foundation from resisting any lateral load developed by environmental loads. The displaced articulated tower in rotational mode is reverted into the equilibrium due to its buoyancy. The vertically positioned legs are inter-connected at the top by beams through universal joints, and the turbine tower is mounted over the intersection of the beams. The turbine is positioned on top of the tower. The articulated tower is held upright by an excess of buoyancy over the weight of the structure. Thus the universal joint at the base coupled with the angular stiffness, and excess of buoyancy, yields a compliant structure which moves horizontally on wave action. The performance advantage of the articulated tower lies in the fact that it lowers the tilts appreciably in waves, with no moment transfer to the base.

However the preliminary challenge in this type of design is that, weight, thickness, the size of the members, ballast etc are to be fixed so that a control over natural frequency is realised and these frequencies are placed in a desirable limit. The natural frequency of the system should be designed in such a way that resonance will not occur with most commonly occurring waves. The general rule is that the surge, sway and yaw motions must be inertia dominated in the first order wave force frequency range in order to eliminate resonance. This means natural periods of these modes are longer than 25 s. It is presumed that second order wave forces will be negligible for an articulated tower because of the relatively small diameter.

Before moving on to the detailed free vibration analysis to get natural frequencies, the basic dimensions of the structure are to be determined based on basic stability checks, i.e. the buoyant force should not be less than total weight and a proper restoring is attained when deflected. To get an idea on basic mechanics of articulated tower, a well investigated articulated platform proposed by Kirk and Jain (1977) was selected for detailed study. It is single legged articulated tower, whose dynamics is entirely different from multi legged tower. But the basic stability criteria may be considered same. The structure is evaluated to find Buoyancy Force to Weight ratio (B.F/W) and Restoring Moment to Overturning Moment ratio (RM/OM). The Buoyancy Force to Weight ratio (B.F/W) of this is estimated to be 2.0. The Restoring Moment [is given by $F_b \times C_b$, where F_b is buoyancy force and C_b, the distance

from hinge to centre of buoyancy] to Overturning Moment [is given by W × Cg, where W is the total weight of structure and Cg, the distance from hinge to centre of gravity] ratio, RM/OM, is found to be 1.6.

In the light of this investigation, the Three Legged Articulated Support is proposed. Efforts are made to keep the B.F/W ratio and RM/OM at a level similar to that of articulated tower proposed by Kirk and Jain, (1977) It is found that, since the top loads on the proposed platform weighs about 900 tonnes, the diameter of the legs are fixed so as to get a fairly high B.F/W ratio. The weight of the turbine, tower and supporting beams are distributed above the water surface, increasing the lever arm corresponding to centre of gravity, and thereby increasing the overturning moment. In order to reduce the lever arm corresponding to centre of gravity, a ballasting is provided at the bottom of the tower.

The dimensions of leg, ballasting height, thickness etc. could be only fixed by trial and error process. Fig. 3.4 shows the methodology adopted for the design. When the model satisfies the basic stability check, a free vibration analysis is done to determine the natural frequencies. If the natural frequencies are not within the desired limits, changes are made and analysed further till the natural frequencies are within desirable limits. The properties of the finalised preliminary design are given in Table 3.1. The Buoyancy Force to Weight ratio (B.F/W) is found to be 1.5 and Restoring Moment to Overturning Moment ratio (RM/OM) is found to be 1.3.

3.4 INPUT DATA

Offshore wind turbine platforms are subjected to marine environmental forces. The governing loads for these structures are hydrodynamic and aerodynamic. These are presented by wave and wind loading. Therefore the input data depends on the site where wind turbine is to be installed, wind and wave data of the site, the turbine and its tower. A detailed description of these design inputs are given below

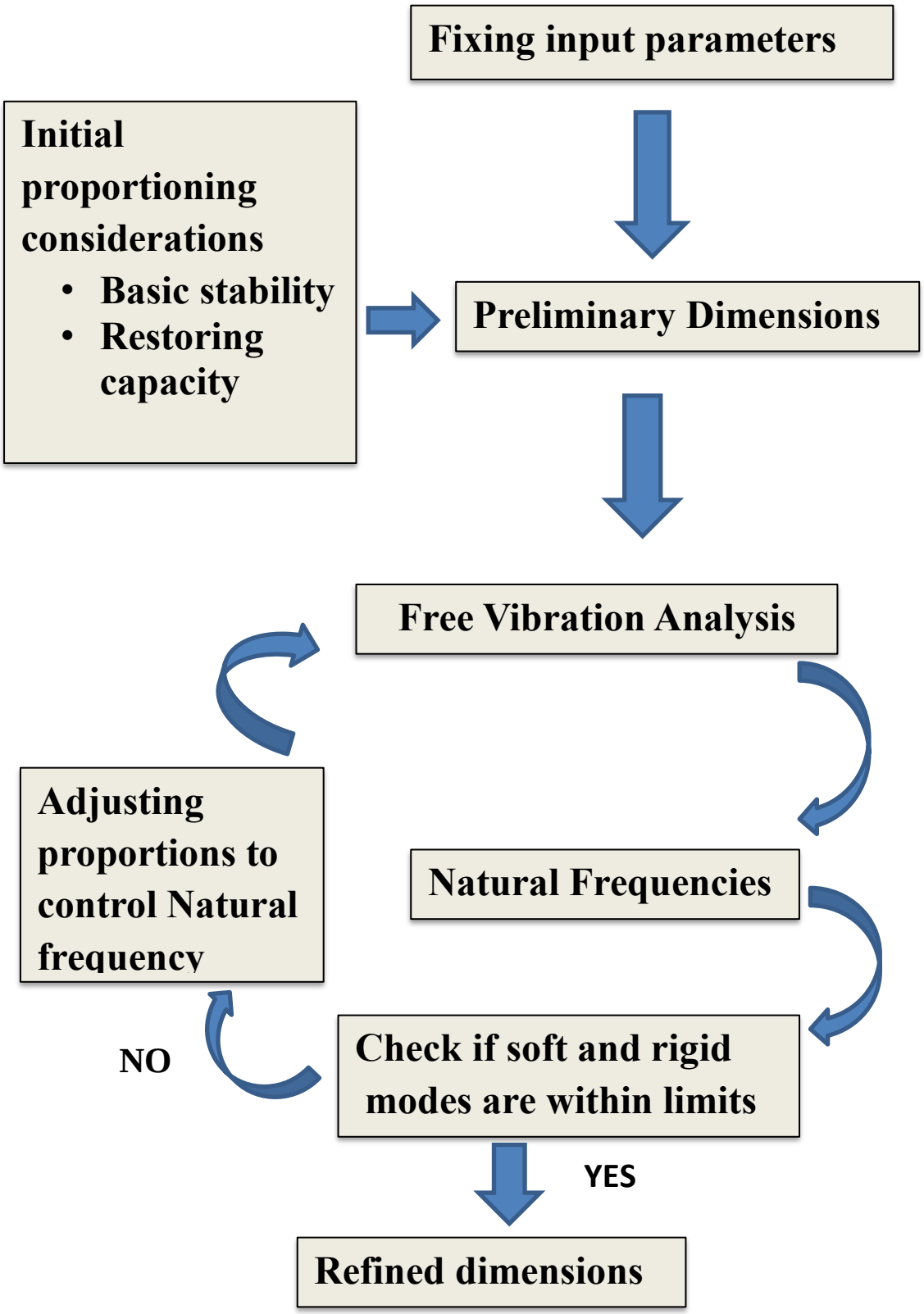

Fig. 3.4 Methodology adopted for the design

Table 3.1 Properties of the structure

Total mass of the structure	11232000 kg
Mass of nacelle system	350000 kg
Depth	144 m
Displacement	17947440 kg
Diameter of tower legs	7.2 m
Diameter of wind tower	4.8 m
Diameter of supporting beam	3 m
Total ballast mass	5175360 kg

3.4.1 Wind Turbine

NREL's (National Renewable Energy Laboratory) 5 MW wind turbine is used for the study. The details of the 5 MW turbine are taken from NREL website. This is a three bladed upwind type of turbine. To encourage concept studies intended for assessing offshore wind technology, Jonkman et al., (2009) developed the specifications of the "NREL offshore 5 MW baseline wind turbine. The technical details of 5 MW NREL wind turbine is shown in Fig 3.5.

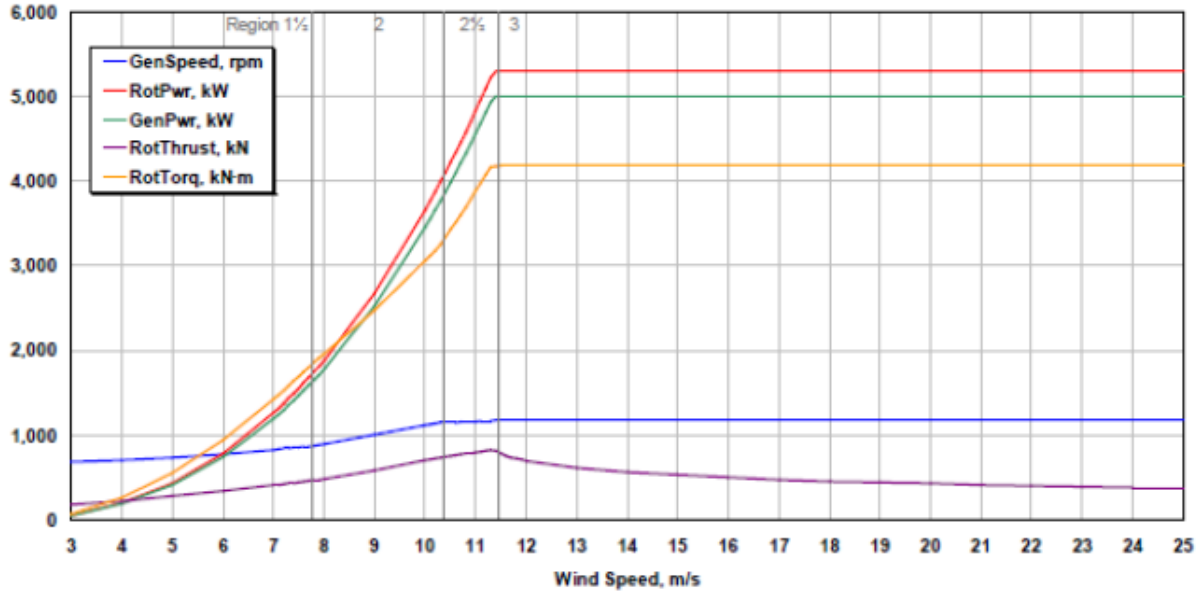

Fig. 3.5 Details of 5 MW wind turbine (Jonkman et al. 2007)

The gross properties of the NREL 5 MW wind turbine are listed below in Table 3.2. The tower base is placed 10 m above the still water level.

Table 3.2 Gross Properties - NREL 5 MW Offshore Wind Turbine (Jonkman, 2009)

Rating	5 MW
Rotor Orientation, Configuration	Upwind, 3 Blades
Rotor, Hub Diameter	126 m, 3 m
Hub Height	90 m
Cut-In, Rated, Cut-Out Wind Speed	3 m/s, 11.4 m/s, 25 m/s
Cut-In, Rated Rotor Speed	6.9 rpm, 12.1 rpm
Rated Tip Speed	80 m/s
Overhang, Shaft Tilt, Precone	5 m, 5^0, 2.5^0
Rotor Mass	110,000 kg
Nacelle Mass	240,000 kg
Tower Mass	347,460 kg
Coordinate Location of Overall CM	(-0.2 m, 0.0 m, 64.0 m)

Aero-Servo Loads on Wind Turbine

Forces on the wind turbine includes aerodynamic blade loads during operation and parking condition, drag forces on tower and nacelle, gravitational loads, servo loads and wave induced loads causing motion of the platform which affects the aerodynamics.

3.4.2 SITE

Location of wind turbine is identified within a rectangular section of 400 sq.km area, at east coast of India. Points $8^0$50’40’’N, $78^0$40’33’’E and $8^0$29’40’’N, $78^0$45’47’’E conforms the diagonal points of the area selected. Area identified is about 52 kilometers from Tuticorin coast. The depth at this area is found to be about 144 m. Depth at the site is determined using data from Google Earth. The Google Earth has the inbuilt provision to display the latitude, longitude and depth of the sea at the point selected.

3.4.3 WAVE FORCES AND HYDRODYNAMICS

The platform concept and specifications of the site affects certain hydrodynamic aspects of offshore wind turbine support structures. These aspects include selection of wave kinematics models, hydrodynamic models for required water depth and whether structural members are slender or large-volume. There are numerous methods recommended for hydro loads that include the panel method, Morison formula and pressure integration method or a combination of these methods. Generally, for slender structures, the diffraction effects are insignificant as the structure does not considerably disturb the wave pattern. Therefore to represent wave loads acting on slender structural members (eg. wave load on cylinder submerged in water), the Morison formula can be applied. The importance of diffraction, inertia and drag forces on the structures is shown in Fig.3.6. Referring the Fig.3.6 it is clear that Morison formula can represent the wave forces if the diffraction forces are negligible while comparing to other wave forces.

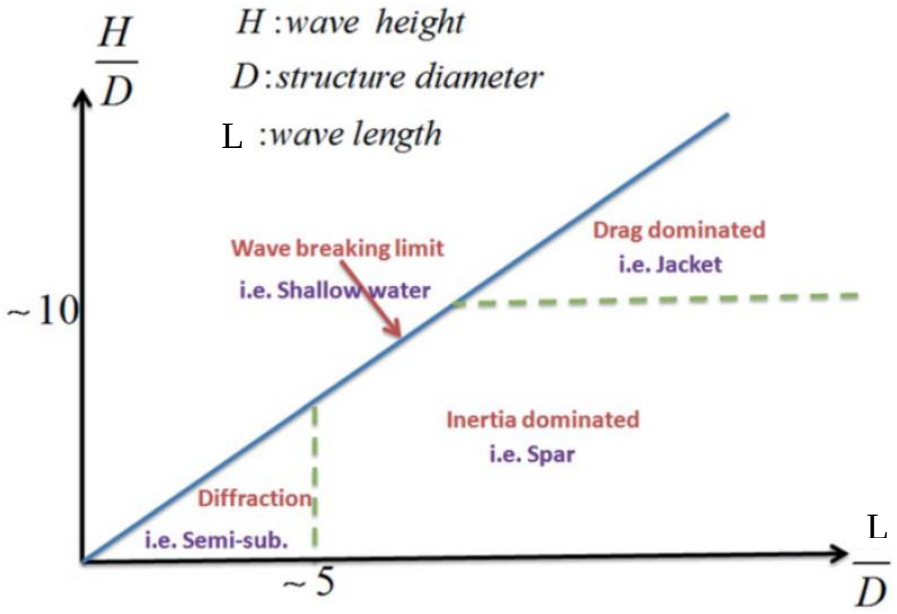

Fig. 3.6 Importance of wave forces (Karimirad 2014)

The Morison formula is applied for slender members where the diameter of the structure is very small compared to the wave length, i.e. $D < 0.2L$ where D is the characteristic diameter and L is the wave length, i.e. it is presumed that the structure does not have a substantial effect on the waves. The hydrodynamic forces of the Morison formula include the inertial and quadratic viscous excitation forces. The inertial forces in the Morison formula include

diffraction and Froude- Krylov forces. The force on the cross section of a slender cylinder is expressed as:

$$dF = \frac{1}{2}\rho D C_d |u_f - u_s|(u_f - u_s) + \rho A C_m \dot{u}_f - \rho A (C_m - 1)\dot{u}_s$$

$$= \frac{1}{2}\rho D C_d |u_f - u_s|(u_f - u_s) + \rho A (1 + C_a)\dot{u}_f - \rho A C_a \dot{u}_s \quad \text{.....3.1}$$

where C_d and C_m are quadratic drag and inertia coefficients, respectively. ρ is the sea water density, D is the diameter of the cylinder, u_f is the fluid particle velocity, u_s is the structure velocity, $\dot{u}_f$ is the fluid particle acceleration, $\dot{u}_s$ is the structure acceleration and A is the cross-sectional area. The positive direction of force is in the wave propagation direction.

3.5 DESIGN OF THE SCALED MODEL

For understanding the dynamics and responses of a prototype, the model tests data is scaled up by using scaling laws. The dynamic similitude between the two physical systems, prototype and the scaled model is achieved by satisfying the scaling laws. The various forces that come across in a hydrodynamic test setup model are gravity force, inertia force, viscous force, drag force, pressure force and elastic force. The scaling laws are ascertained from the ratio of these forces. The gravitational effect predominates in the case of water flow with a free surface. The effects of other forces like viscous force, surface tension and elastic compression forces are relatively small and can be ignored in most of the ocean engineering problems. Therefore Froude's law is the most common scaling law in water wave problem. The Froude number considers the effect of gravity and is defined as the ratio of inertia force to the gravitational force. It is expressed as

$$\text{Froude number, Fr} = \frac{u}{\sqrt{gl}} \text{.....3.2}$$

u = velocity

g = acceleration due to gravity

l = characteristic dimension

The advantage of choosing Froude's scaling law is that it straightly scales the most significant criteria of the mechanism. The Table 3.3 shows the scale factor of the parameters used under Froude scaling.

A scale ratio of 1:60 ($\lambda = 60$) is adopted in compliance with the water depth available at the testing facility. The Properties of Scaled Model are given in the Table.3.4.

Table 3.3 Scale factor of the parameters used under Froude scaling.

PARAMETERS	SCALE FACTOR
Length	$1/\lambda$
Diameter	$1/\lambda$
Wave height	$1/\lambda$
Wavelength	$1/\lambda$
Wave period	$1/\lambda^{1/2}$
Acceleration	1
Velocity	$1/\lambda^{1/2}$
Wave force	$1/\lambda^3$
Mass	$1/\lambda^3$
Buoyancy	$1/\lambda^3$
Moment of inertia	$1/\lambda^5$
Angle	1

Table 3.4 Properties of Scaled Model

Total mass of the structure	52 kg
Mass of nacelle assembly	1.620 kg
Depth	2.40 m
Displacement	83.09 kg
Diameter of tower legs	0.12 m
Diameter of upper tower	0.08 m

3.6 SUMMARY

The chapter explains the design details of the proposed three-legged articulated platform for 5 MW offshore wind turbine are described. The properties of the prototype structure as well as the scaled model are also presented.

CHAPTER 4

EXPERIMENTAL INVESTIGATION

4.1 GENERAL

In the present work, the motion response of a three-legged articulated structure is investigated using scaled model tests in a 4m wide wave flume at the Department of Ocean Engineering, Indian Institute of Technology, Madras. Towards this objective, a scaled model of the candidate structure is fabricated based on Froude scaling. Tests are done for regular waves of different wave periods and wave heights and for different orientations of the platform. The descriptions of the fabrication of scale model, details of testing instruments and other facilities used along with their calibration are addressed in this chapter. The details of free vibration tests, sample calibration graphs, measured time series of wave elevation and the captured motion responses are also discussed.

4.2 FABRICATION OF THE MODEL

The three-legged articulated structure designed to support the 5 MW wind turbine is fabricated out of acrylic tubes and plates. A 1:60 scale model of a prototype designed as per the Froude Law is adopted for the experimental study. Three-legged articulated support comprises of three separate vertical legs to which ballast is attached near the bottom on each leg. The vertically positioned legs are inter-connected at the top by beams through universal joints, and the turbine tower is mounted over the intersection of the beams. The model geometry is given in Fig. 4.1.

The model is fabricated using acrylic tubes and plates, assembled together using chemical adhesives araldite and chloroform to make it water tight. In order to lower the centre of gravity, steel rods are inserted inside the tube as ballast. The beams for connecting the three legs are ISA 50mm×50mm @ 37 kg/m. The wind turbine tower is modeled using a single acrylic tube; the turbine weight at the nacelle is simulated by a steel disc of mass 1.62 kg. The properties and mass distribution of the model are given in Tables 4.1 and 4.2 respectively. The model is shown in Fig. 4.2.

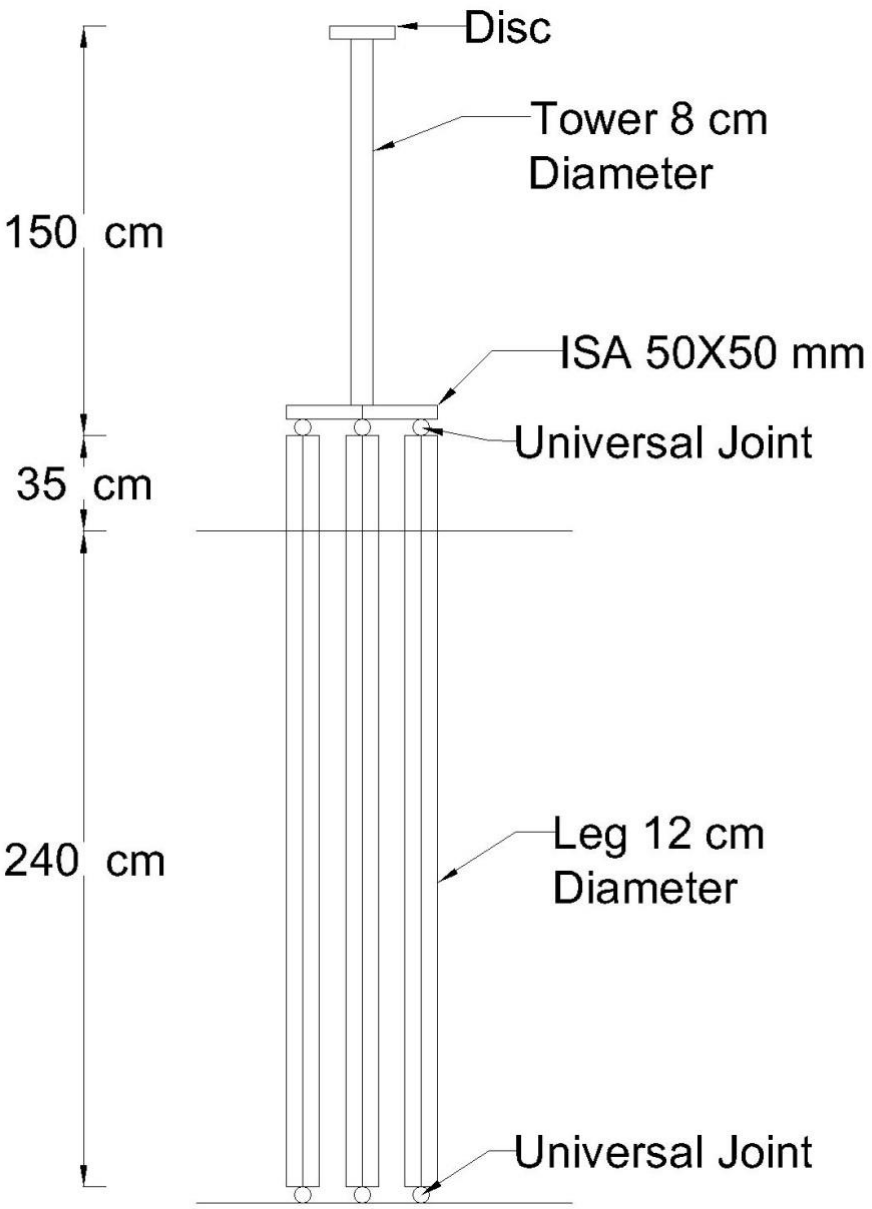

(a) Elevation

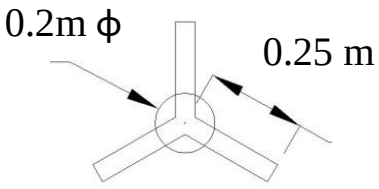

(b) Plan

Fig. 4.1 Details of Model (Three Legged Articulated Wind Tower - Scale 1:60)

Table 4.1 Properties of Scaled Model

Total mass of the structure	52 kg
Mass of nacelle assembly	1.620 kg
Draft	2.40 m
Height above SWL	1.85 m
Displacement	83.09 kg
Diameter of tower legs	0.12 m
Diameter of upper tower	0.08 m

Table 4.2 Mass distribution of Model

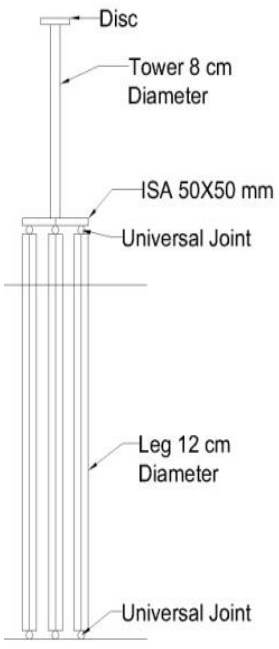

Description	Mass (kg)
Steel disc	1.62
Tower – 80 mm diameter, 4 mm thick acrylic tube	1.9
Tower base -200 mm diameter, 20 mm thick acrylic plate and three spokes ISA 50 mm × 50 mm, 250 mm length	4.84
Three legs - each 120 mm diameter and 5 mm thick	19.48
Ballast - steel rods 50 mm diameter, 500 mm length	23.96

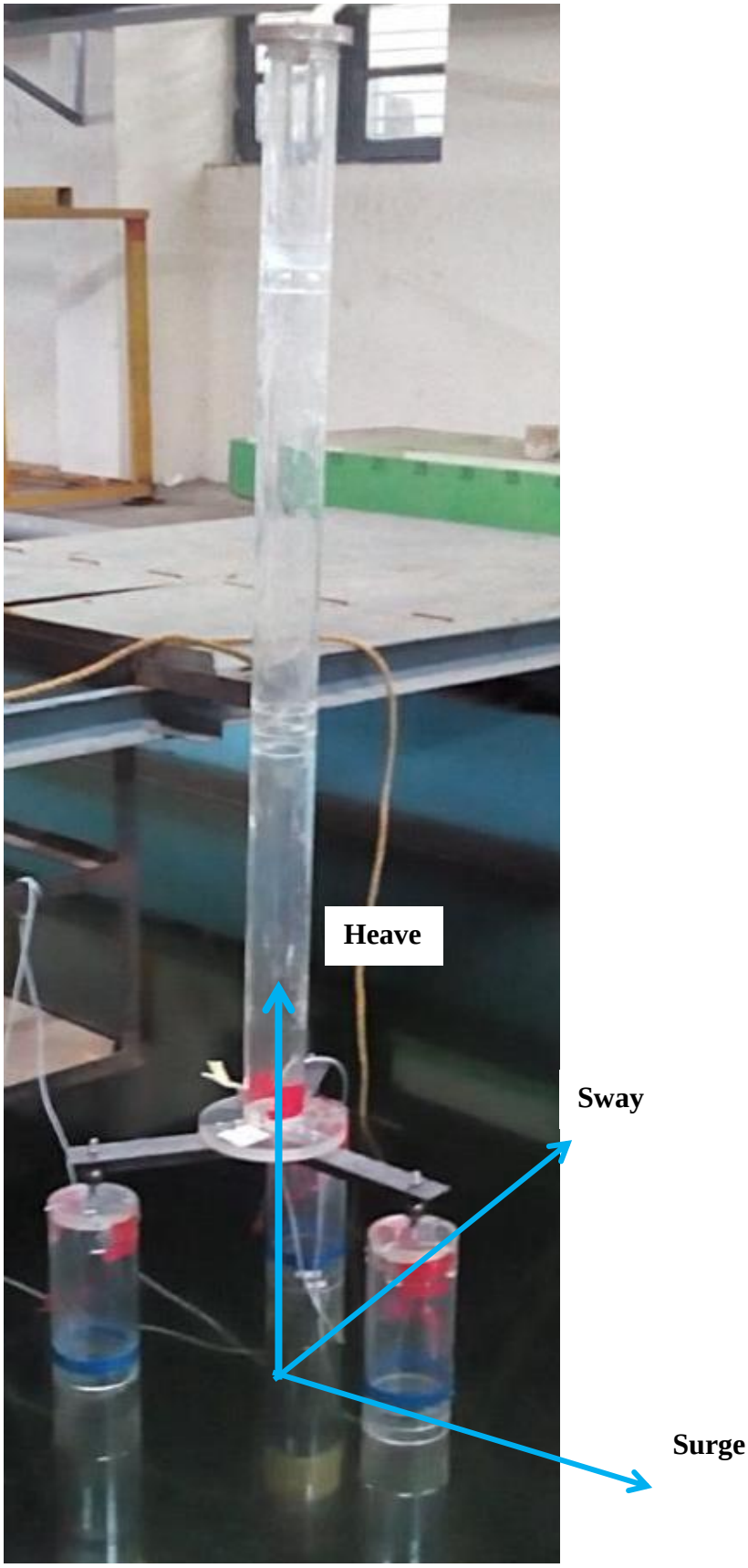

Fig. 4.2 Model (Scale 1:60) showing coordinate system

4.3 TEST FACILITY

The tests are performed in the 85 m long, 4 m wide and 3 m deep wave flume with 2.4 m water depth at the Department of Ocean Engineering, IIT Madras. The flume is fitted at one end with a dual hinged flap type wave maker (Fig.4.3) that can produce both regular and random waves (unidirectional) and a sloping rubble beach wave absorber at the other end. Fig. 4.4a, 4.4b and 4.4c show the three views of the test set up in wave flume.

Fig.4.3 Wave flume with wave maker

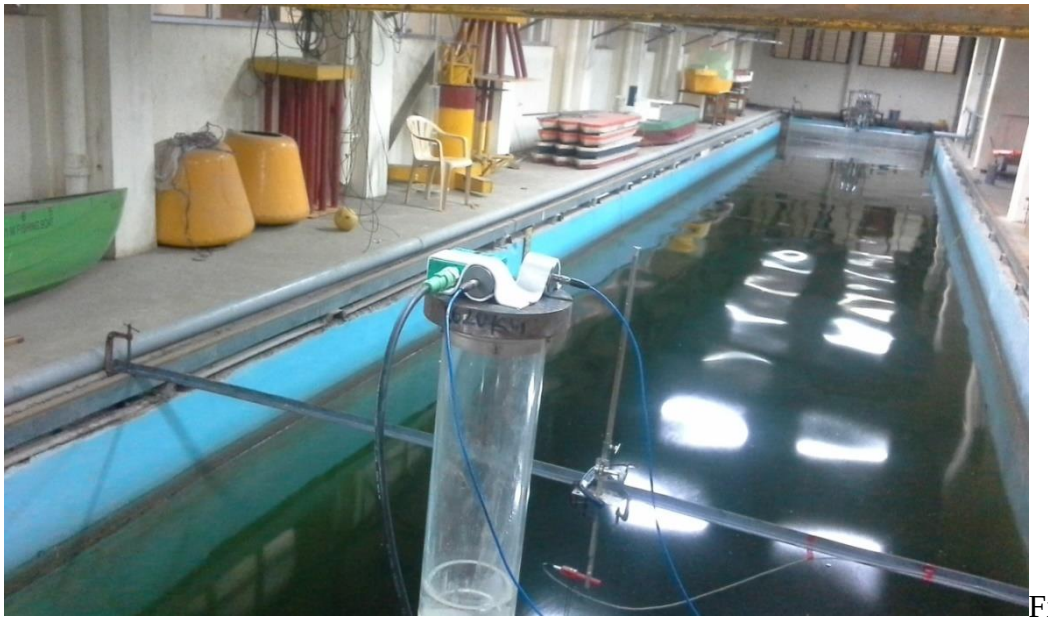

Fig. 4.4(a) Model in wave flume

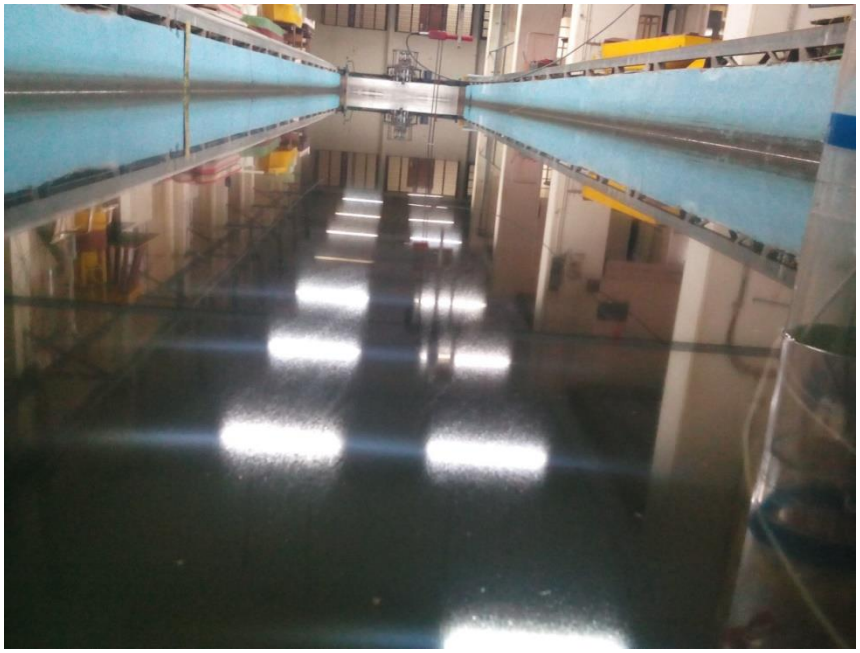

Fig. 4.4(b) Model in wave flume

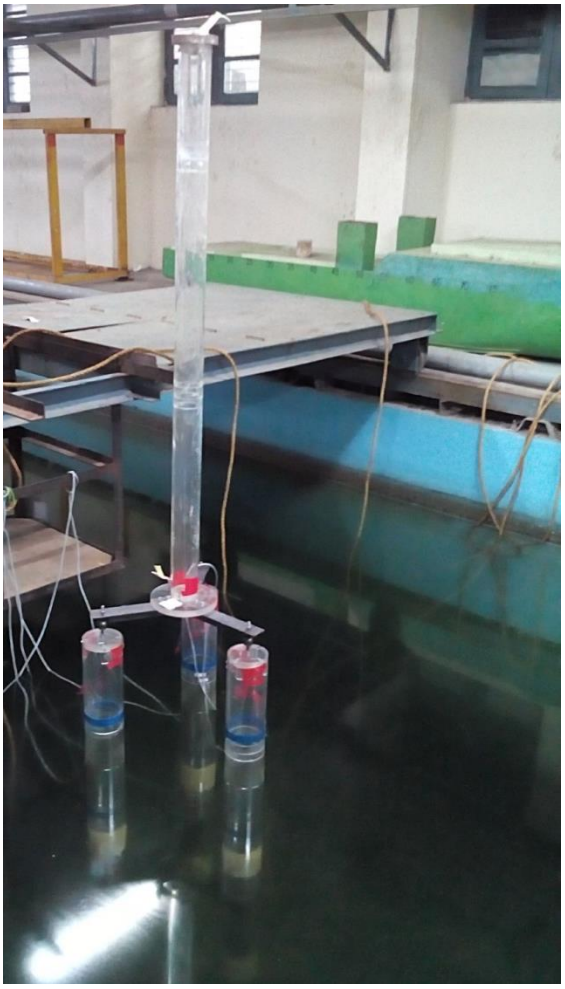

Fig. 4.4(c) Model in wave flume

4.4 INSTRUMENTATION

For the experimental investigation, the wave surface elevation, and the corresponding motion response in surge, sway, pitch and roll degrees of freedom are recorded with the help of suitable instruments. The details of these instruments are presented here. The wave probe is used for measuring wave elevation, accelerometers are used for the measurement of surge and sway motion responses and a dual axis inclinometer for the pitch and roll responses. Model with instrumentation is shown in Fig. 4.5

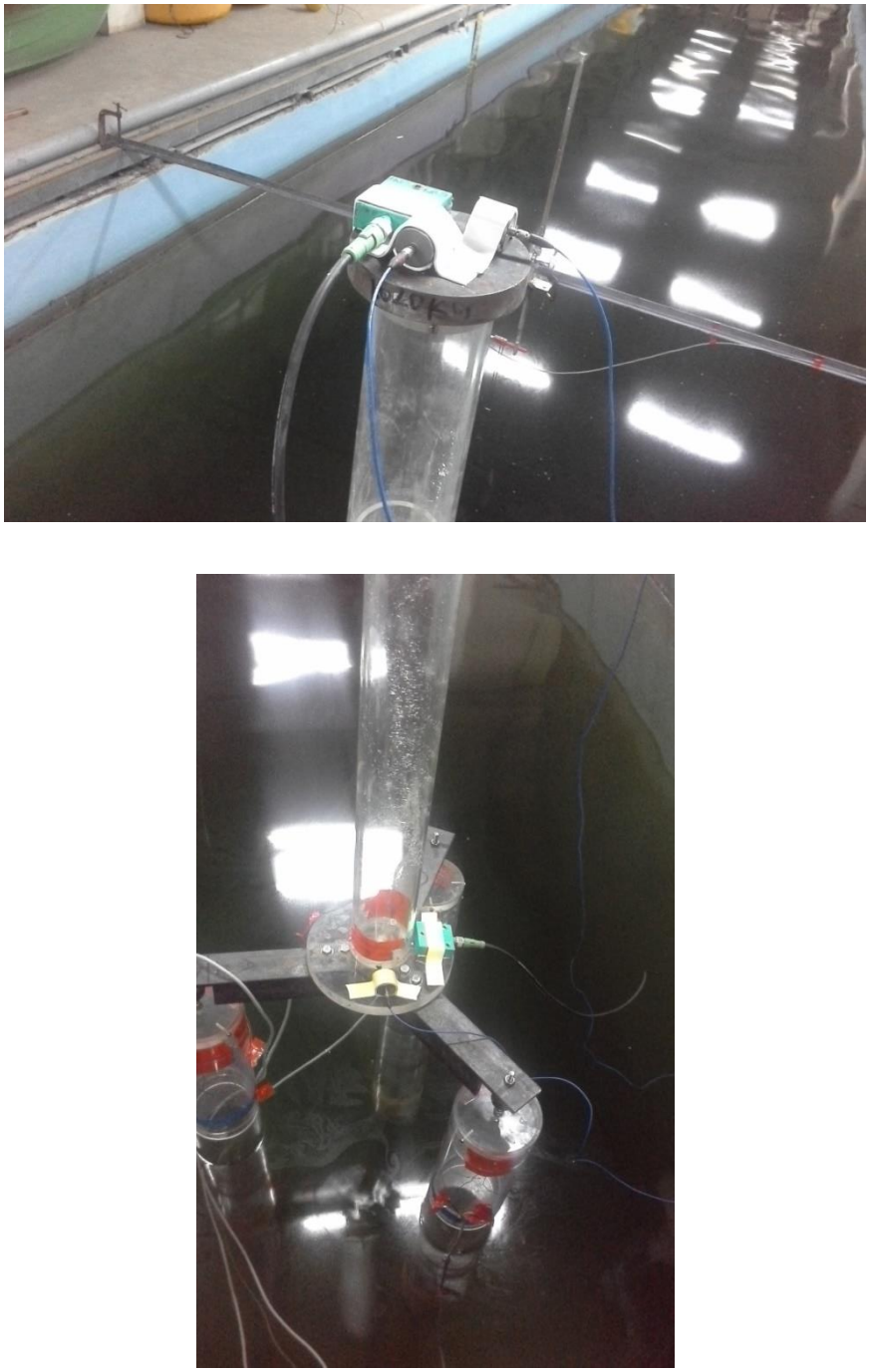

Fig. 4.5 Model with instrumentation

4.4.1 Wave Probe

The wave surface elevation in front of the model is measured by a wave probe shown in Fig. 4.6. A conductivity type wave gauge along with a wave meter is used to measure the wave elevations. The measuring range of the wave probe is 0 to 500mm with an accuracy of 1mm. The wave gauge consists of two thin, stainless steel electrodes placed parallel. When immersed in water, the meter measures the conductivity based on the instantaneous water volume between the two electrodes. The calibration of the wave probe is carried out by lowering and raising the probe all along a known depth of immersion in still water, and recording the changes in the corresponding voltages. The calibration curve plotted is shown in Fig. 4.7.

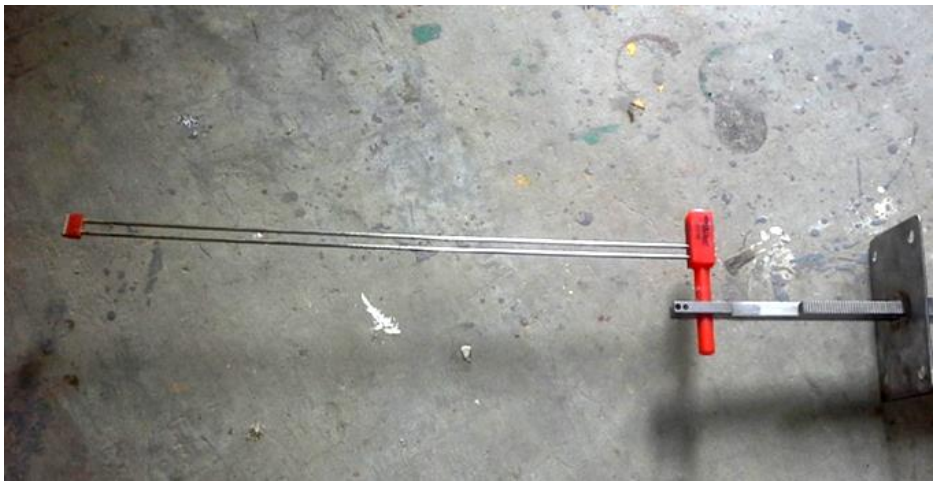

Fig. 4.6 Wave probe

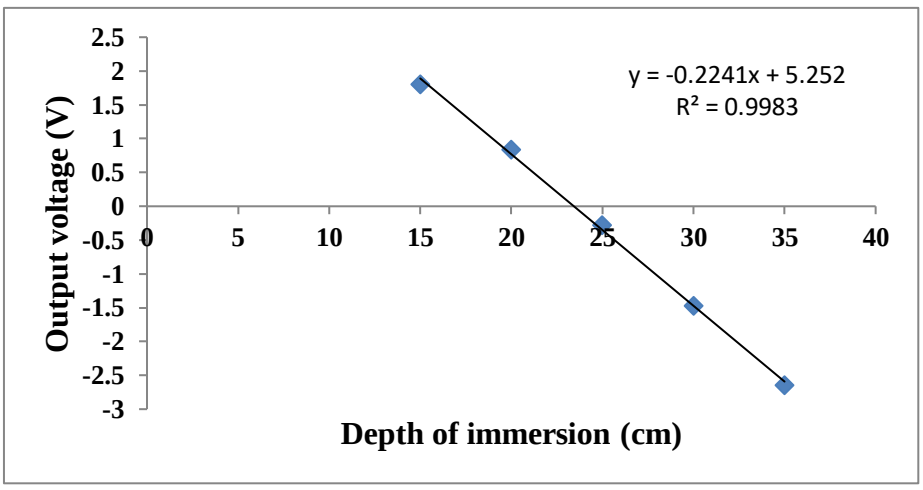

Fig. 4.7 Calibration plot for wave probe

4.4.2 Accelerometer

A single axis, piezoelectric accelerometers (sensitivity 1000 mV/g) is used to measure the surge and sway motion response. Fig. 4.8 shows the accelerometer utilised for measuring the response. The voltage fluctuation is converted to acceleration by using the calibration constant furnished by the manufacturer. The signal from the accelerometer is fed into to the spider 8 (data acquisition system) through a three channel sensor signal conditioner.

Fig. 4.8 Accelerometer

4.4.3 Inclinometer

A Dual axis inclinometer with an accuracy of 0.1^0 is used to measure the pitch and roll motion response. The maximum range of inclinometer is $\pm 80^0$. For calibration, the inclinometer is kept on the movable arm of the calibration set-up and turning the arm from –80˚ to +80˚ and at every 10^0 interval, the output voltages are noted. The

inclinometer used and calibration set up are shown in Fig. 4.9 and Fig. 4.10 respectively. The calibration curve for inclinometer is shown in Fig. 4.11. The calibration constant is arrived as one volt equal to 40^0.

Fig. 4.9 Inclinometer

Fig. 4.10 Calibration set up

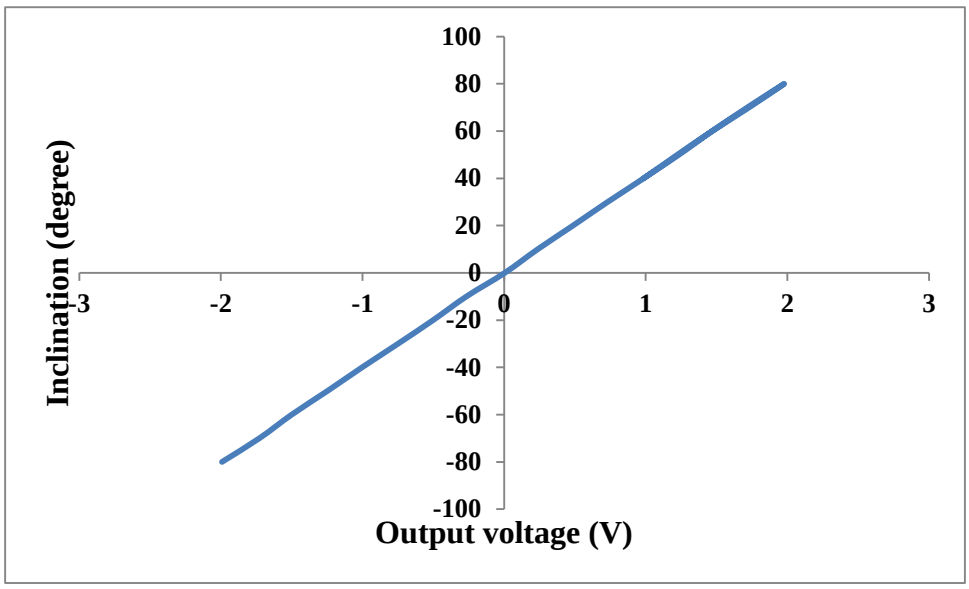

Fig. 4.11 Calibration curve for inclinometer

4.4.4 Data Acquisition System

The data acquisition is done using Holtinger Baldwin Messtechnik (HBM) Spider-8. It is an electronic multi-channel PC measuring device for real time data acquisition. The signal from the wave probe is conditioned and amplified by the wave meter and fed forward to the data acquisition system. The signal from the inclinometer and accelerometers are also connected to the different channels of Spider-8 data acquisition system. The Spider-8 is connected to a PC with Catman software using which the output is recorded as needed. The data acquisition system is capable of sampling rates between 25 Hz. and 2500 Hz. 50 Hz is fixed as sampling rate for the measurement of motions. The block diagram for the data acquisition scheme is shown in Fig. 4.12. Fig. 4.13 shows the data acquisition set up.

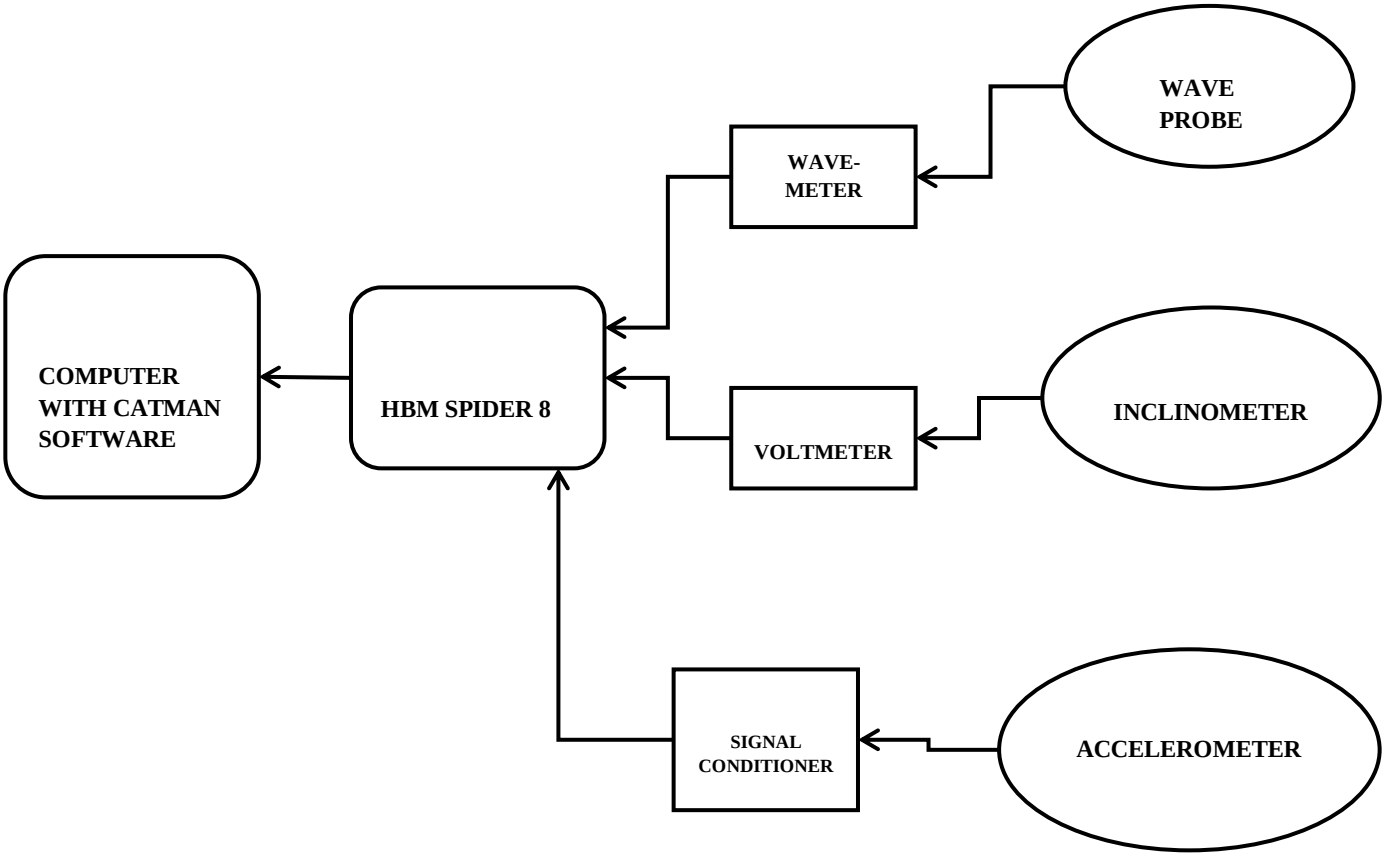

Fig. 4.12 Block diagram showing data acquisition scheme

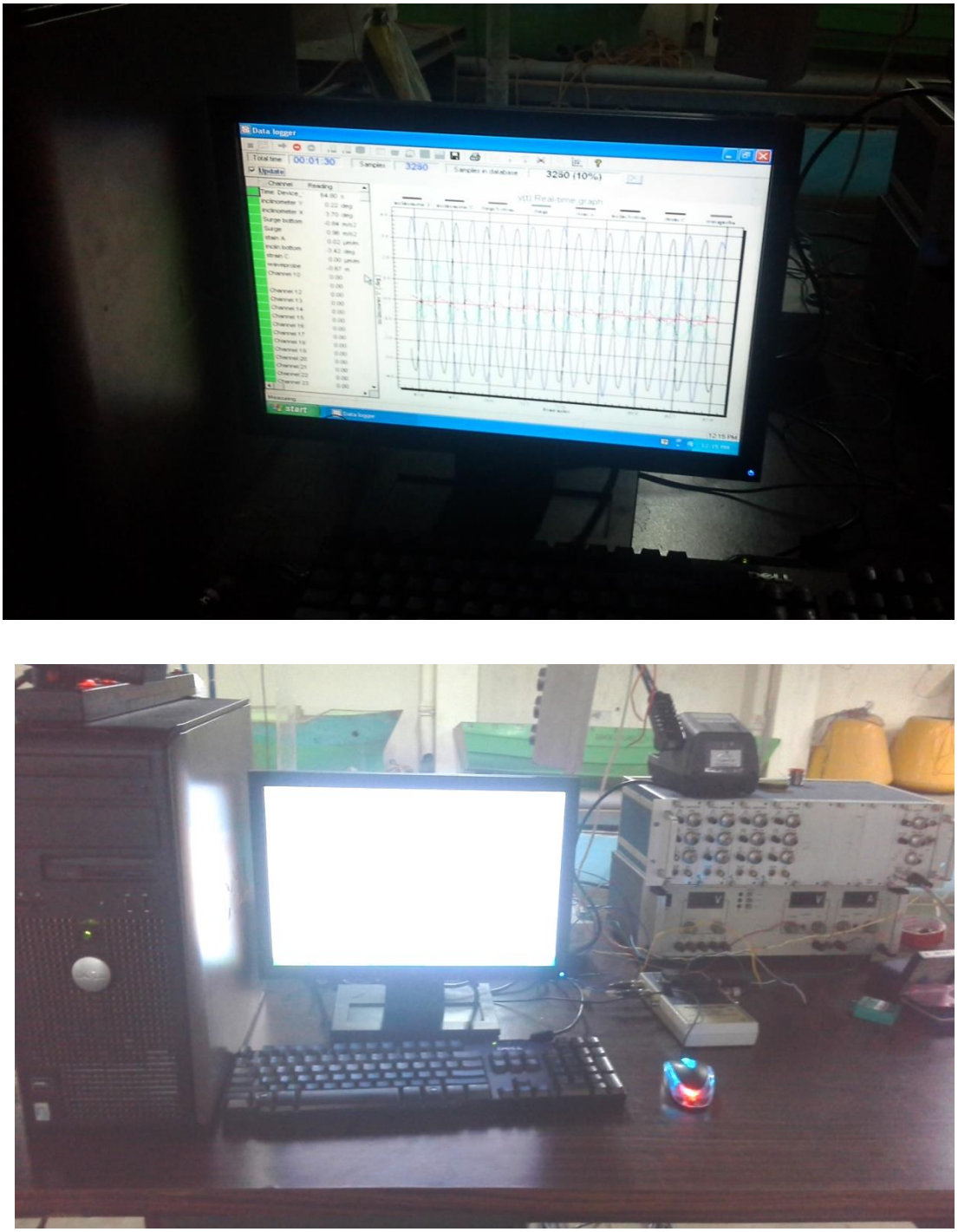

Fig. 4.13 Data acquisition set up

4.5 FREE VIBRATION TEST

Free vibration tests are conducted to determine the natural periods. The tests are conducted in still water by giving displacement in the respective degree of freedom and releasing it suddenly. The response is recorded as time series and shown in Fig. 4.14 and Fig. 4.15. From the plot of response amplitude decay, the natural frequency

is computed. Pitch and surge are fully coupled as sway and roll. Natural period of the structure is 5.5s and 5.36s for surge and sway respectively.

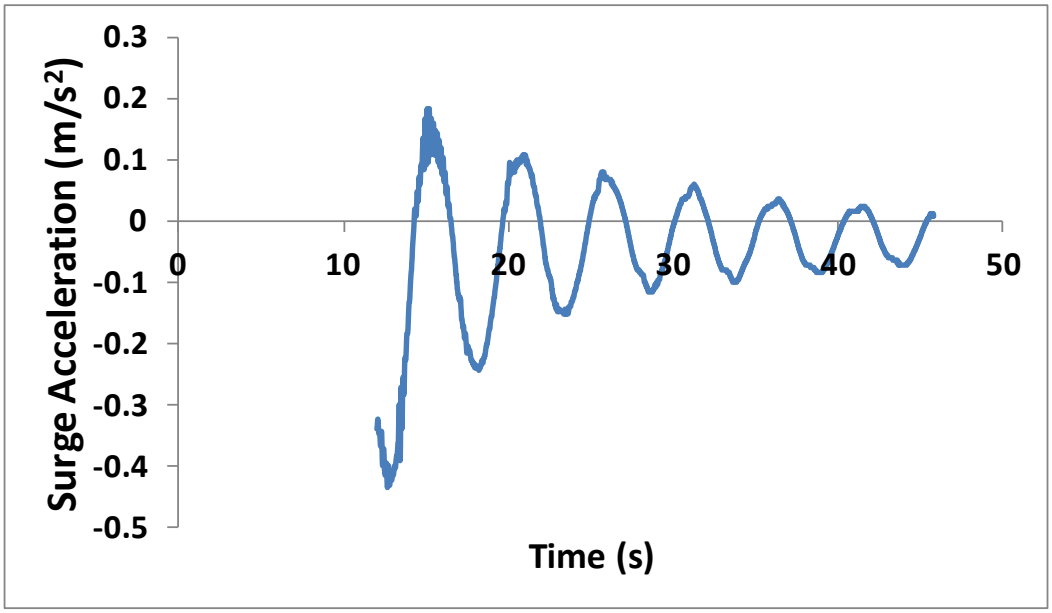

Fig. 4.14 Time history of surge free decay

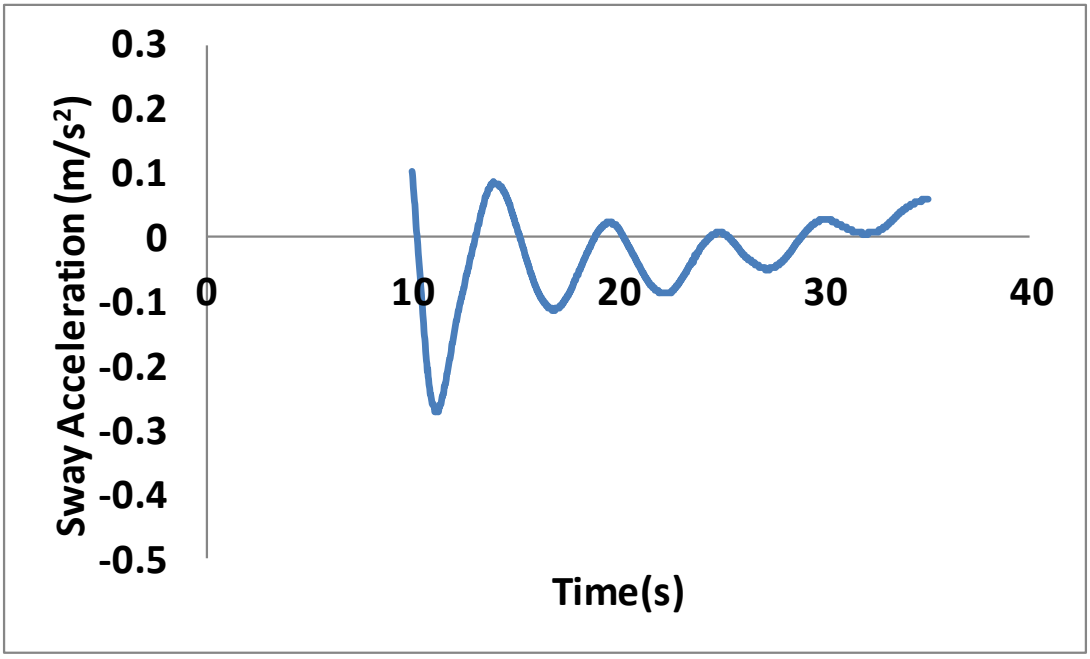

Fig. 4.15 Time history of sway free decay

4.6 TESTING IN REGULAR WAVES

For the experimental study, the model is placed in the wave flume. The wave probe is positioned near to the model to record the surface elevation of the incident wave. Understanding of the system behavior in an environment of controlled wave height and frequency is accomplished with the help of regular waves. Testing is performed for a wave period ranging from 1s to 2.75s at an interval of 0.25s for three wave heights 8cm, 10cm and 12cm, and for three orientations of the platform (0^0, 90^0 and 180^0) so that the wave hits at 0^0, 90^0 and 180^0 on the platform. The plan showing the 0^0 wave direction is shown in Fig. 4.16. Measurements and recordings for the motion response surge, sway, pitch and roll have been done at two locations - the nacelle and the tower base. Fig. 4.17 presents two views of the model under wave action. With the help of a data acquisition system, the responses from wave probe, inclinometer and accelerometers are simultaneously recorded as time series for duration of 50-60 sec. Typical measured records of time histories of wave surface elevation and related surge, sway, pitch and roll responses corresponding to 0^0 wave direction are shown in Fig. 4.18. The responses of the surge and pitch are significant whereas the response of the sway and roll of the structure is found to be close to zero when the wave hits at zero degree.

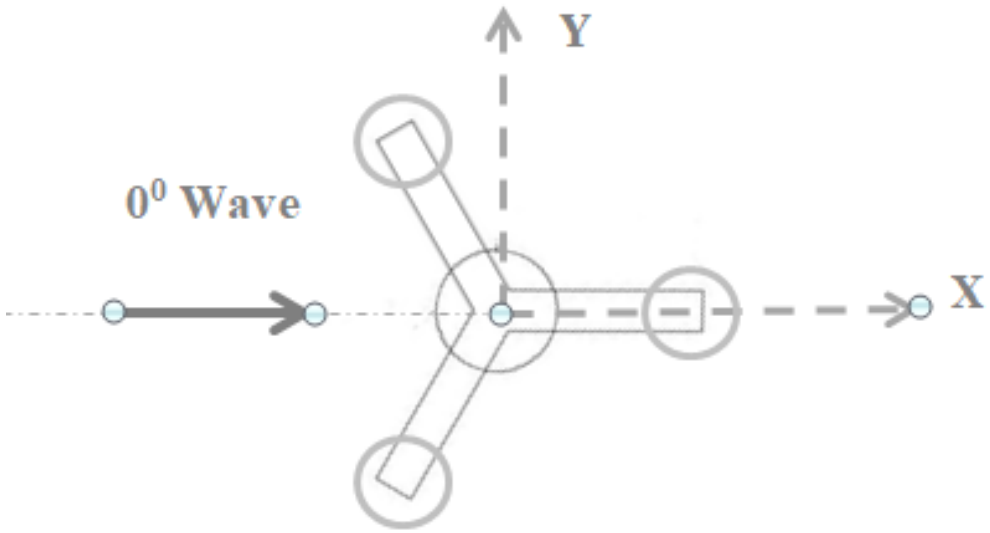

Fig. 4.16 Plan showing the 0^0wave direction

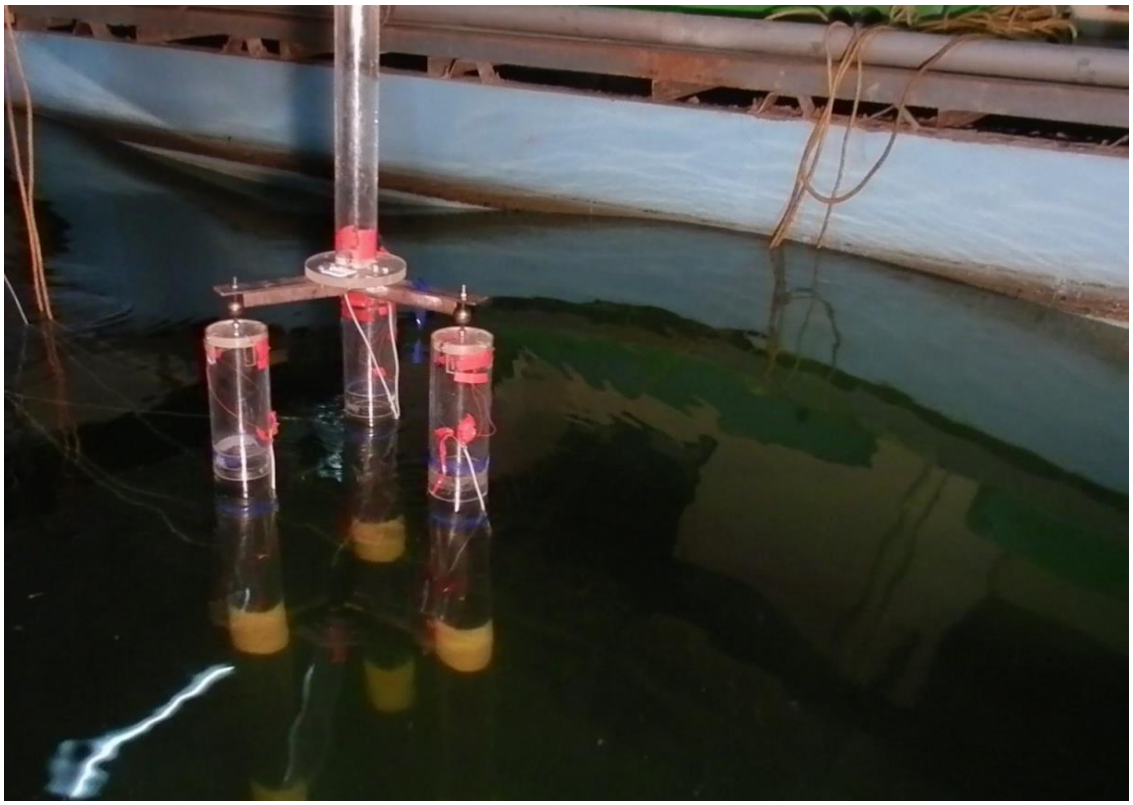

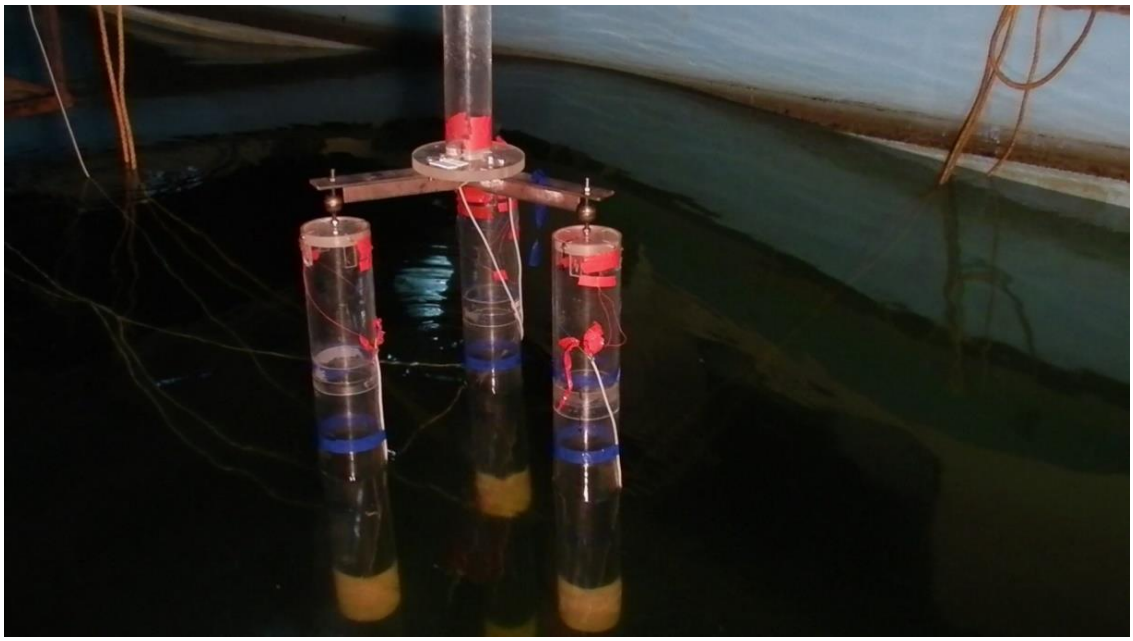

Fig. 4.17 Model under wave action

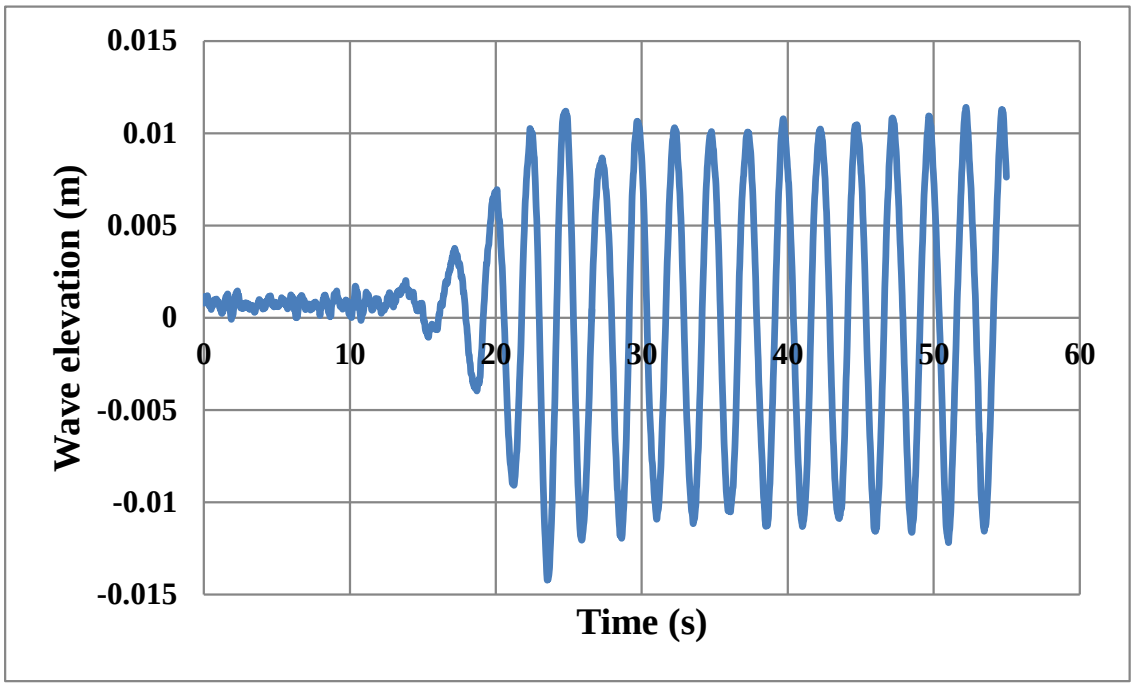

Fig. 4.18 (a) Time history of wave elevation

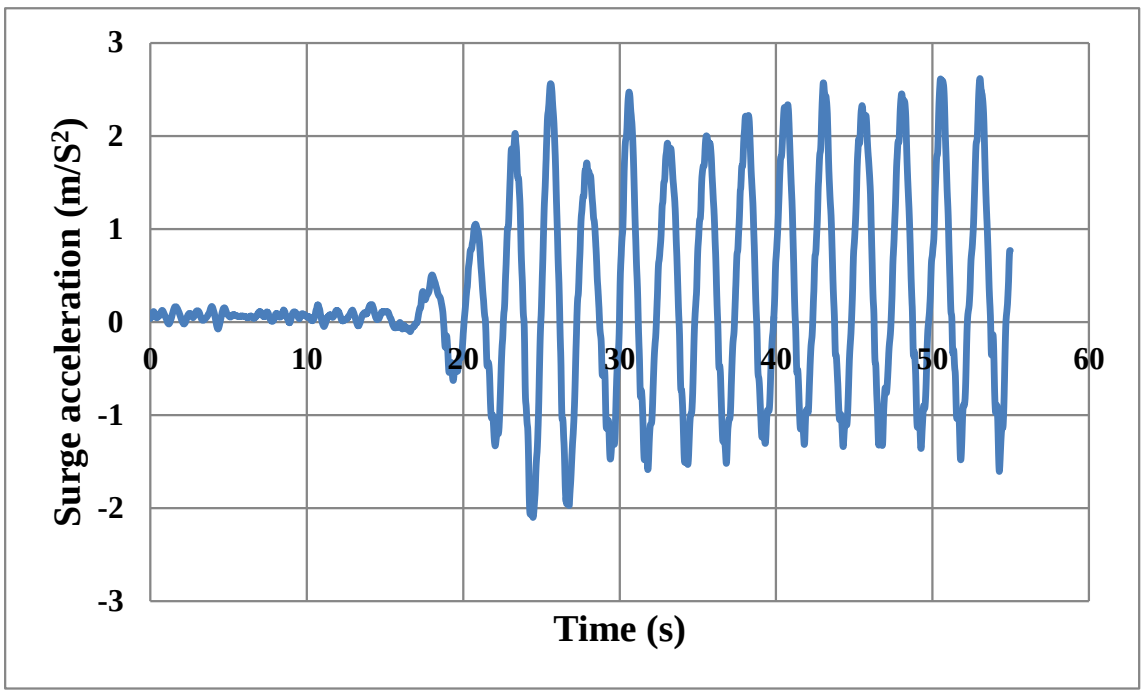

Fig. 4.18 (b) Time history of surge acceleration

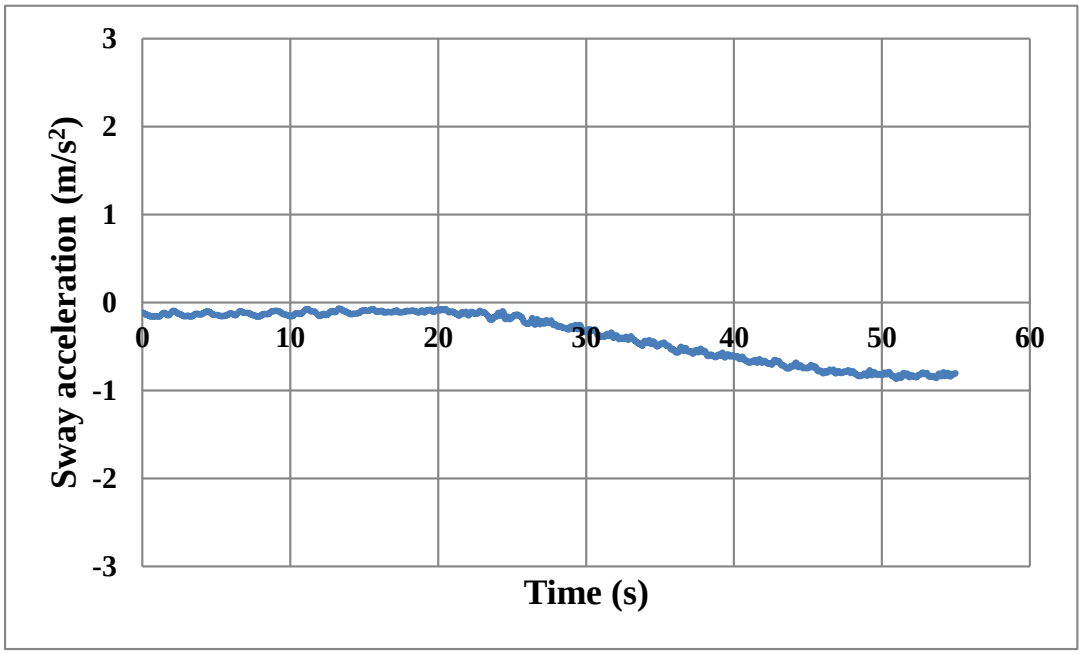

Fig. 4.18 (c) Time history of sway acceleration

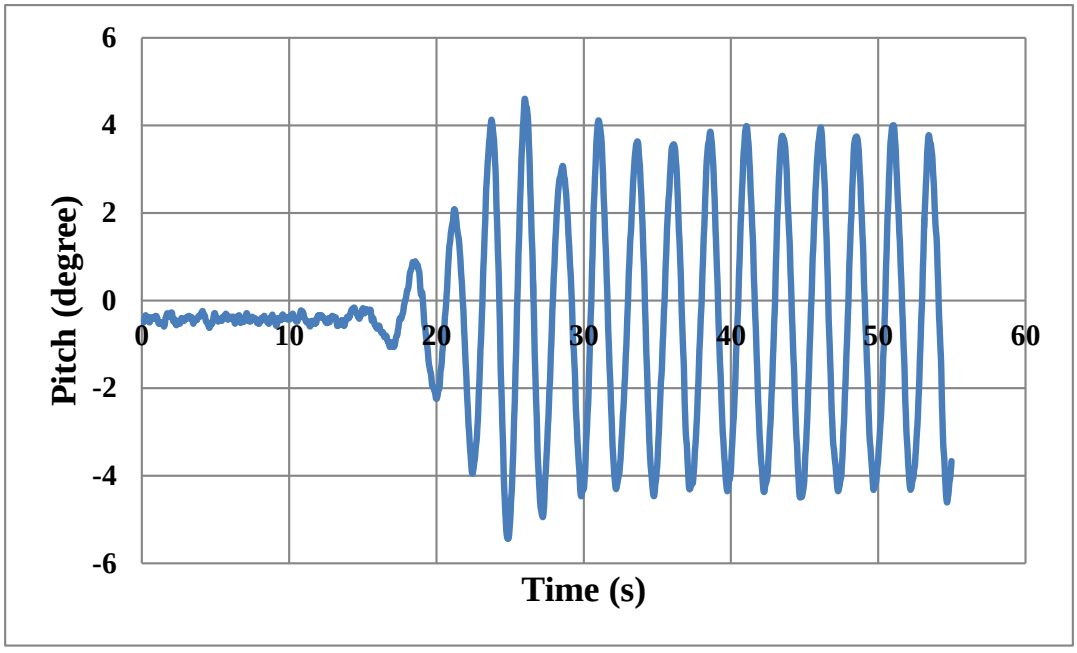

Fig. 4.18 (d) Time history of pitch response

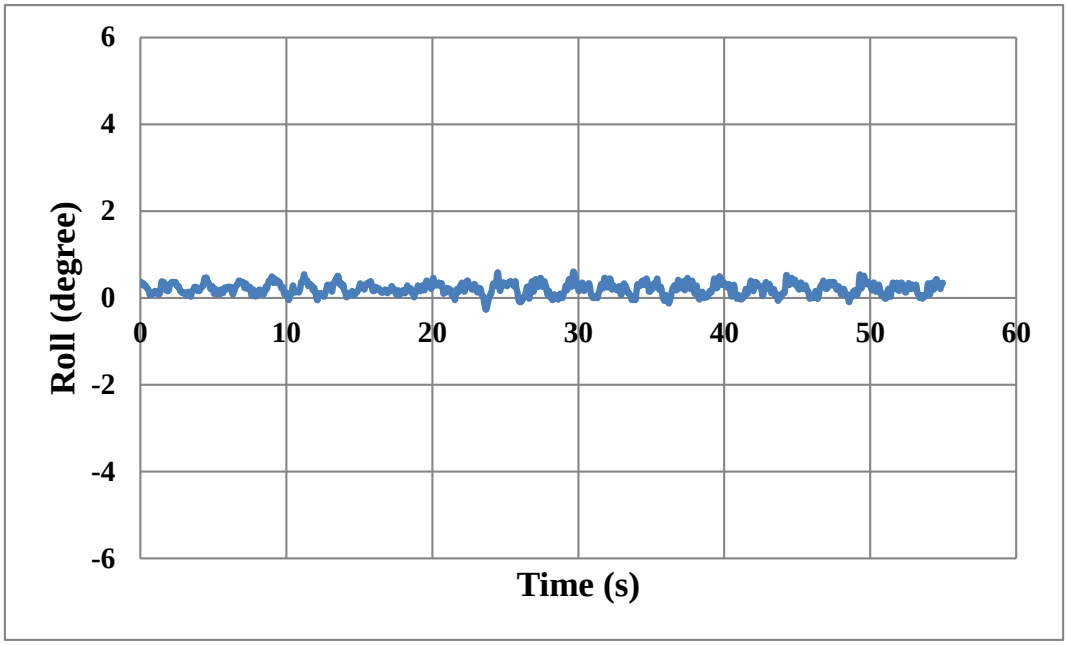

Fig. 4.18 (e) Time history of roll response

For regular waves, the amplitude of response is usually normalized with reference to the amplitude of incident wave. In the case of linear systems, these normalized responses are independent of the wave amplitude at a frequency and these are known as the Response Amplitude Operator (RAO) given by

$$RAO(f) = \frac{amplitude\ of\ response\ (f)}{amplitude\ of\ wave\ (f)}$$

RAO's are plotted for all data sets to normalise the results and study the general trend with regard to changes in wave amplitude and period. RAOs corresponding to the surge and pitch degrees of freedom of the model measured at the nacelle and bottom of the tower are shown in Fig. 4.19 and Fig. 4.20. Surge motion shows an excitation at the time period at which the pitch RAO is maximum. This indicates that there is a coupling between the surge and pitch motion. The responses of sway and roll are found to be close to zero as expected. The maximum pitch response for the highest wave given is found to be four degree. From the experimental observations it can be concluded that there exists a stable dynamic behaviour. This stable behaviour is mainly contributed by the presence of the universal joints. The joints provided at the top of the legs helps to maintain the top disc in a horizontal position while the structure is moving with the waves. The results indicate a stable dynamic behavior of the structure which implies that the design is feasible.

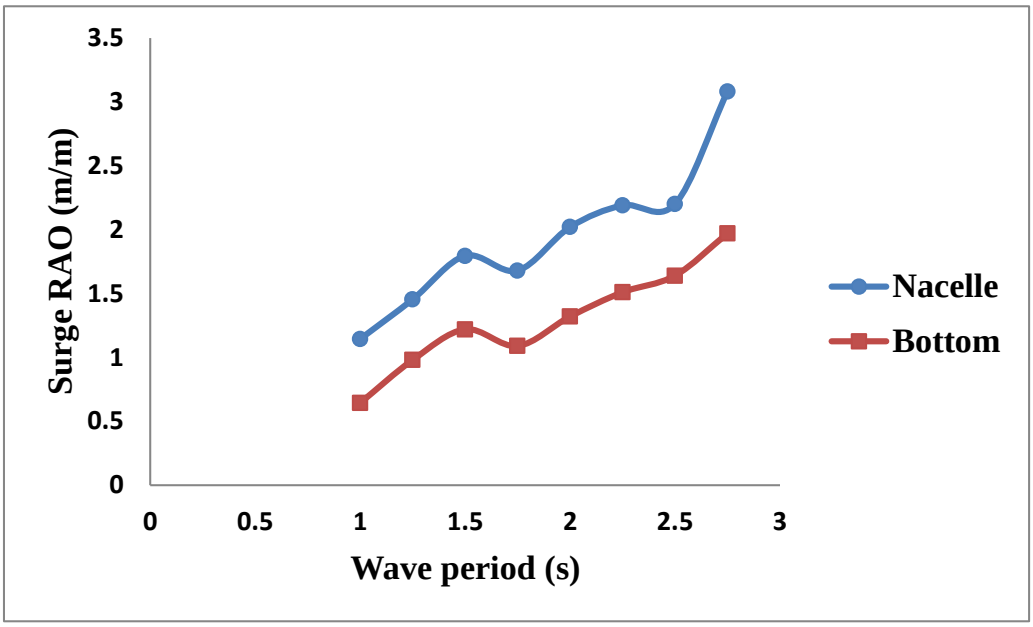

Fig. 4.19 Surge RAO at nacelle corresponding to 0^0 wave approach

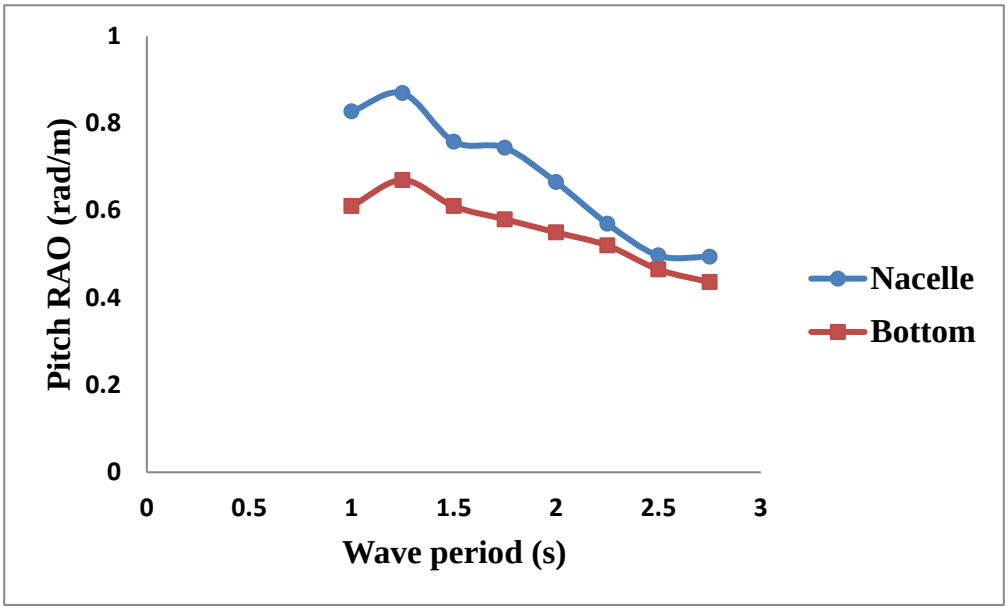

Fig. 4.20 Pitch RAO at nacelle corresponding to 0^0 wave approach

The motions are simultaneously measured at the nacelle and the bottom of the tower for 90^0 and 180^0 wave approach. Comparison between the motion at the nacelle and the tower bottom is shown in Fig. 4.21, Fig. 4.22, Fig. 4.23 and Fig. 4.24. The pitch at the base of the tower is due to the elastic deformation of the legs and bending of the three cantilever rackets connecting the tower to the legs. In addition to this there will be a small additional rotation at the nacelle due to the bending of the tower.

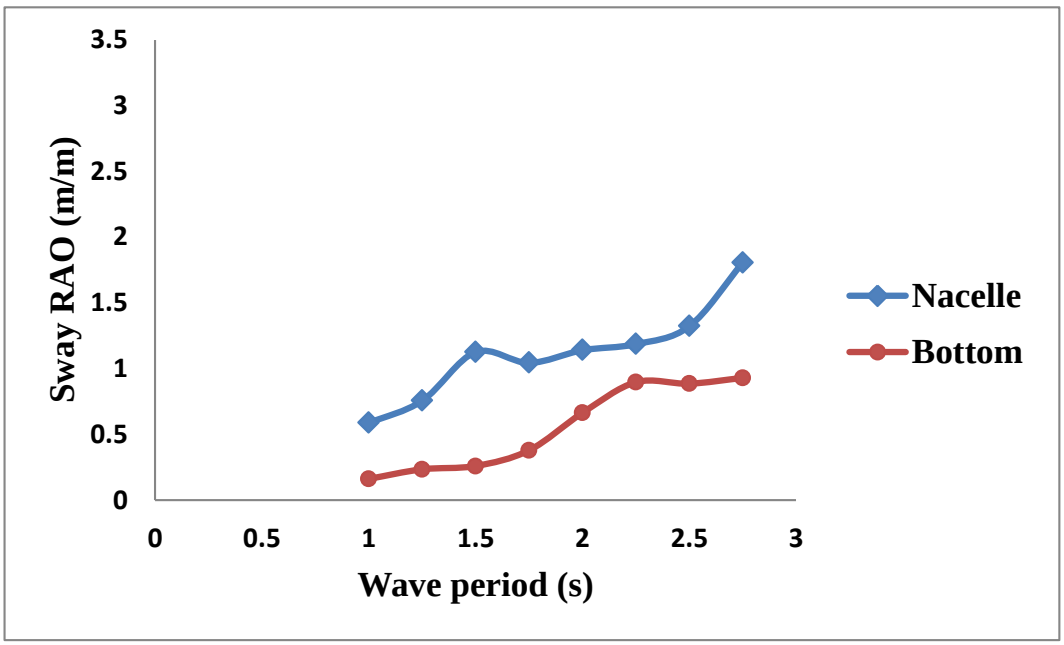

Fig. 4.21 Sway RAO at the nacelle and bottom corresponding to 90^0 wave approach

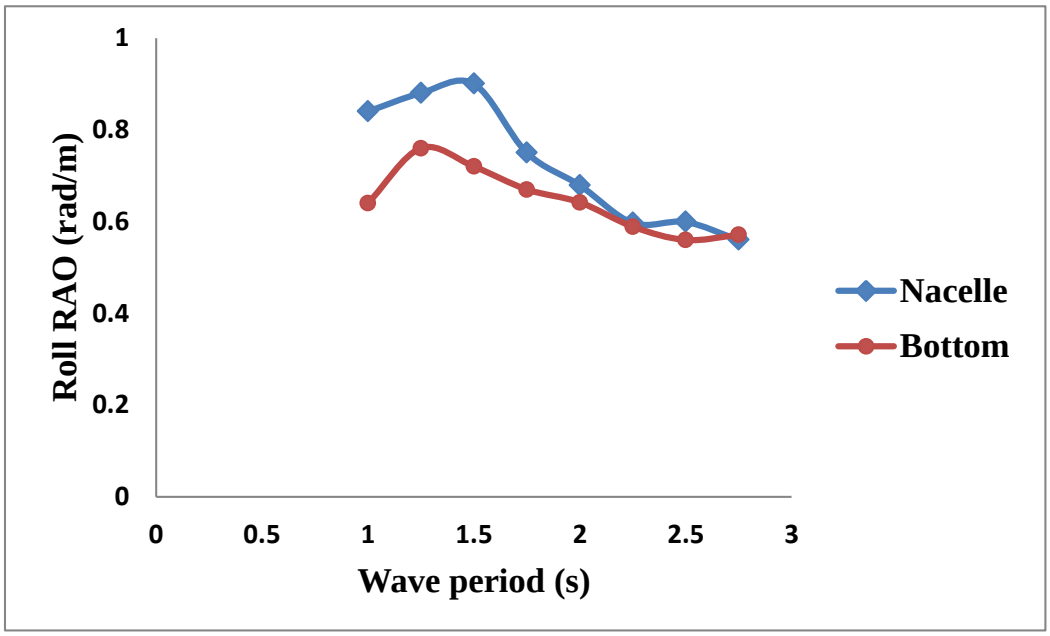

Fig. 4.22 Roll RAO at the nacelle and bottom corresponding to 90^0 wave approach

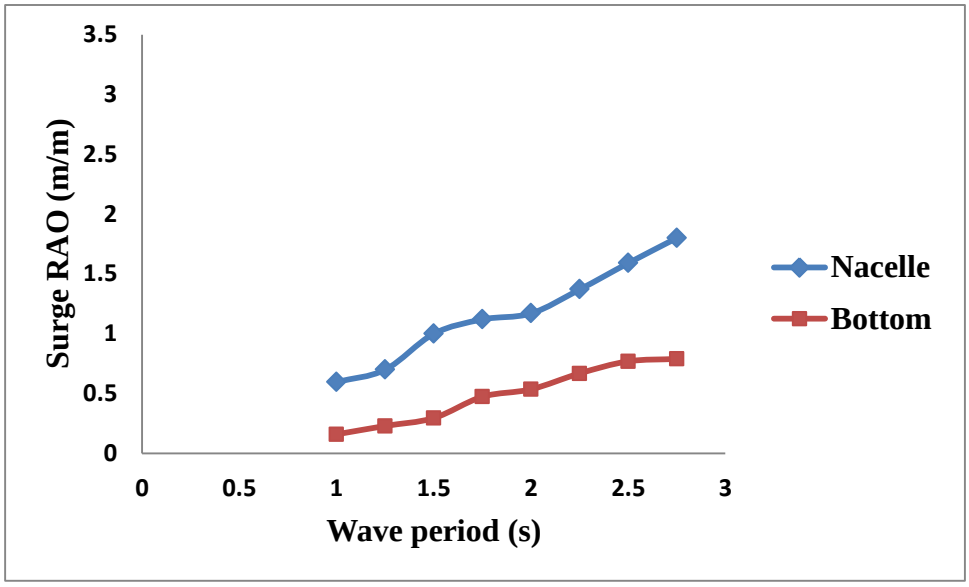

Fig. 4.23 Surge RAO at the nacelle and bottom corresponding to 180^0 wave approach

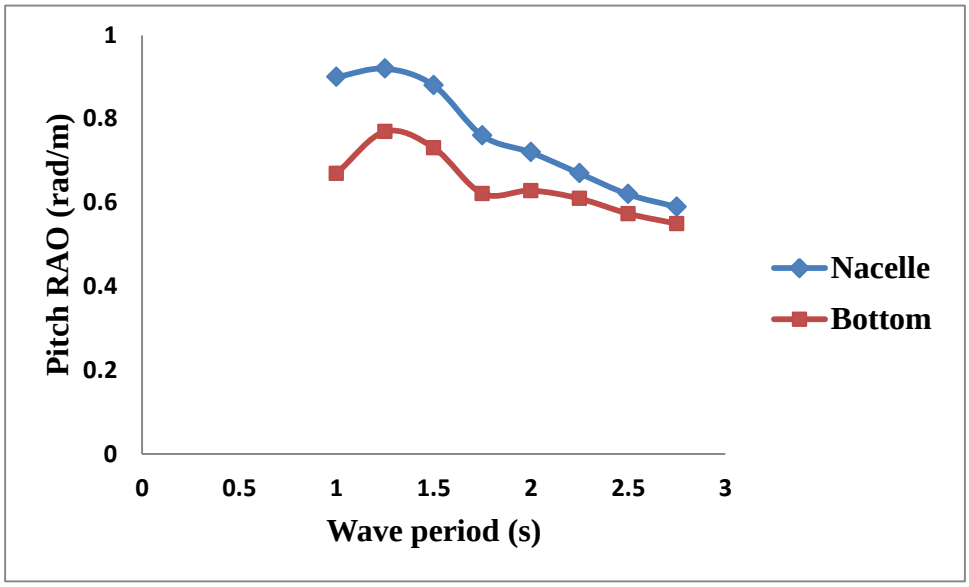

Fig. 4.24 Pitch RAO at the nacelle and bottom corresponding to 180^0 wave approach

The variation of motion response at the nacelle with the wave direction is shown in Fig. 4.25 and Fig. 4.26. To investigate the influence of wave height on the motion response surge acceleration at the nacelle for each wave height is plotted against the wave period and is shown in Fig. 4.27. The variation shows that the surge acceleration decreases with wave period.

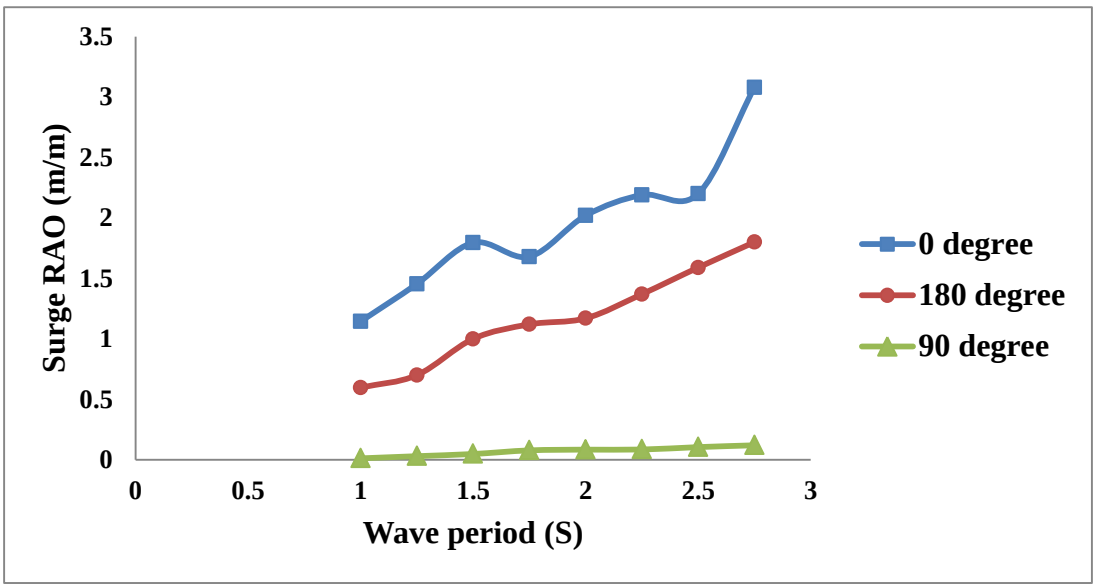

Fig. 4.25 Surge RAO corresponding to different platform orientation

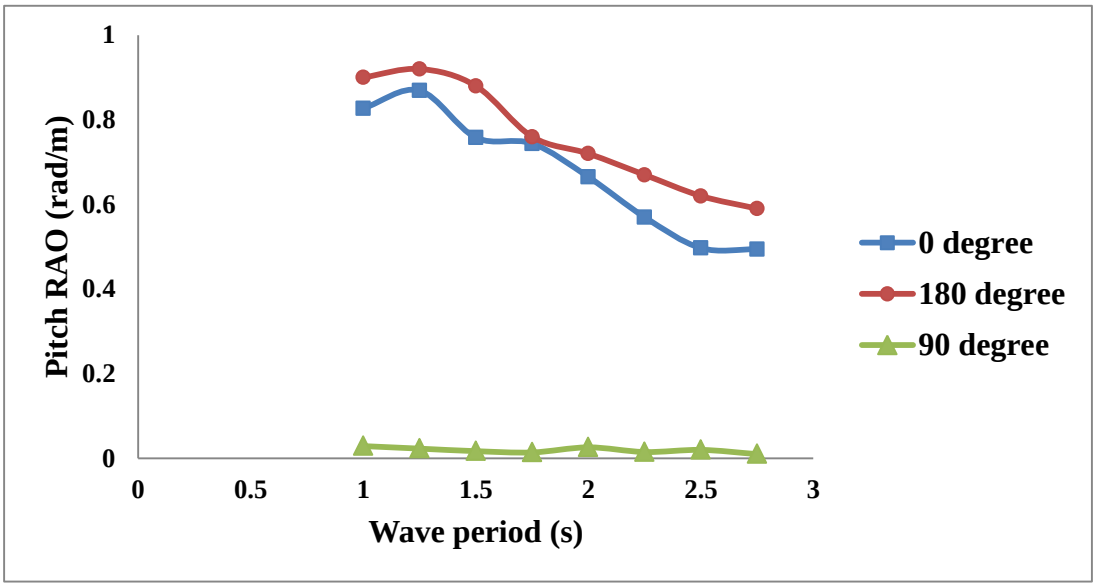

Fig. 4.26 Pitch RAO corresponding to different platform orientation

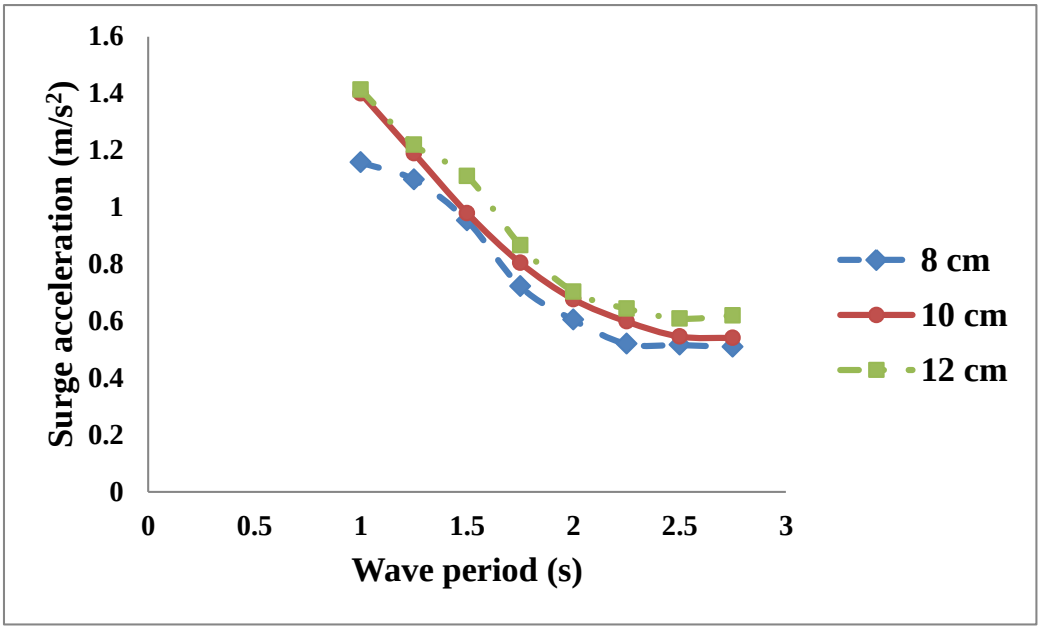

Fig. 4.27 Motion response with wave height

4.7 SUMMARY

Details of fabrication of the three-legged articulated wind tower model are presented. The measurement instrumentation and its calibration are described. The experiments on free oscillation studies also are discussed. Details of experiments on the motion response under regular waves and sample records of measured quantities are given. RAOs of responses are also presented.

CHAPTER 5

NUMERICAL INVESTIGATION ON SCALED MODEL

5.1 GENERAL

Ocean engineering problems which are very complex in nature can be modeled and solved efficiently and inexpensively by means of numerical simulations. In ocean engineering, for several years, the fluid structure interaction problems have been solved with some degree of approximation by numerical methods. In the recent past, these solutions have been proved to have attained acceptable precision. They must therefore be experimentally validated. In the present work, the motion response analysis of the scaled model of three legged articulated wind tower in the time domain is investigated using hydrodynamic software ANSYS AQWA. This type of analysis, alternatively called simulation, seeks motion response of the compliant structure in waves. This does not involve either material nonlinearity or large strains whereas geometric nonlinear behaviour involving large displacements and rotations are considered.

5.2 NUMERICAL MODELING

The numerical model of the scaled model of three-legged articulated platform with tower is developed using the software ANSYS AQWA so that the complexities that rise due to modeling the structure with six degrees of freedom can be controlled. This software package provides a toolset for studying the influence of various environmental forces on both floating and fixed offshore structures. AQWA can model hydrodynamic fluid wave loading on fixed and floating structures, by using three-dimensional diffraction theory or Morison's equation. AQWA can evaluate the equilibrium characteristics (static and dynamic stability) of moored or connected bodies subjected to environmental forces like wind, wave and current. The linearized drag due to Morison elements can also be simulated in ANSYS AQWA. This tool can produce a time history of the simulated motions of compliant platforms, connected by articulated joints, under the action of wave and wind forces.

As the characteristic dimension of the legs (D) is less than 0.2 times the wave length (L) for the considered waves then wave forces can be calculated using Morison equation. In order to model the Morison elements in the DesignModeler of ANSYS AQWA, TUBE elements are used. ANSYS DesignModeler is a tool for creating geometry for hydrodynamic analysis. The

geometric properties such as mass, the center of gravity and moment of inertia are given as separate inputs for articulated legs, beams and tower in ANSYS DesignModeler. The ballast weight is given as point mass in each leg. The details of leg and the point mass given on the leg are listed in the Table 5.1 and 5.2 respectively.

The tower is supported at the intersection of beams and the beams are connected to the legs by articulated joints. These articulated joints are modeled as the joint, which transfers only translational responses from articulated legs to the tower These articulated legs are connected to the seabed also by articulated joints.. The model of the joint used in the analysis is shown in the Fig. 5.1. The turbine weight is given as a point mass at the tower top. The input details of turbine point mass are given in the Table 5.3.

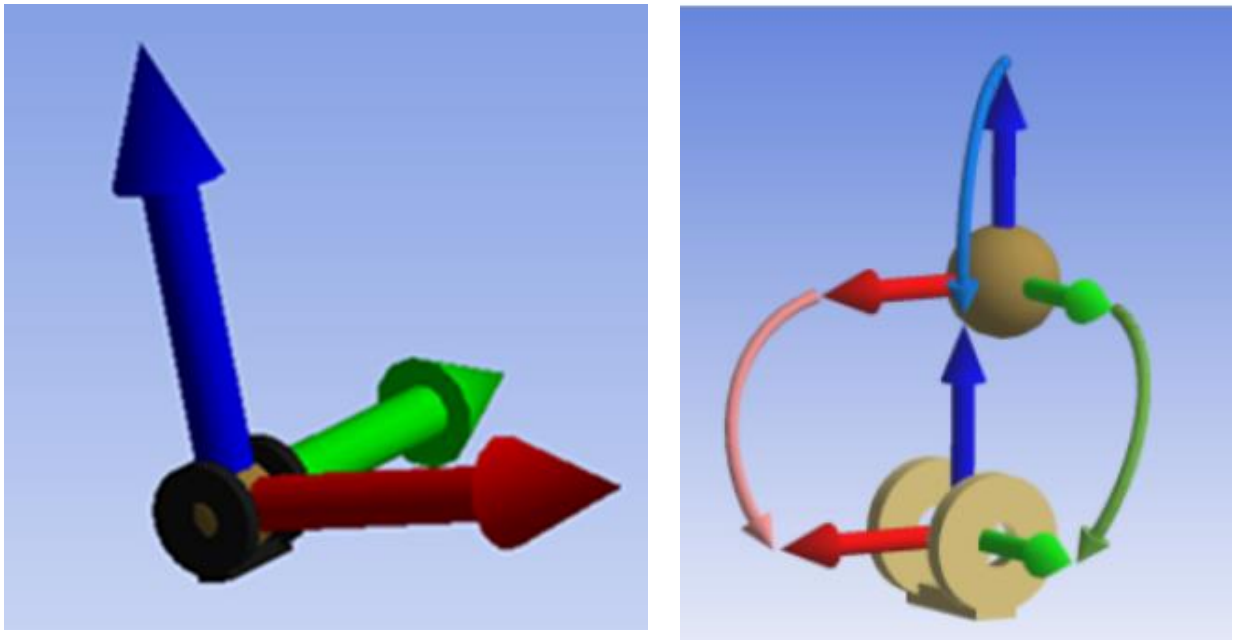

Fig. 5.1 Model of the joint

Table 5.1 Details of leg A

Body Visibility	Visible
Activity	Not Suppressed
Line Type	Tubular
Tube Type	Sealed
Tube End Discs	None
Diameter	0.12 m
Thickness	0.005 m
Material Density	1300 kg/m³
Mass	6.46 kg
X Position of Body COG	0.0 m
Y Position of Body COG	0.0 m
Z Position of Body COG	-1.025 m
Viscous Drag Coefficient	0.75
Added Mass Coefficient	1

Model generated in DesignModeler software is shown in Fig.5.2. The geometry is imported to ANSYS AQWA module where it is meshed and the details of point mass and joint details are given. The inertia and drag coefficients for the tube elements are given as 2.0 and 0.75 respectively. In ANSYS AQWA, the meshing is then carried out by program controlled optimum meshing. Since the articulated legs are given as tube elements, the meshing quality will not influence the accuracy of hydrodynamic properties of the model. Model imported into ANSYS AQWA Diffraction software is shown in Fig. 5.3. Generated numerical model of three-legged articulated platform with tower is shown in Fig.5.4.

Table 5.2 Details the point mass given on the leg A

Name	Point MassA
State	Fully Defined
Details of Point MassA	
Visibility	Not Visible
Activity	Not Suppressed
Mass Properties	
X	0.0 m
Y	0.0 m
Z	-2.15 m
Mass	10.0 kg
Inertia Properties	
Define Inertia Values By	Radius of Gyration
Kxx	0.125 m
Kyy	0.125 m
Kzz	0.177 m
Ixx	0.156 kg.m²
Ixy	0.0 kg.m²
Ixz	0.0 kg.m²
Iyy	0.156 kg.m²
Iyz	0.0 kg.m²
Izz	0.313 kg.m²

Table 5.3 Details of turbine point mass

Name	Point Mass top
State	Fully Defined
Visibility	Not Visible
Activity	Not Suppressed
Mass Properties	
X	0.125 m
Y	0.216 m
Z	1.85 m
Mass	1.62 kg

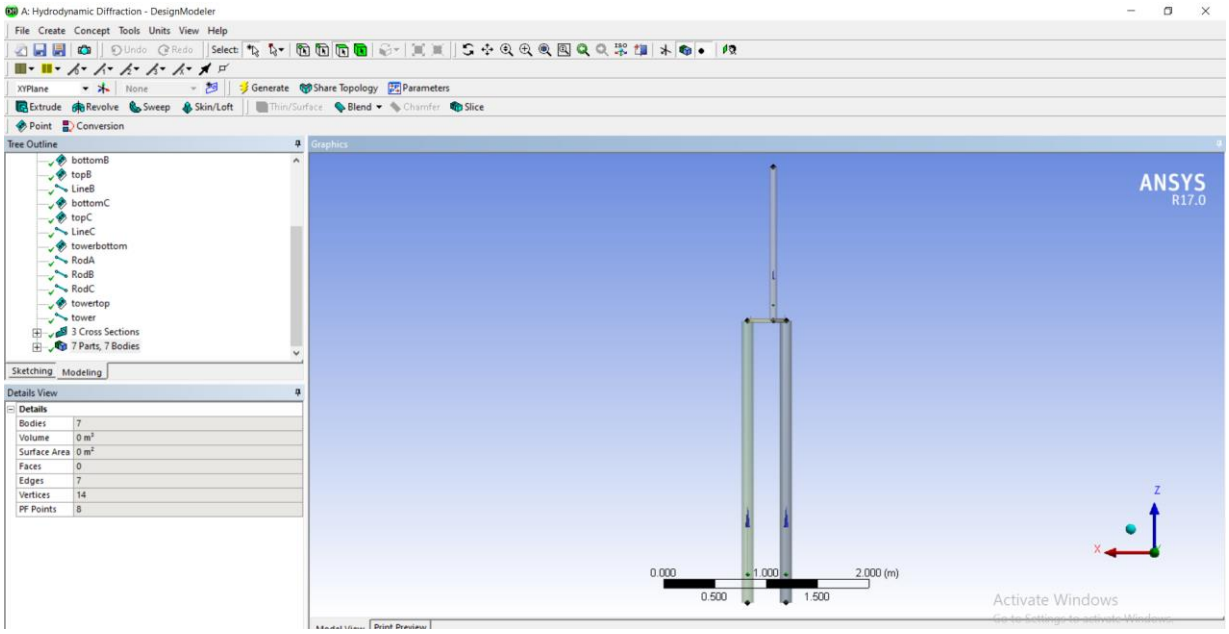

Fig.5.2 Geometry of Three- legged articulated platform in ANSYS DesignModeler software

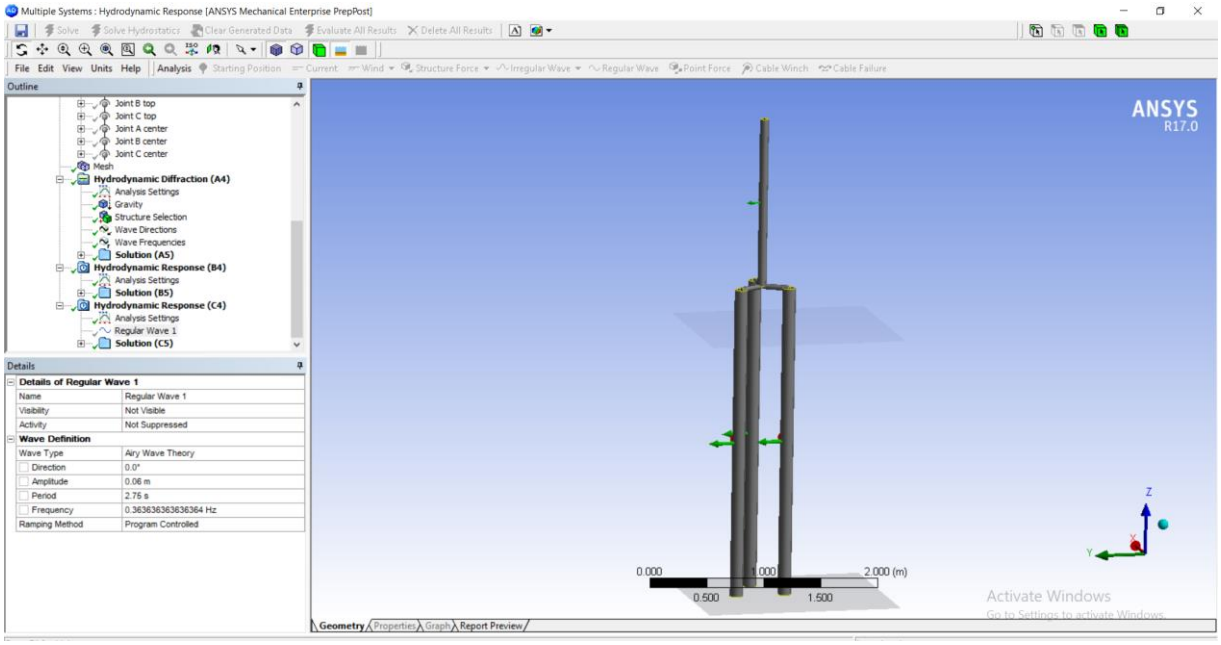

Fig.5.3 Model imported into ANSYS AQWA Diffraction software and meshed

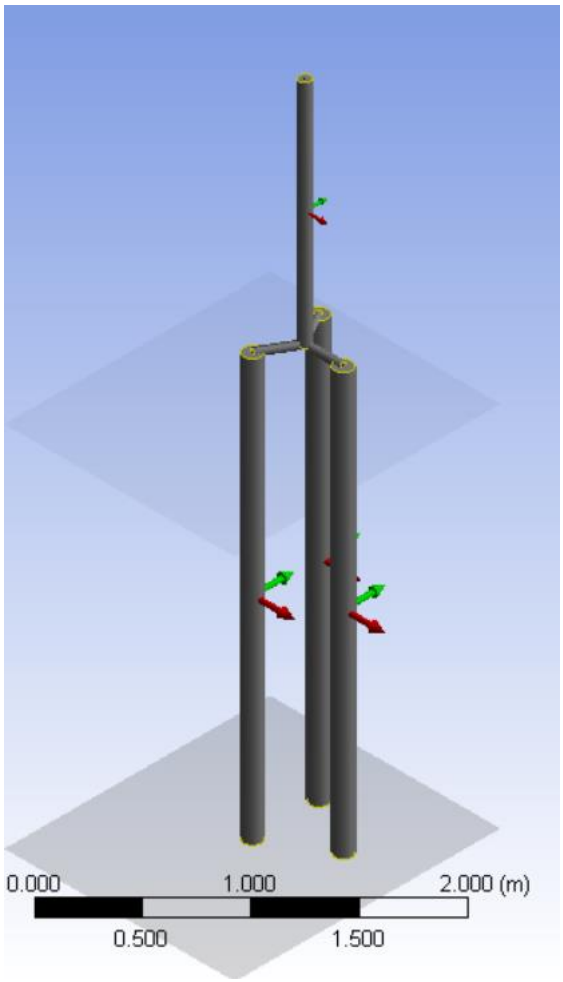

Fig.5.4 Generated model

5.3 VALIDATION STUDY

Free oscillation studies are conducted to assess the surge and sway natural periods. Natural periods determined experimentally for various degrees of freedom are verified with that of the numerical results from ANSYS. The natural periods obtained from numerical simulation are found slightly shorter than those obtained from experiments. The free oscillation results from the numerical simulation compared well with the experiment. The surge and sway natural periods variations are within 12% and 9% respectively as shown in Table 5.4.

Table 5.4 Free oscillation results

Description	Time period (s)	
	Experimental	Numerical
Surge	5.5	4.83
Sway	5.36	4.83

Numerical response analysis is performed on the model. The wave force acting on the articulated legs are computed with well-known Morison's formula. The drag coefficient for the tube elements is taken as 0.75 and the inertia coefficient is taken as 2. In ANSYS AQWA, the meshing is then executed using program controlled optimum meshing. Since the articulated legs are treated as slender elements, the accuracy of the hydrodynamic properties of the model is unaffected by the quality of meshing. Numerical analysis is then carried out by solving the equation of motion under wave loads. As the analysis continues the Morison force components are evaluated at each time step considering the effects of variation of immersion Equation of motion is solved at each time step by considering the variable submergence effect. A time step of 0.1 seconds is considered for the analysis.

The response $\{X\}$of the structure is computed by solving the equation of motion

$$[M]\{\ddot{X}\} + [C]\{\dot{X}\} + [K]\{X\} = \{F_{(t)}\} \ldots\ldots\ldots\ldots\ldots\ldots 5.1$$

where $[M]$, $[C]$ and $[K]$ are the total mass, damping and hydrostatic stiffness matrices of the three legged articulated platform. F is wave force, $\{\ddot{X}\}$ is the acceleration vector, $\{\dot{X}\}$ is the velocity vector and $\{X\}$is the displacement vector.

The water particle kinematics is calculated by Airy's wave theory for the calculation of hydrodynamic loads. The displacements and velocities of the platform are evaluated at each time step by integrating the accelerations due to the environmental forces in the time domain, by means of predictor-corrector numerical integration scheme. In the initial time step of the analysis, displacements, velocities and accelerations are assumed. Using these assumed values, restoring and damping forces are calculated and accelerations for the next time step is calculated by equating total force to inertia force. This process is repeated for all time steps.

Time history analyses are done in regular waves for 0^0, 90^0 and 180^0 wave directions and the motion responses are obtained. The plan showing the 0^0 wave direction is shown in Fig.5.5

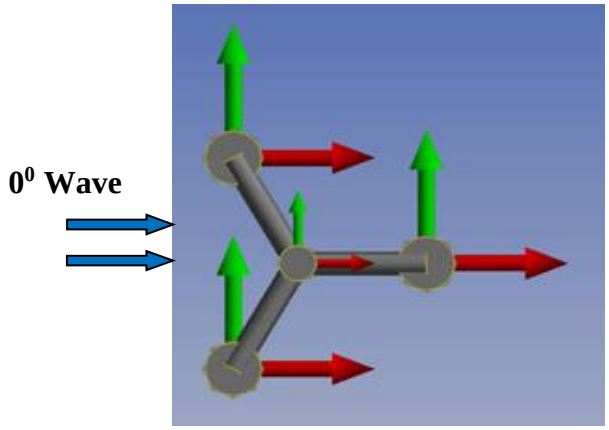

Fig.5.5 Plan showing the 0^0 wave direction

RAO's of the tower under regular wave for these wave directions are obtained in surge and pitch degree of freedom and compared with that of the experimental results. It is found that the surge motion dominates the other motions. The numerical simulations are validated against the experiments conducted and are demonstrated through favourable comparison of RAO in the predominant degree of freedom (surge).Deviation is noted in pitch response of the tower as numerical model is not able to predict the frictional resistance served by the articulated joint (Chandrasekaran and Madhuri, 2015). The RAO's obtained numerically and experimentally are compared in Fig. 5.6, 5.7 and 5.8.

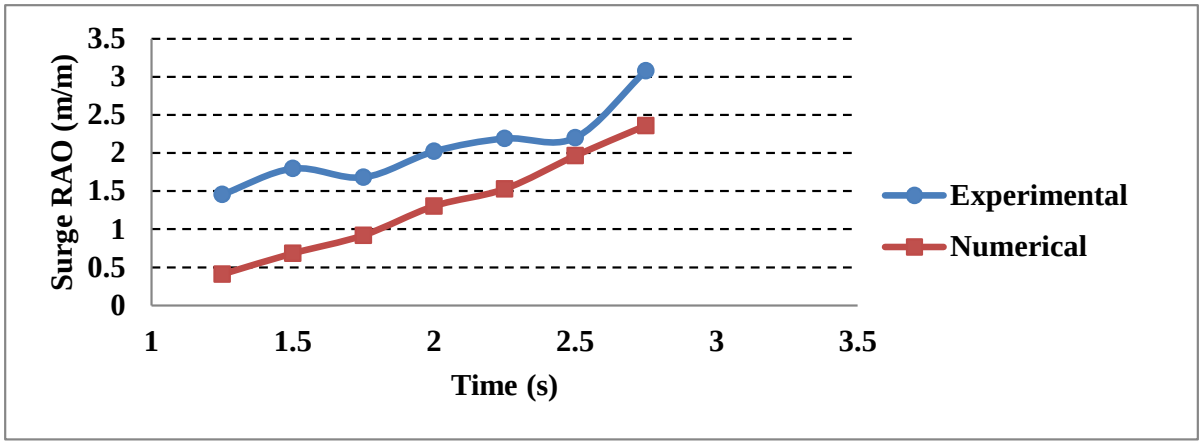

Fig.5.6 Comparisons of experimental and numerical results in terms of RAO's when the wave approach angle is 0 degree

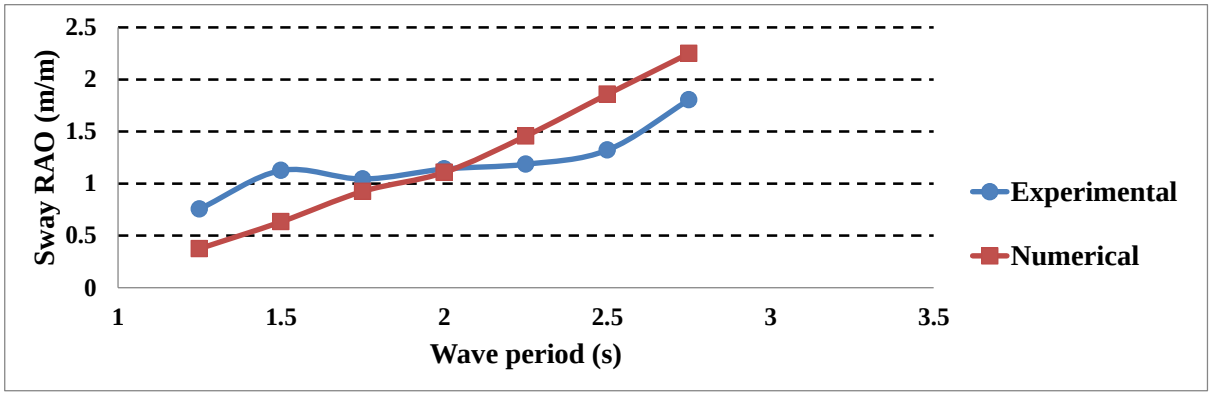

Fig.5.7 Comparisons of experimental and numerical results in terms of RAO's when the wave approach angle is 90 degree

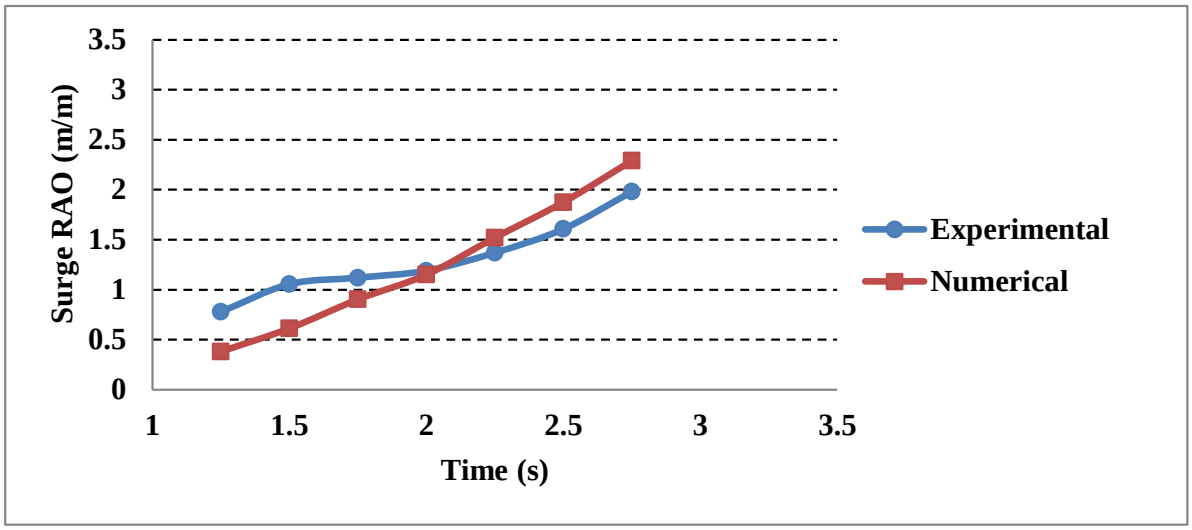

Fig.5.8 Comparisons of experimental and numerical results in terms of RAO's when the wave approach angle is 180 degree

5.4 SUMMARY

In this chapter, details of numerical simulation of the scaled model using ANSYS AQWA and the validation by experimental results are presented. The computed and experimental natural periods are in good agreement, indicating that all principal effects are incorporated in the numerical model. The comparison of the experimental and numerical results show that the surge responses agreed well with the experiments conducted and is revealed through favourable comparison of Response Amplitude Operator in the active degree of freedom.

CHAPTER 6

NUMERICAL INVESTIGATION ON PROTOTYPE

6.1 GENERAL

In the present work, the design and the dynamic response of a three-legged articulated platform is investigated. To investigate the complete behaviour of this compliant support system under the actual ocean environment, a numerical investigation on the dynamic response characteristics of the prototype of three-legged articulated wind tower are evaluated. Numerical analyses are conducted on the prototype, using ANSYS AQWA to investigate the effects of various parameters that influence the response. The investigations are carried out under regular waves and random waves, for wave induced as well as wind-wave induced cases.

6.2 NUMERICAL MODELING AND FREE VIBRATION STUDY

The numerical model of the prototype of three legged articulated tower is developed using ANSYS AQWA. As the characteristic dimension of the legs is less than 0.2 times the wave length for the considered waves the wave forces can be computed using Morison equation. For modeling the Morison elements in the DesignModeler of ANSYS AQWA, TUBE elements are used. Articulated joints are modeled as the joint, which transfers only translational responses. The turbine weight is given as a point mass at the tower top. Generated numerical model of prototype is depicted in Fig 6.1.

The free vibration analysis is carried out and the natural periods of surge, sway and yaw are found to be 37.4 s, 37.4 s and 34.1s respectively. The natural periods for these modes do not fall in the range of typical ocean wave periods, these being approximately from 5 to 17s.

6.3 BEHAVIOUR UNDER REGULAR WAVES

Articulated structure is compliant with respect to the horizontal degrees of freedom while it is stiff with respect to the vertical degrees of freedom. Motion response analysis of the three legged articulated platform under regular waves is conducted. Time domain analysis is done in ANSYS AQWA for a water depth of 144m under the action of regular waves. The time step considered in the analysis is 0.1 s. Equation of motion is solved at every time step. The

wave loads on the legs are evaluated by Airy's wave theory and Morison's equation, without considering the diffraction effects. Response Amplitude Operator (RAO) of the tower under regular wave loading is obtained in the active degree of freedom (surge) and is depicted in Fig 6.2. From the analysis it is shown that surge RAO reaches its maximum at the corresponding natural frequency showing less coupling with other modes.

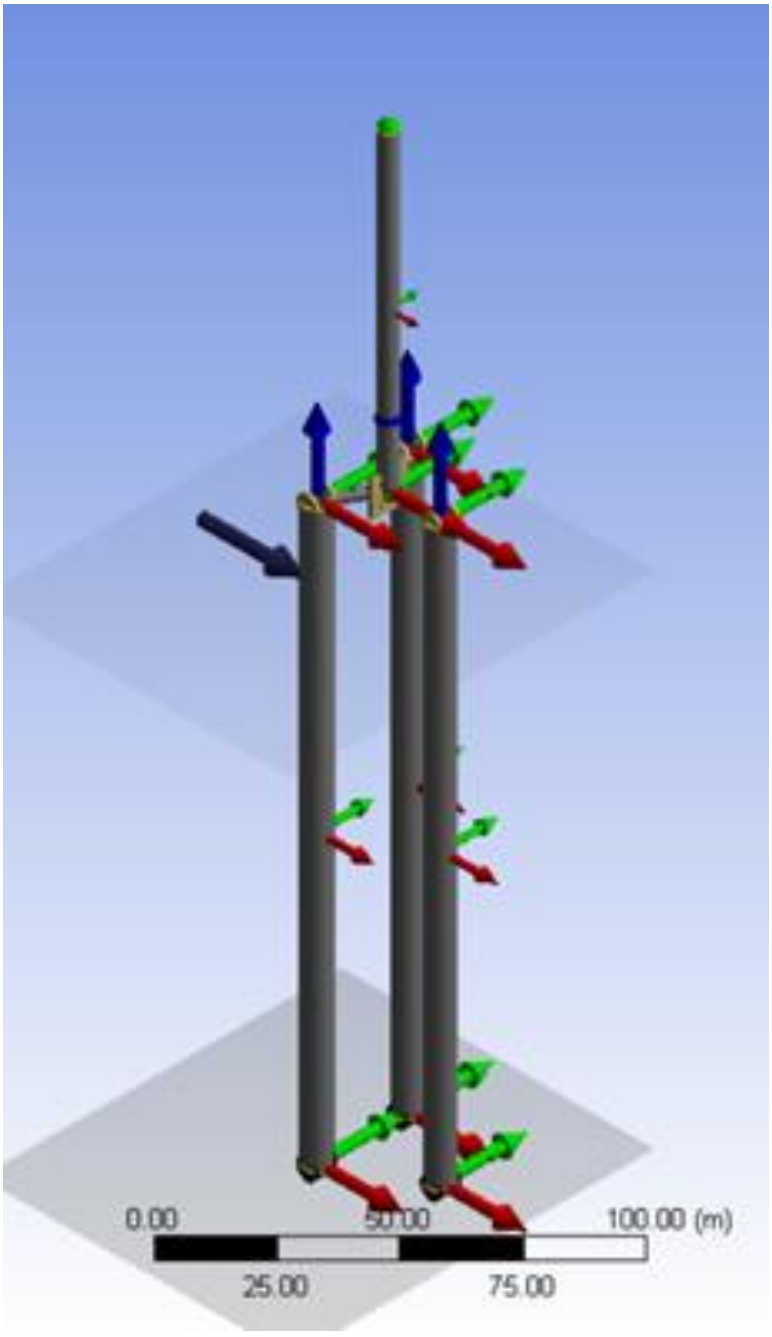

Fig. 6.1 Generated numerical model of prototype

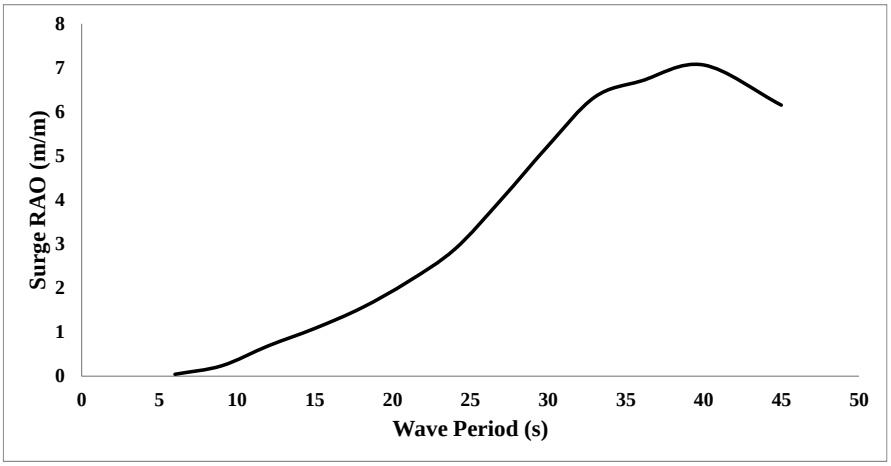

Fig. 6.2 Response Amplitude Operator (RAO) of the tower in the surge

6.3.1 Responses corresponding to different wave directions

Influence of wave direction on the motion response of the prototype is studied to determine the critical orientation of the platform. For this, the wave data of the site is taken from www.waveclimate.com, a site run by BMT ARGOSS, a leading maritime, meteorological, and oceanographic company. A wave height of 7 m with 12 seconds wave period is selected as design site wave. Details of wave height and its probablity of exceedance are given in table 6.1. Details of wave time period and its probablity of exceedance are given in Table 6.2. This data is also obtained from www.waveclimate.com. A tabulation of one year data is given.

Table 6.1 Wave height and probability of exceedance (courtesy BMT AGROSS)

Wave Height (m)	**Prob. of exc. (%)**	**Wave Height (m)**	**Prob. of exc. (%)**	**Wave Height (m)**	**Prob. of exc. (%)**	**Wave Height (m)**	**Prob. of exc. (%)**
0	100.0	3.5	34.0	7.0	4.1	10.5	0.3
0.5	100.0	4.0	25.8	7.5	3.0	11.0	0.2
1.0	96.4	4.5	19.2	8.0	2.2	11.5	0.1
1.5	83.8	5.0	14.4	8.5	1.5	12	0.1
2.0	69.5	5.5	10.8	9.0	1.1	12.5	0
2.5	55.8	6.0	8	9.5	0.8	13	0
3.0	44.2	6.5	5.7	10.0	0.5	13.5	0

Table 6.2 Wave period and probability of exceedance (courtesy BMT AGROSS)

Wave Period (s)	Prob. of exc. (%)	Wave Period (s)	Prob. of exc. (%)	Wave Period (s)	Prob. of exc. (%)	Wave Period (s)	Prob. of exc. (%)
0	100.0	7	81.3	14	0.4	8.3	50.0
1	100.0	8	58.0	15	0.1	8.8	40.0
2	100.0	9	35.8	16	0	9.3	30.0
3	100.0	10	19.6	6.5	90	10	20.0
4	100.0	11	9.2	7.1	80	10.9	10.0
5	99.8	12	3.7	7.5	70	12.4	2.5
6	95.6	13	1.2	7.9	60	13.2	1.0

The wave direction is rotated and responses in various degrees of freedom corresponding to 0^0, 30^0, 60^0, and 90^0 are obtained. Schematic diagram showing the zero degree direction of wave is shown in Fig.6.3

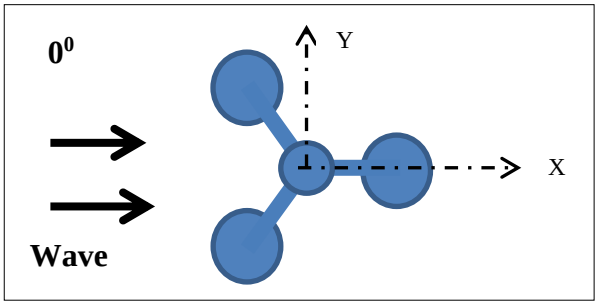

Fig. 6.3 Schematic diagram showing wave direction

0^0 wave approach

Time history of responses corresponding to various degrees of freedom when the incident wave direction is 0 degree is shown in Fig.6.4. It is found that only surge (3.2m) response is significant, but within limit. All other responses are nil.

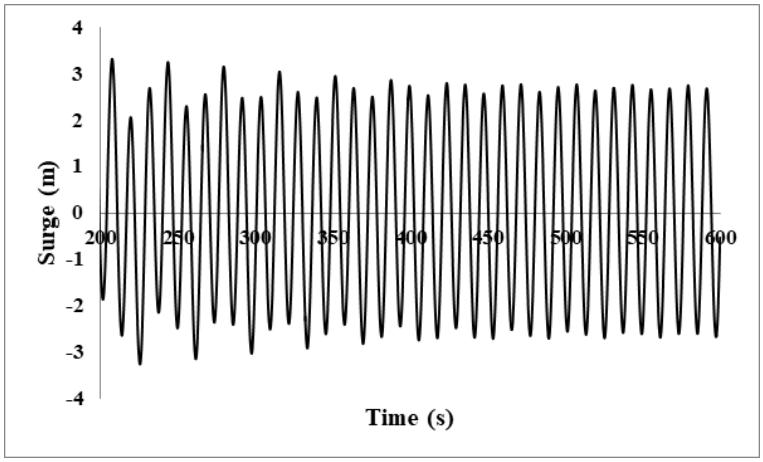

Fig. 6.4 (a) Time history of surge response when the incident wave direction is 0 degree

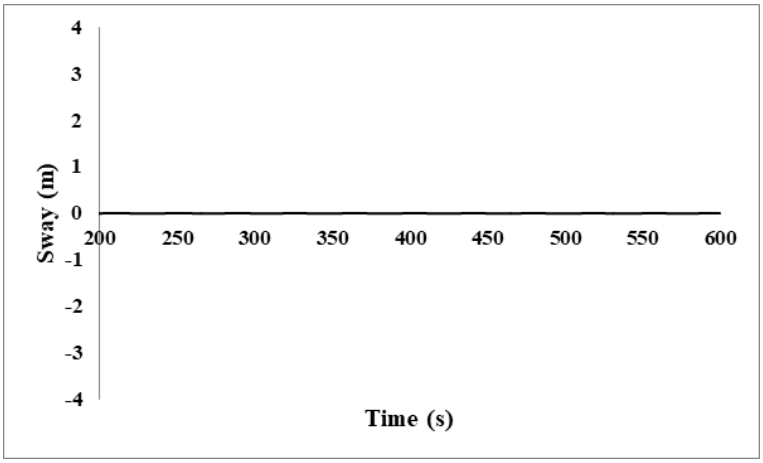

Fig. 6.4 (b) Time history of sway response when the incident wave direction is 0 degree

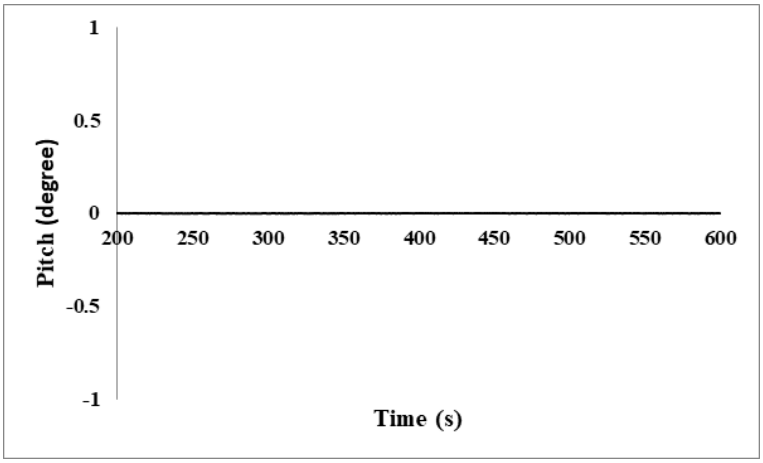

Fig. 6.4 (c) Time history of pitch response when the incident wave direction is 0 degree

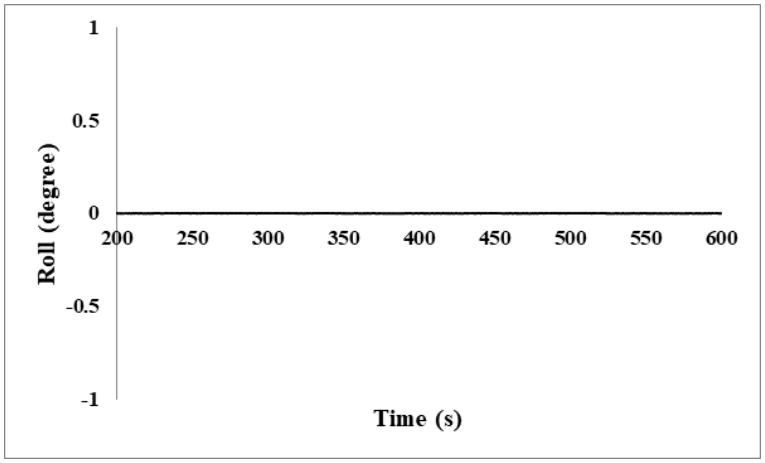

Fig. 6.4 (d) Time history of roll response when the incident wave direction is 0 degree

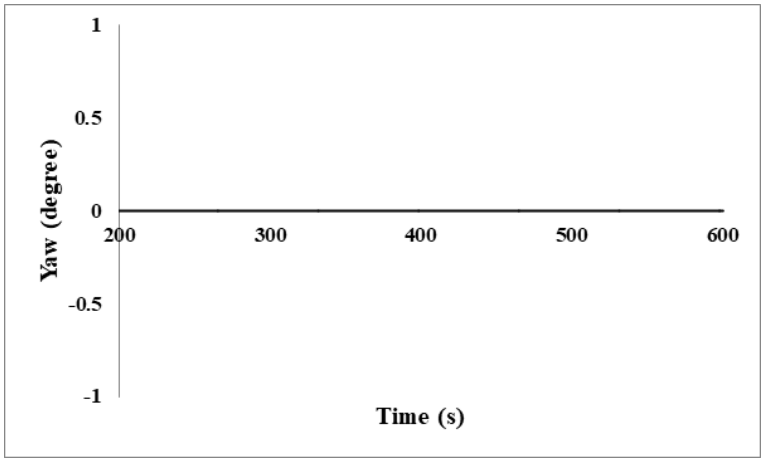

Fig. 6.4 (e) Time history of yaw response when the incident wave direction is 0 degree

30^0 wave approach

Time history of responses corresponding to various degrees of freedom when the incident direction of wave is 30 degree is shown in Fig.6.5. When the main approach angle is 30 degree, the surge response is slightly reduced (2.9 m). But a sway response of 1.5 m is also observed when the wave approaches in an angle. All other rotational responses are almost nil, small yaw response is occurred at 30 degree.

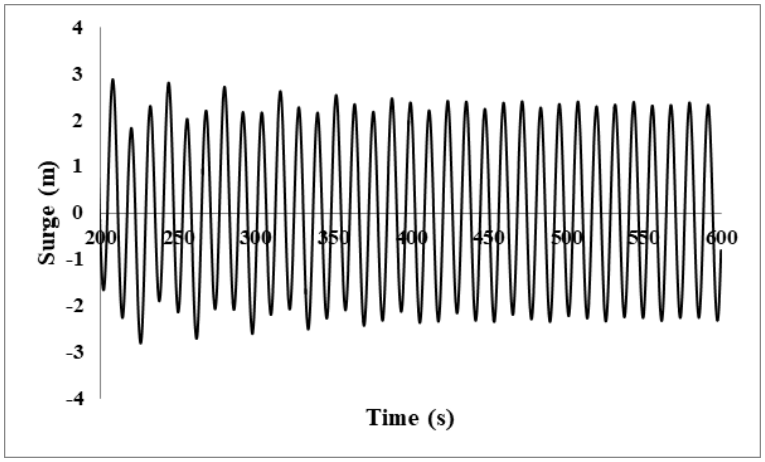

Fig. 6.5 (a) Time history of surge response when the incident wave direction is 30 degree

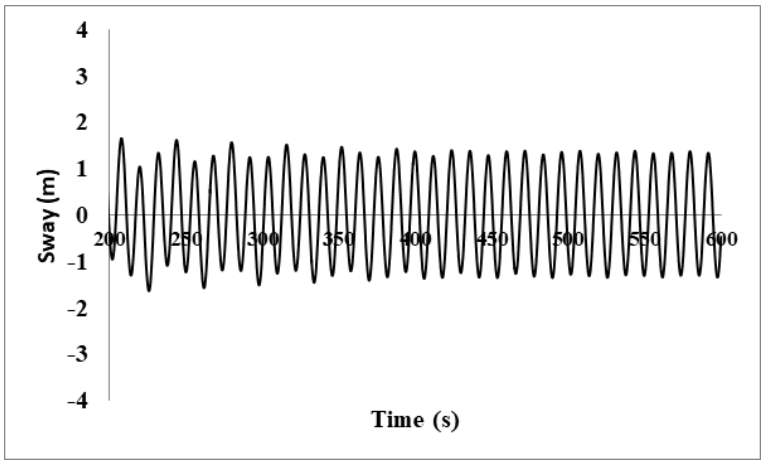

Fig. 6.5 (b) Time history of sway response when the incident wave direction is 30 degree

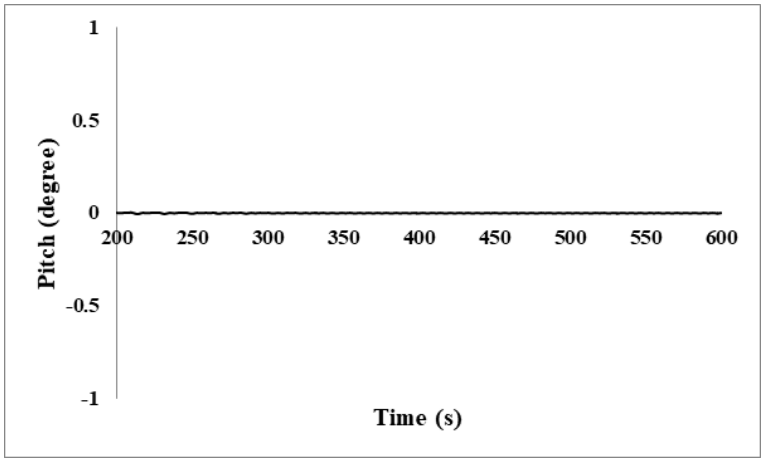

Fig. 6.5 (c) Time history of pitch response when the incident wave direction is 30 degree

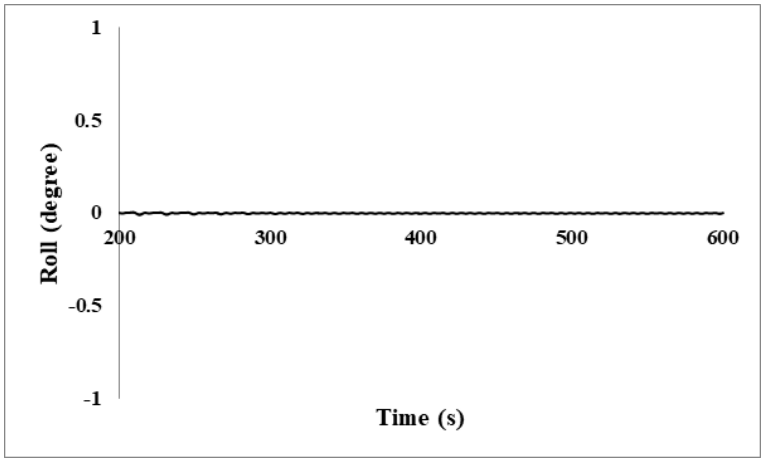

Fig. 6.5 (d) Time history of roll response when the incident wave direction is 30 degree

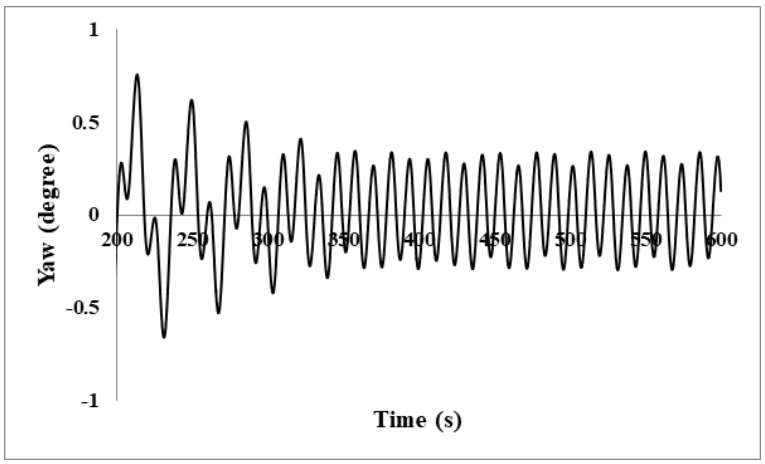

Fig. 6.5 (e) Time history of yaw response when the incident wave direction is 30 degree

60^0 wave approach

Time history of responses corresponding to various degrees of freedom when the incident wave direction is 60 degree is shown in Fig.6.6. When the main approach angle is 60 degree, the surge response is reduced (1.7 m). But a sway response of 2.9 m is also observed when the wave approaches in an angle. All rotational responses are nil.

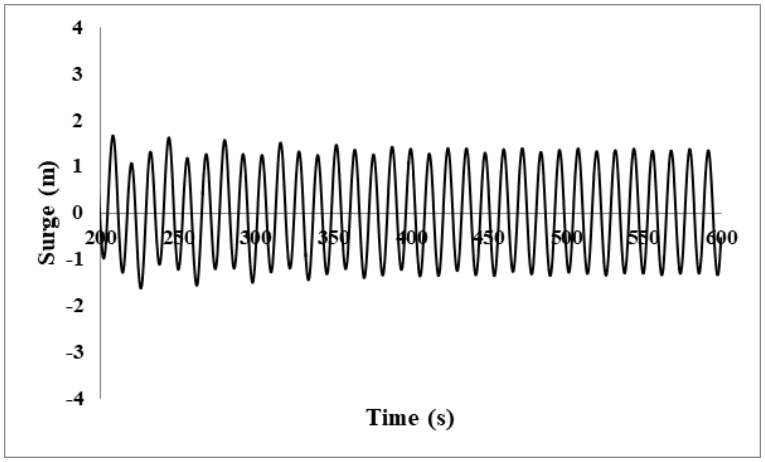

Fig. 6.6 (a) Time history of surge response when the incident wave direction is 60 degree

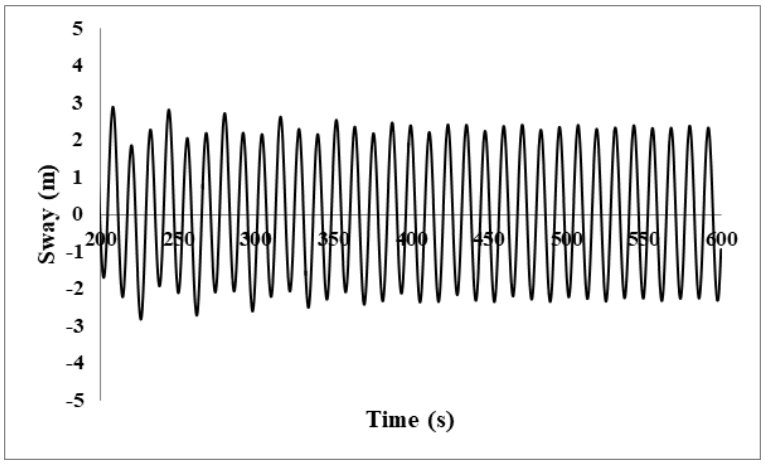

Fig. 6.6 (b) Time history of sway response when the incident wave direction is 60 degree

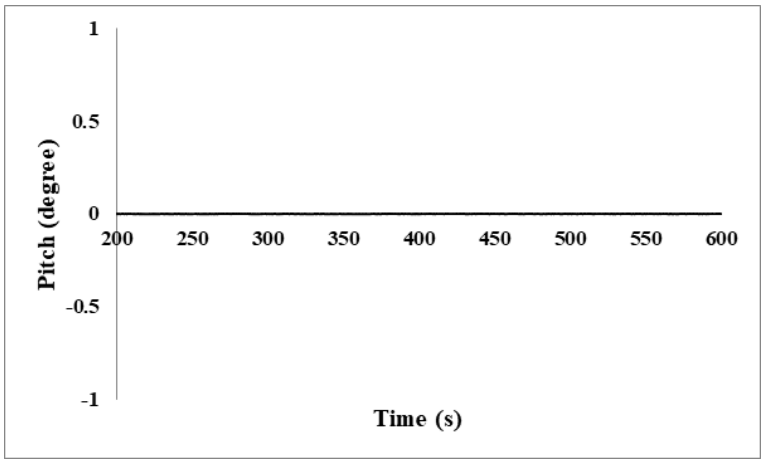

Fig. 6.6 (c) Time history of pitch response when the incident wave direction is 60 degree

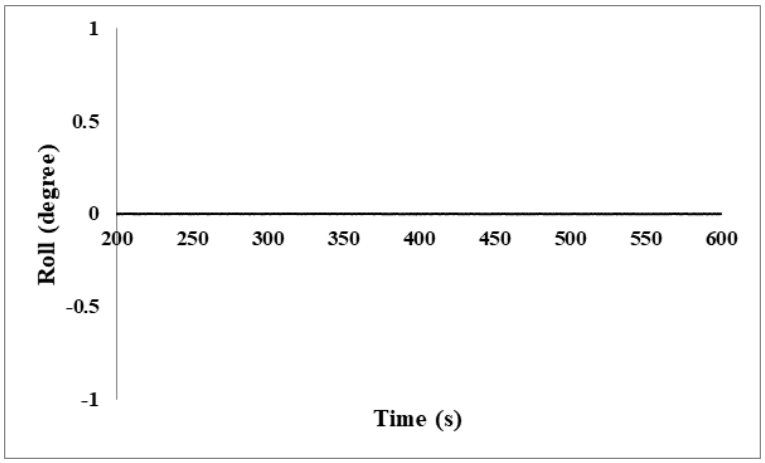

Fig. 6.6 (d) Time history of roll response when the incident wave direction is 60 degree

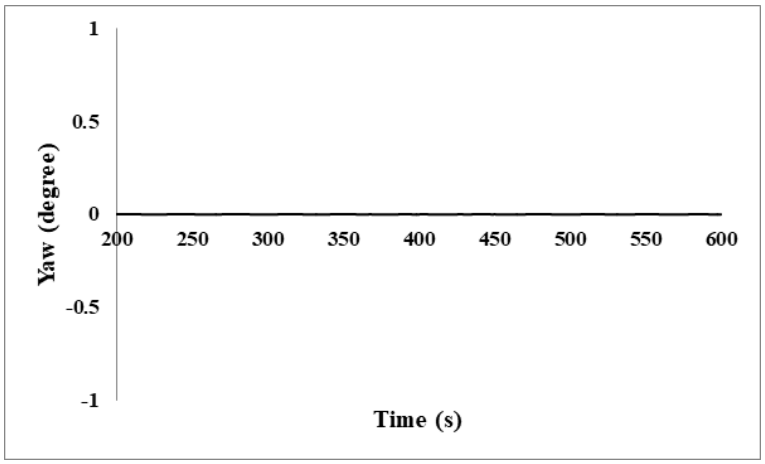

Fig. 6.6 (c) Time history of yaw response when the incident wave direction is 60 degree

90^0 wave approach

Time history of responses corresponding to various degrees of freedom when the incident wave direction is 90 degree is shown in Fig.6.7. It is found that only sway (3.2m) response is significant, but within limit. All other responses are nil, but a small yaw response occurred at 90 degree.

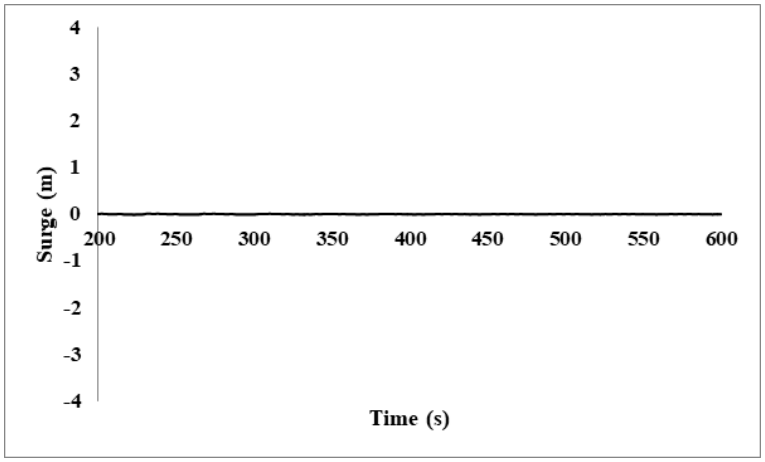

Fig. 6.7 (a) Time history of surge response when the incident wave direction is 90 degree

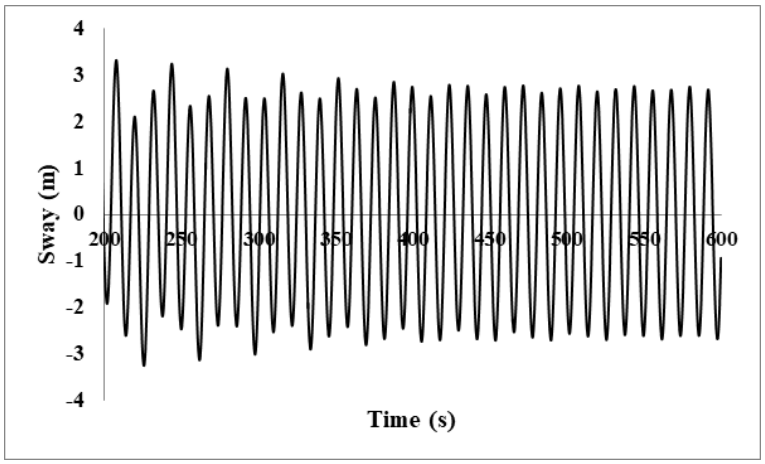

Fig. 6.7 (b) Time history of sway response when the incident wave direction is 90 degree

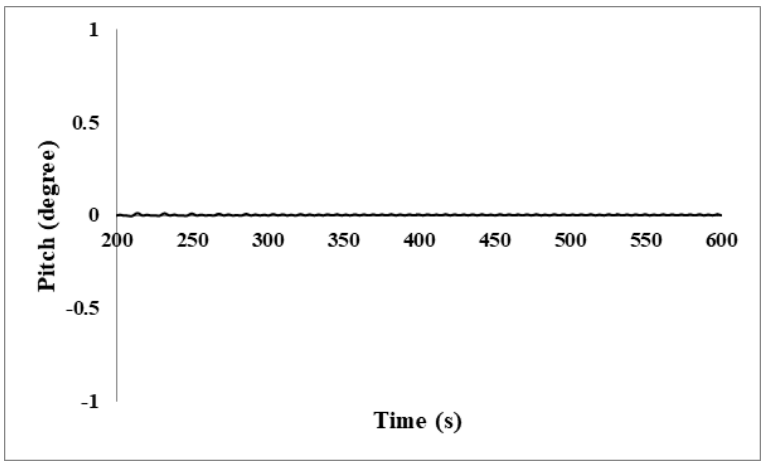

Fig. 6.7 (c) Time history of pitch response when the incident wave direction is 90 degree

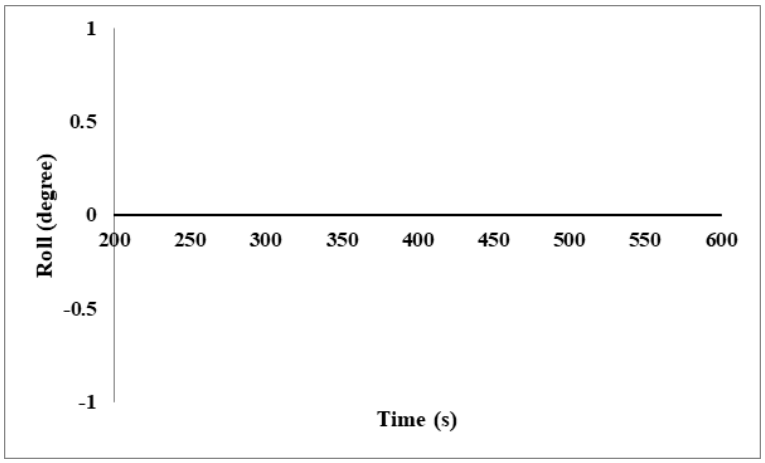

Fig. 6.7 (d) Time history of roll response when the incident wave direction is 90 degree

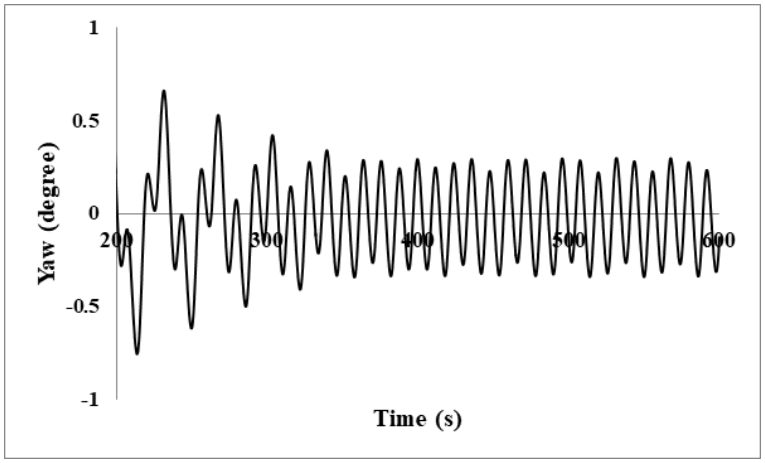

Fig. 6.7 (e) Time history of yaw response when the incident wave direction is 90 degree

The result shows that the orientation with respect to predominant direction of wave during installation of the platform is useful to reduce the response of the structure.

6.3.2 Influence of wave height on the motion response of the articulated platform

The primary loading on offshore platforms is the load due to waves. So the behaviour of these platforms under wave loading is of design interest. For the calculation of wave forces three load cases are selected. The load cases are mentioned in Table 6.3. The effect of variation in wave height is studied.

Table 6.3 Load cases for wave force calculation

load cases	Wave height in m	Wave period (s)
1	8	10
2	10	10
3	12	10

When the wave period is 10 s, for an increase of 25% in the wave height (from 8 m to 10 m), the corresponding increase in response is 33% and similarly for an increase in wave height of 50% (from 8 m to 12 m), the corresponding increase in response is 61% and is shown in Fig.6.8.

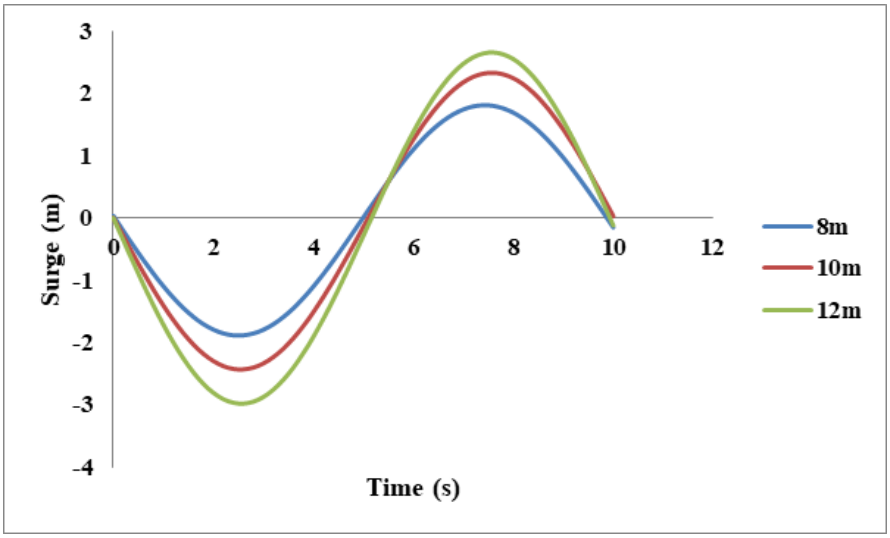

Fig. 6.8 Influence of wave height on the motion response of the articulated platform

6.4 BEHAVIOUR UNDER RANDOM WAVES

Analysis under random wave environment will give the behaviour of the structure exactly since the ocean waves are a combination of waves with various frequency and direction. Wave loading on offshore structures is usually presumed to be more important than wind loading, but articulated platforms having low frequency show reduced response to high frequency wave loads. These articulated platforms, with natural periods of 30 s and more, vibrates within the range of the most energetic low frequency wind forces (Zaheer and Islam, 2017), as depicted in Fig.6.9. This shows the critical impact of wind on the behavior of articulated structures. So to obtain the actual behavior of the proposed three legged

articulated platform, numerical analysis under combined action of wind and wave are to be done.

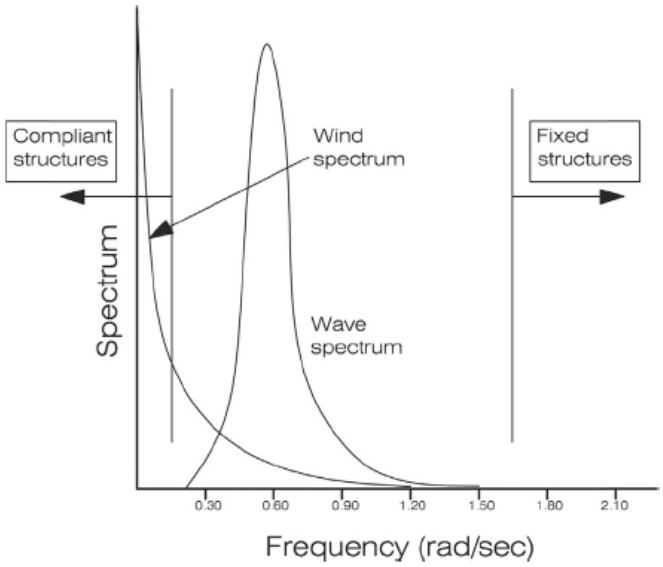

Fig. 6.9 Excitation and frequency ranges of offshore structures (Zaheer and Islam, 2017)

6.4.1 Motion response analysis for operational and survival conditions

In this section, motion response analysis of the three legged articulated wind tower is studied under operational and survival conditions of the wind turbine. For this time and frequency domain simulations are performed using ANSYS AQWA. The numerical simulations are done for investigating the motion response of the articulated wind tower due to:

(i) Wave only
(ii) Combined action of wind and wave

Different wind speeds (operational and survival conditions) as given in Oguz et al. (2018) is selected to study the motion responses of the compliant wind turbine. The constant wind is used to analyse the motion response of the compliant wind turbine subjected to combined action of wind and wave. The cut-in speed, rated speed and cut-out speed of NREL turbine are 3 m/s, 11.4 m/s and 25 m/s respectively. The ocean environmental conditions chosen for operational and survival cases are presented in Table 6.4. One more severe environment for a wind speed of 38.76 m/s (survival condition) as given in Oguz et al. (2018) is also analysed.

Table 6.4 Load Cases for Operational and Extreme Conditions, Oguz et al. (2018)

Load cases	Significant wave height [m]	Tp [s]	Gamma	Wind Speed [m/s]	Turbine Status
Load case 0	0.75	5.44	1	6.05	Operating
Load case 1	4.55	9.00	2.45	11.4	Operating
Load case 2	6	10.28	2.52	25	Parked
Load case 3	8.46	10.13	5	38.76	Parked

The random sea is modeled by a JONSWAP spectrum. The spectral ordinate at a frequency is represented as

$$S(\omega) = \frac{\alpha g^2 \gamma^a}{\omega^5}\, exp\left(-\frac{5{\omega_p}^4}{4\omega^4}\right) \ldots\ldots\ldots\ldots\ldots\ldots 6.1$$

Where ω_p is the peak frequency in rad/s, γ is the peak enhancement factor, α is a constant and

$$a = exp\left[-\frac{\left(\omega - \omega_p\right)^2}{2\sigma^2 {\omega_p}^2}\right]$$

$$\sigma = \begin{cases} 0.07 \;\; where\; \omega \leq \omega_p \\ 0.09 \;\; where\; \omega > \omega_p \end{cases}$$

The maximum force of the NREL 5 MW turbine happens at rated wind speed in operating condition of turbine when the control is active and the blades are rotating. In the parked condition of a turbine, the blades are feathered 90 degree, i.e. the blades are kept in locked position. So the parked case is a non-operating condition where the blades are not rotating and the control is not active. During harsh conditions, the turbines are parked in order to avoid damage. The aerodynamic thrust generated by wind turbine for operating and parked cases are calculated and given as a point force at the top of the tower (Zang et al. 2013).

For the operating condition, average pressure P_H on rotor swept area is

$$P_H = \frac{\rho_a}{2} C_{FB} u^2 \ldots\ldots\ldots\ldots\ldots 6.2$$

where ρ_a is air density (1.297 kg/m^3), C_{FB} is coefficient (8/9), based upon the Betz momentum theory at maximum power output; and u is speed of wind. So in operating condition, the average wind force acting on the top of tower is

$$F_H = P_H A = P_H \frac{\pi D^2}{4} \ldots\ldots\ldots\ldots\ldots 6.3$$

where A is area swept by the rotor $(\frac{\pi D^2}{4})$ and D is the blade diameter. For parked condition, pressure (P_H) on blade area is calculated as

$$P_H = C_{DD} \rho_a u^2 \ldots\ldots\ldots\ldots\ldots\ldots\ldots\ldots 6.4$$

where C_{DD} is damping coefficient is taken as 1.1. So in parked condition, the horizontal force (F_H) on the tower top is calculated as

$$F_H = P_H S \ldots\ldots\ldots\ldots\ldots\ldots\ldots\ldots 6.5$$

where S is the sum of the area of all blades. This area is taken as 5% of the area swept by the rotor.

Time domain analysis is done using ANSYS AQWA for a water depth of 144m under the combined action of wind and wave loads. The time step of 0.1 s is used for the analysis in AQWA. At each time step the position of legs and tower is obtained by the integration of accelerations. For this predictor-corrector numerical integration technique is used by ANSYS AQWA. For obtaining the motion response of the tower and legs, the solution obtained at the end of each time step is used as the initial condition for the next time step.

To study the dominant effects for operating and parked conditions, responses due to wave only case are compared with simultaneous action of wind and wave responses and are presented here. The same random waves are used in both analyses. The time history of surge response of tower for Load case1 is compared for both the cases and shown in Fig.6.10 Combined wind and wave action results a shift in the mean position. The mean value is shifted from 0 to 4.37.

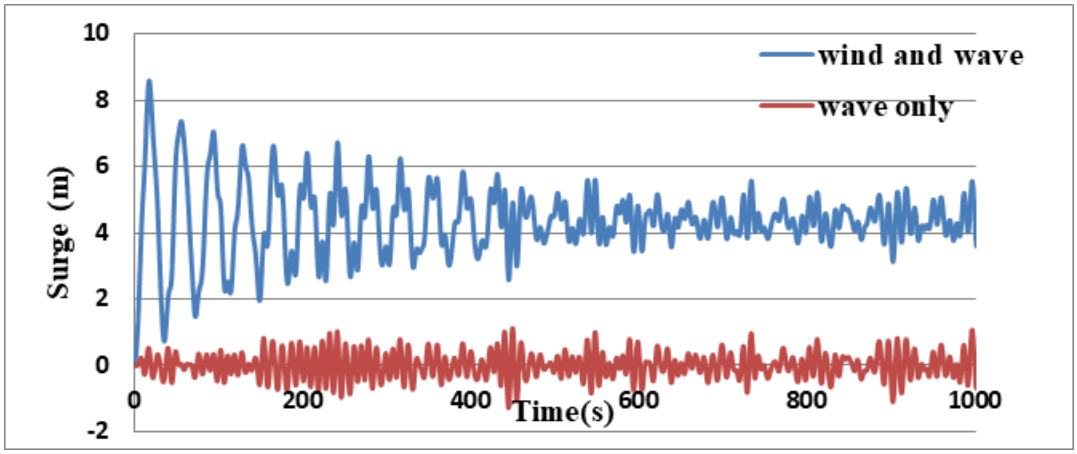

Fig. 6.10 Time history of surge motion of tower, Load case1(Hs=4.55m, Tp=9s, V=11.4m/s)

The Power Spectral Density (PSD) function of the surge response of tower for Load case1 for both the cases is compared in Fig.6.11. Presence of wind does not significantly alter the energy content of the surge power spectral density function. The peak occurs at 0.62 rad/s for the wave only case (Fig.6.11a) and for the combined wind and wave action the peak occurs at 0.65 rad/s (Fig.6.11b). The peak value of PSD for the wave only case is 0.53 m^2s and for the combined action of wind and wave the peak value is 0.61 m^2s.

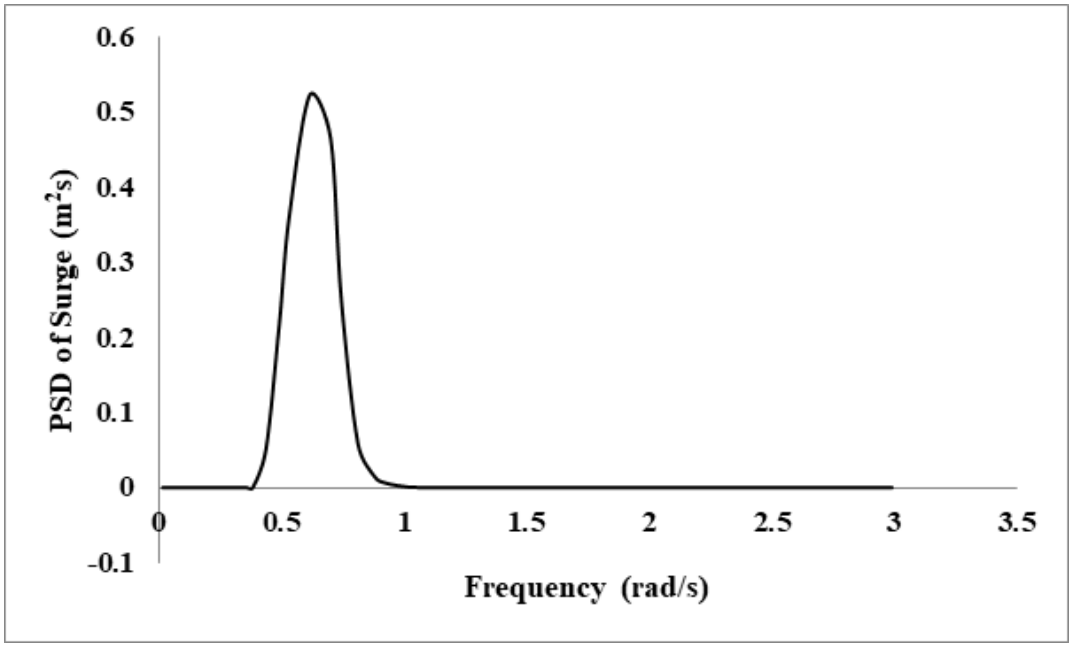

Fig.6.11(a) PSD of surge motion of tower Load case1 (Hs=4.55m, Tp=9s, wave only)

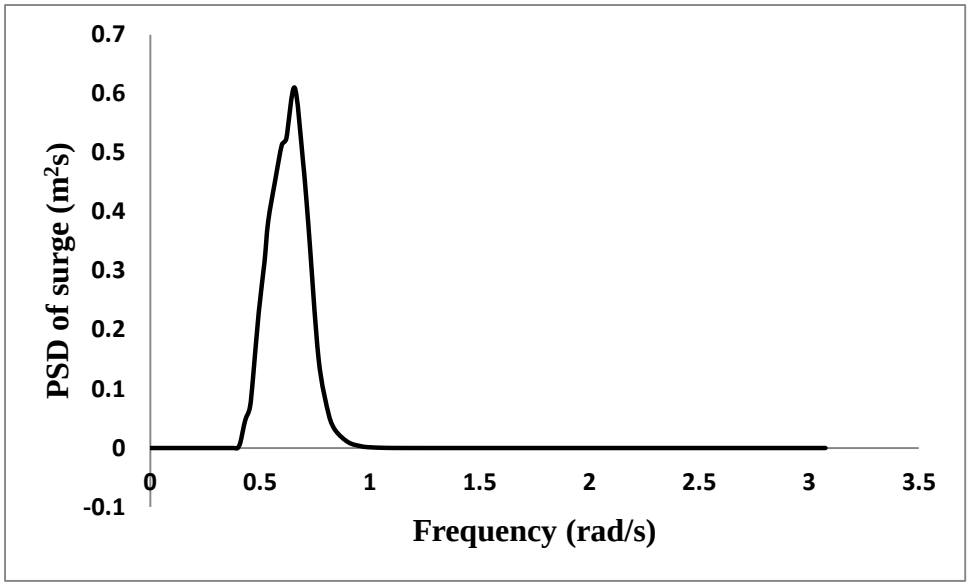

Fig. 6.11(b) PSD of surge motion of tower load case1, (Hs=4.55m, Tp=9s, V=11.4m/s)

The time history of pitch response of the articulated leg for the Load case1 is compared for both the cases and shown in Fig.6.12. Due to the combined wind and wave action, a shift in the mean position is observed.

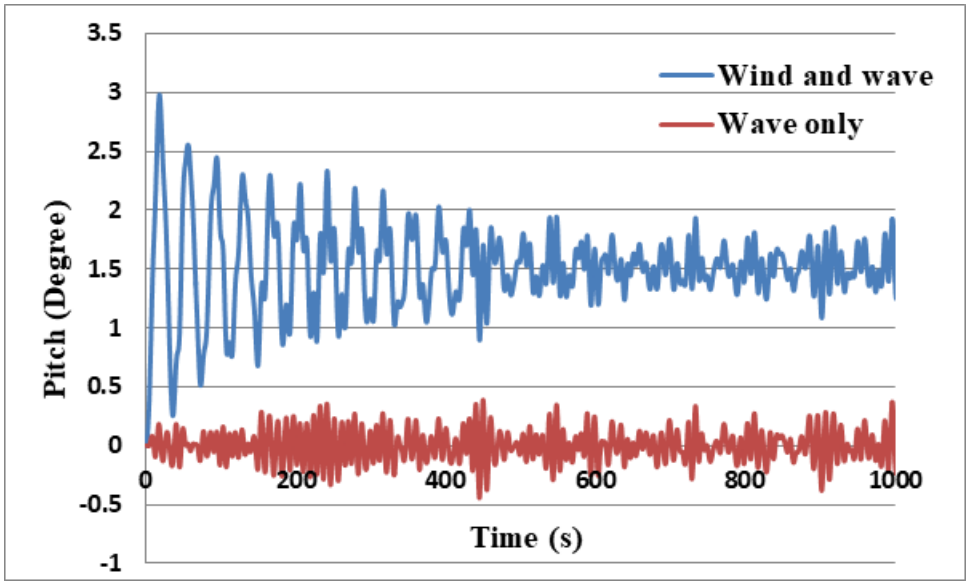

Fig. 6.12 Time history of Pitch of leg load case1, (Hs=4.55m, Tp=9s, V=11.4m/s)

The power spectral density function of the pitch response of articulated leg for Load case1 for both the cases is compared in Fig.6.13 Presence of wind does not significantly alter the

energy content of the pitch power spectral density function. The peak occurs at 0.62 rad/s for the wave only case (Fig.6.13a) and for the combined wind and wave action the peak occurs at 0.65 rad/s (Fig.6.13b). The peak value of PSD for the wave only case is 0.062 degree^{2}s and for the combined action of wind and wave the peak value is 0.07 degree^{2}s.

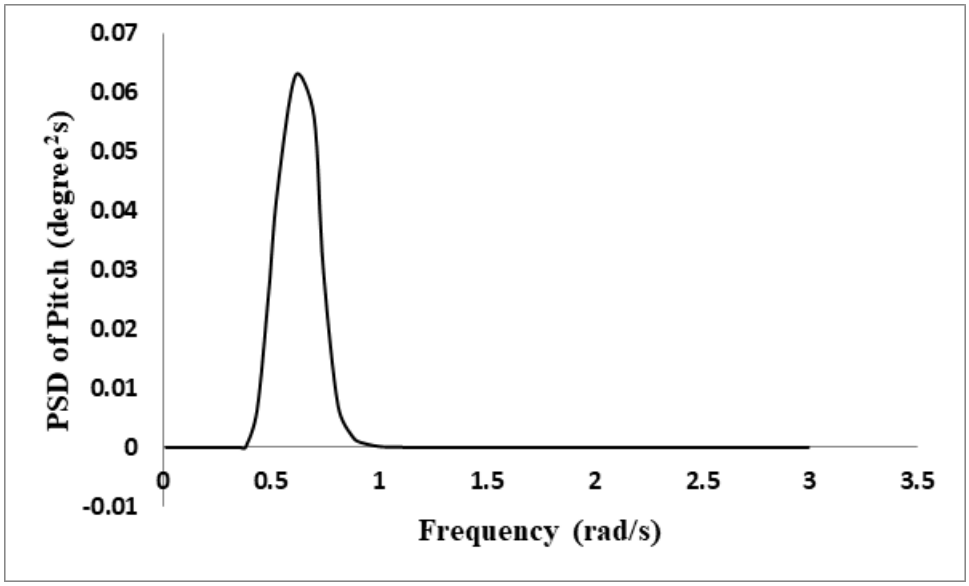

Fig. 6.13 (a) PSD of pitch response of leg load case1, (Hs=4.55m, Tp=9s, wave only)

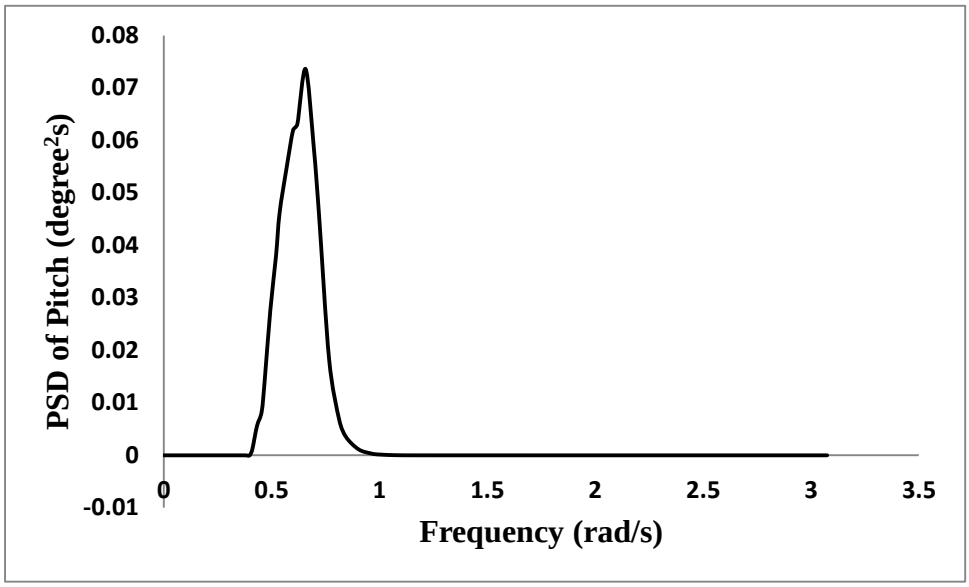

Fig. 6.13(b) PSD of pitch response of leg load case1, (Hs=4.55m, Tp=9s, V=11.4m/s)

Time history of pitch response of articulated leg and tower for load case1is shown in Fig.6.14. Compared to the pitch response of articulated leg, the response of tower is very less. This reduced tower response, as compared to that of the legs shall be due to the presence of

the articulated joints between the beams and the legs. These joints prevent the transfer of rotational responses from legs to the tower. Rotational response of the tower is found to be lesser than that of the leg, indicating that the tower remains almost vertical under the action of the horizontal loads even for the considerable rotation of articulated legs.

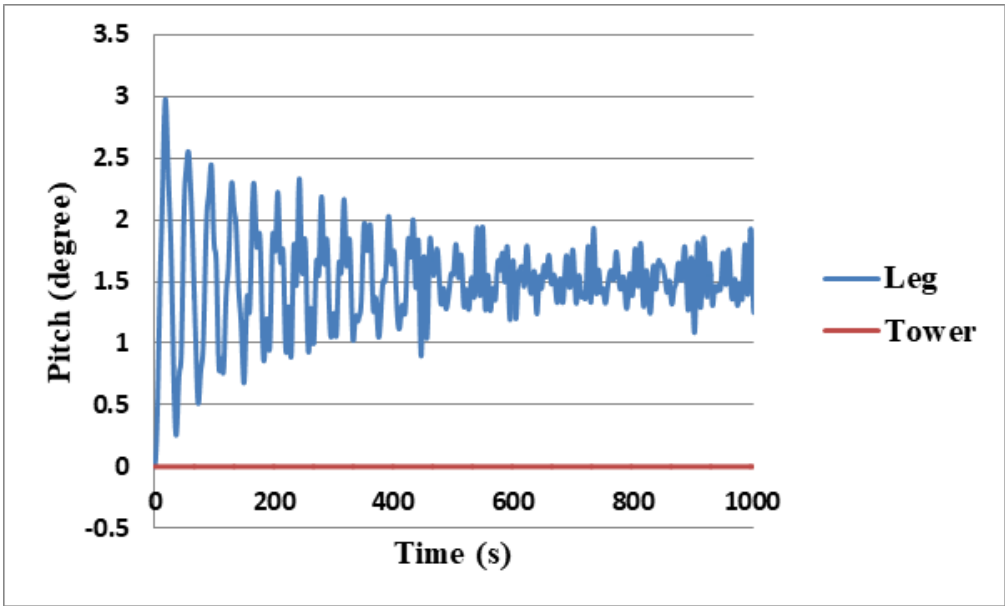

Fig. 6.14 Time history of Pitch of leg and tower load case1, (Hs=4.55m, Tp=9s, V=11.4m/s)

The time history of surge response of tower for Load case 2 is compared for both the cases and shown in Fig.6.15.

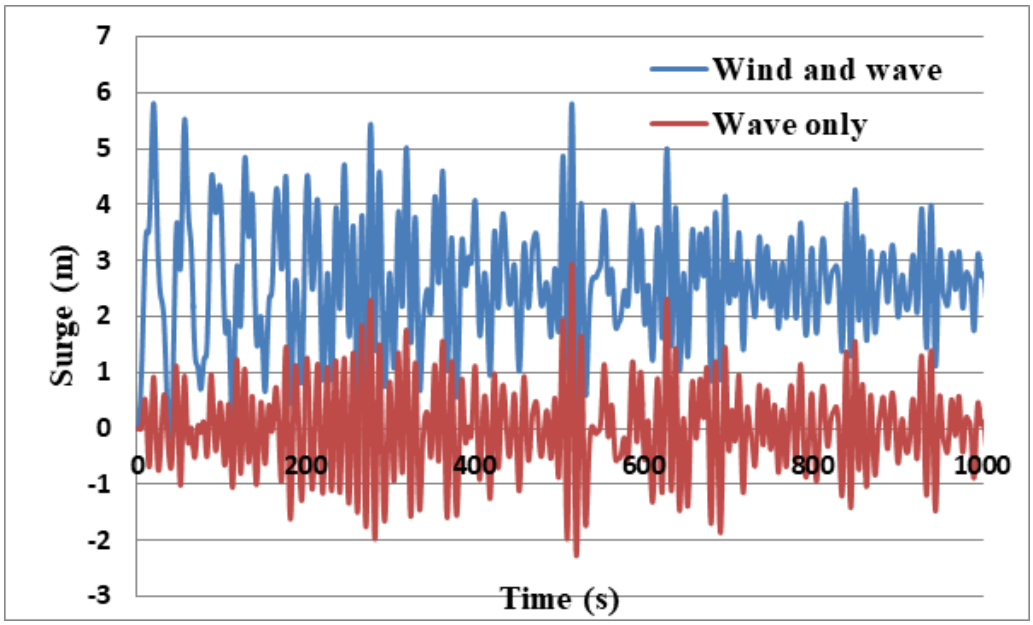

Fig. 6.15 Time history of surge motion of tower, Load case 2 (Hs=6 m, Tp=10.28 s, V=25 m/s)

Due to the combined wind and wave action, shift in the mean position is observed, but the shift is lesser than that in load case 1. In load case 1 the shift in mean value is from 0 to 4.37 whereas in load case 2 the shift is from 0.01 to 2.61. The power spectral density function of the surge response of tower for Load case 2 for both the cases is compared in Fig.6.16. It is shown that the presence of wind does not alter the energy content of the surge power spectral density function. The peak occurs at 0.57 rad/s for the wave only case (Fig.6.16a) and for the combined wind and wave action the peak occurs at 0.59 rad/s (Fig.6.16b). The peak value of PSD for both the cases is 2.6 m^2s. The effect of wind is not significant as the peak value for both the cases remains the same.

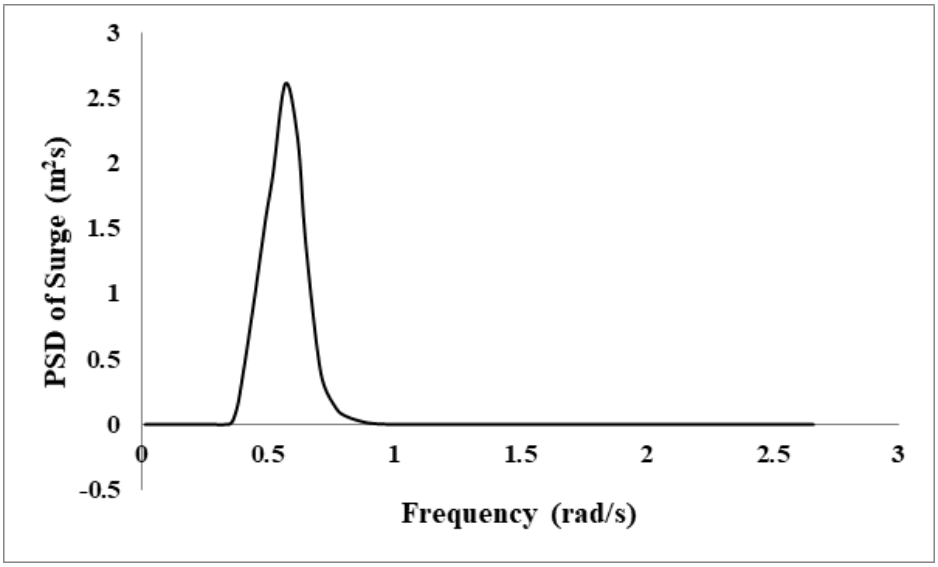

Fig. 6.16 (a) PSD of surge motion of tower Load case 2 (Hs=6m, Tp=10.28s, wave only)

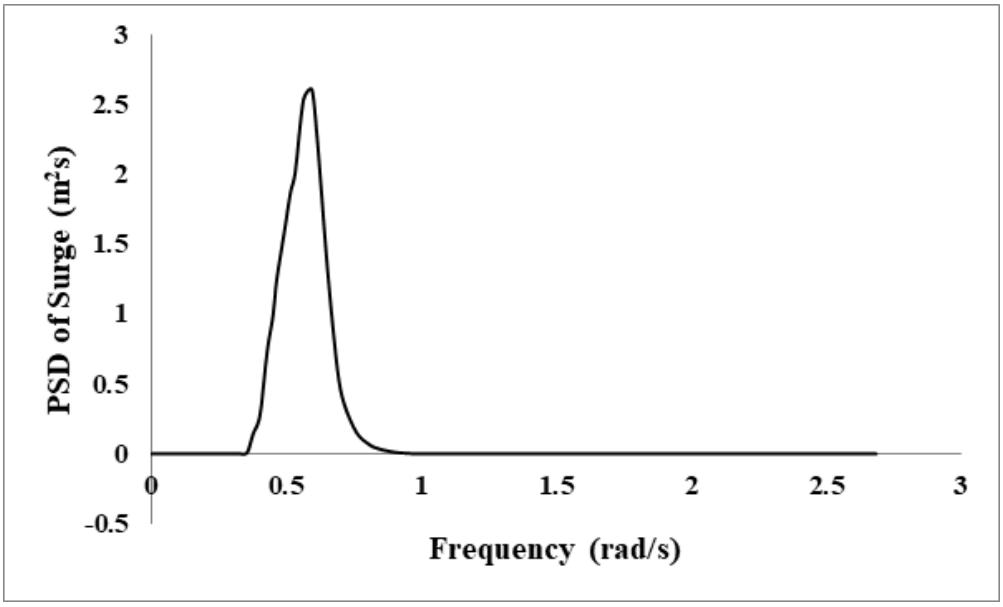

Fig. 6.16 (b) PSD of surge motion of tower Load case 2 (Hs=6 m, Tp=10.28 s, V=25 m/s)

The time history of pitch response of tower for Load case 2 is compared for both the cases and shown in Fig.6.17. The pitch response of tower is very less and remains almost same for both the cases.

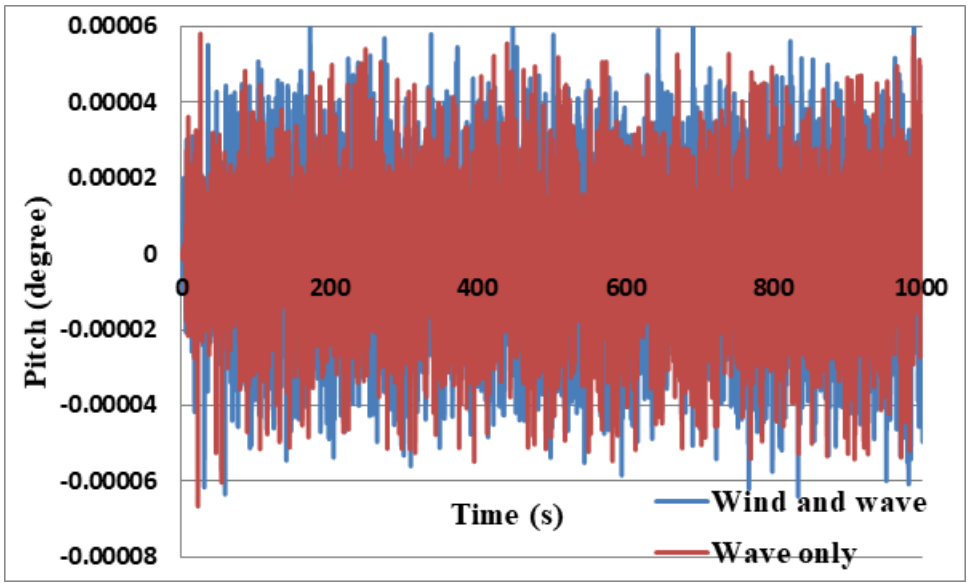

Fig. 6.17 Time history of Pitch of tower Load case2 (Hs=6m, Tp=10.28s, V=25m/s)

The time history of pitch response of leg for Load case 2 is compared for both the cases and shown in Fig.6.18. Due to the combined wind and wave action a shift in the mean position is observed, but the shift is lesser than that in load case 1.

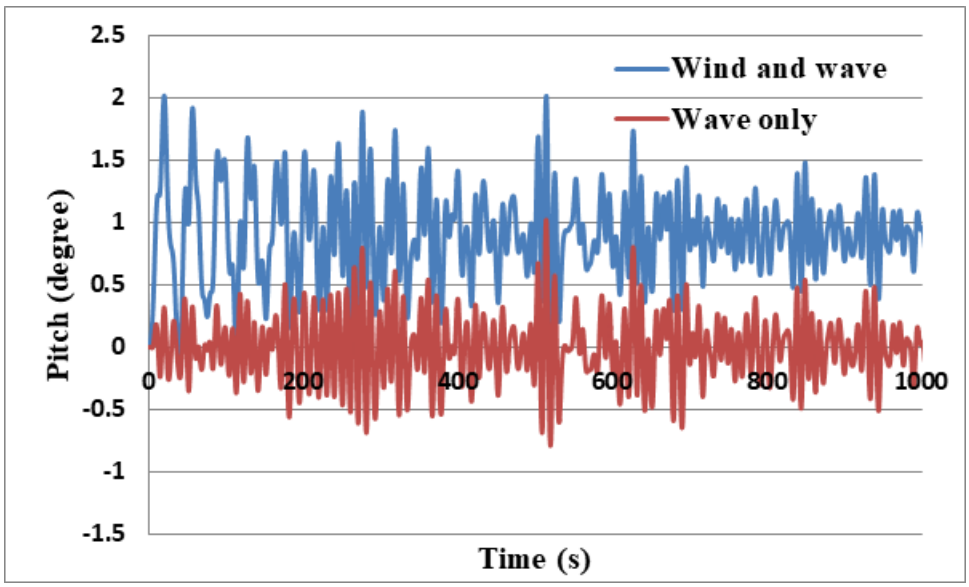

Fig. 6.18 Time history of Pitch of leg Load case2 (Hs=6m, Tp=10.28s, V=25m/s)

The power spectral density function of the pitch response of articulated leg for Load case 2 for both the cases is compared in Fig.6.19. It is shown that the presence of wind does not alter the energy content of the pitch power spectral density function. The peak occurs at 0.57 rad/s for the wave only case (Fig.6.19a) and for the combined wind and wave action the peak occurs at 0.59 rad/s (Fig.6.19b). The peak value of PSD for both the cases is 0.31 degree^{2}s.The effect of wind is not significant as the peak value for both the cases remains the same.

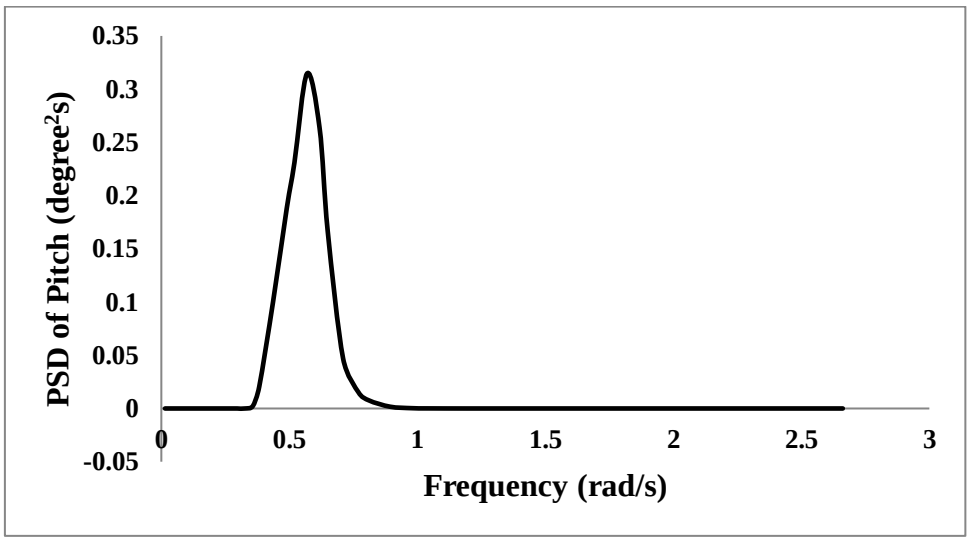

Fig. 6.19 (a) PSD of pitch motion of leg Load case2 (Hs=6m, Tp=10.28s, wave only)

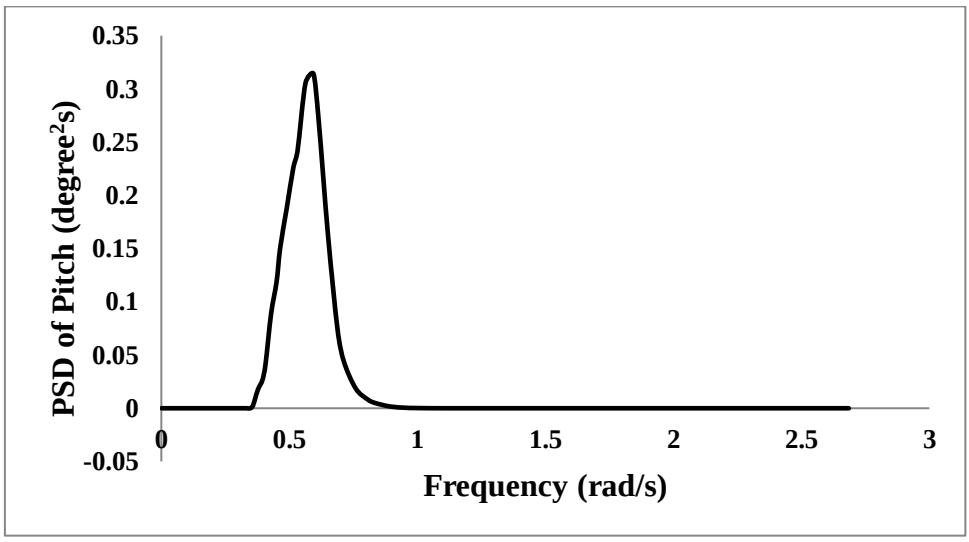

Fig. 6.19 (b) PSD of pitch motion of leg Load case2 (Hs=6m, Tp=10.28s, V=25m/s)

Time history of pitch response of articulated leg and tower for load case 2 is shown in Fig.6.20. Compared to the pitch response of articulated leg, the response of tower is very less

in this load case also. This reduction in the tower response, in comparison to that of the legs shall be attributed to the presence of the articulated joints between the beams and the legs.

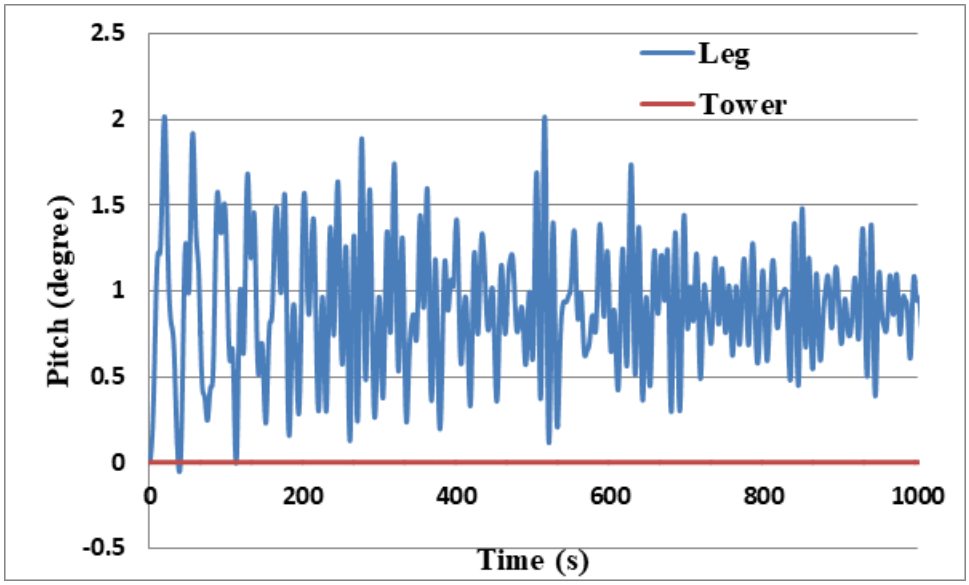

Fig. 6.20 Time history of Pitch of leg and tower Load case2 (Hs=6m, Tp=10.28s, V=25m/s)

The time history of surge response of tower for Load case 3 is compared for both the cases and shown in Fig.6.21. Combined wind and wave action results a shift in the mean position, but the shift is lesser than the other load cases.

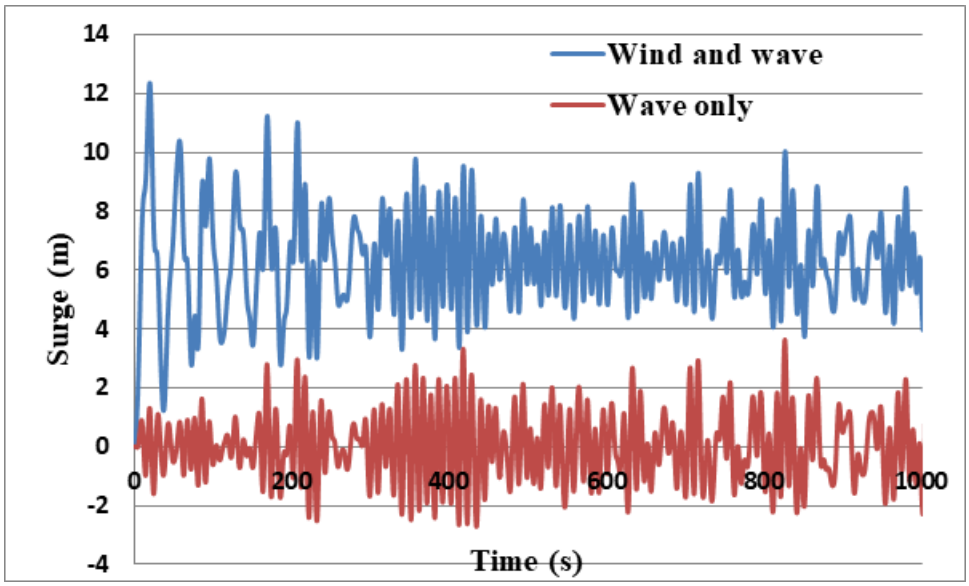

Fig. 6.21 Time history of surge motion of tower, Load case3 (Hs=8.46m, Tp=10.13s, V=38.76m/s)

The power spectral density function of the surge response of tower for Load case 3 for both the cases is compared in Fig.6.22. It is shown that the presence of wind does not alter the energy content of the surge power spectral density function. The peak occurs at 0.6 rad/s for the cases. The peak value of PSD for the wave only case is 6.54 m^2s (Fig.6.22a) and for the combined action of wind and wave the peak value is 6.68 m^2s (Fig.6.22b).

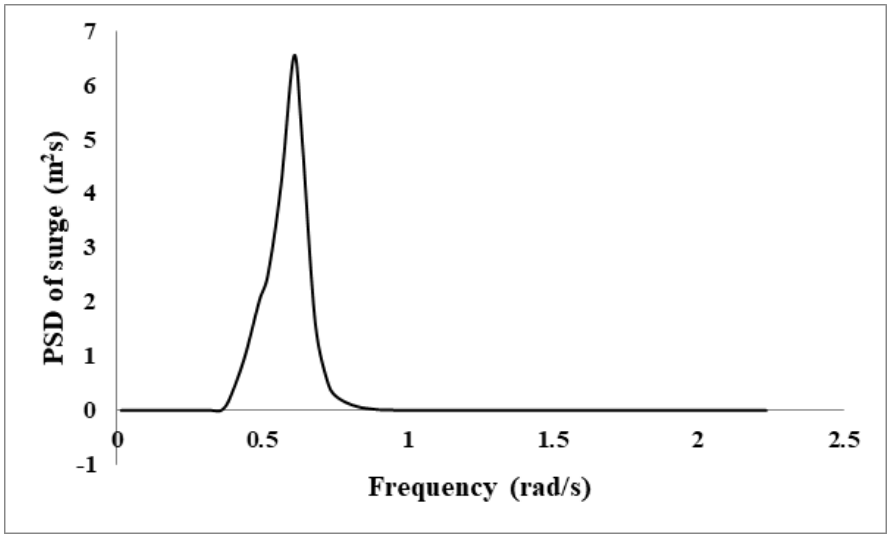

Fig. 6.22 (a) PSD of surge motion of tower Load case3 (Hs=8.46m, Tp=10.13s, Wave only)

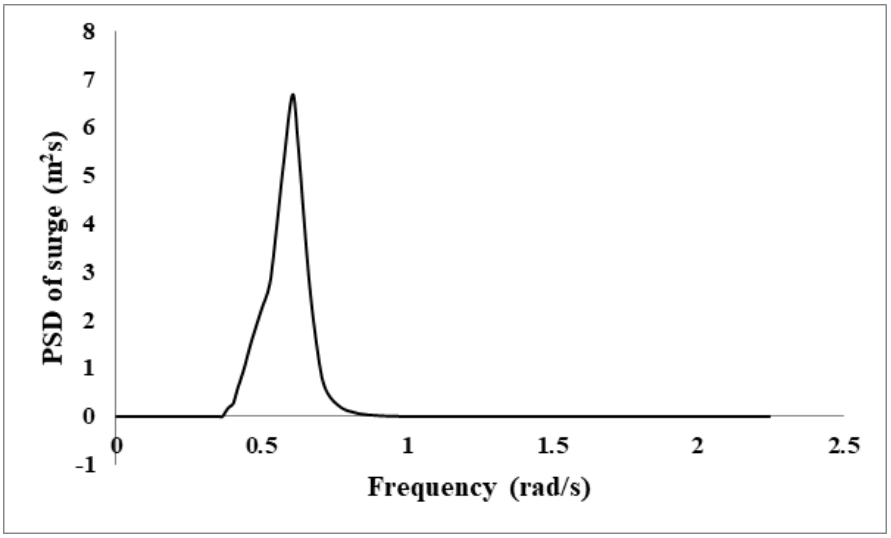

Fig. 6.22 (b) PSD of surge motion of tower Load case3 (Hs=8.46m, Tp=10.13s, V=38.76m/s)

The time history of pitch response of tower for Load case 3 is compared for both the cases and shown in Fig.6.23. The pitch response of tower is very less and remains almost same for both the cases.

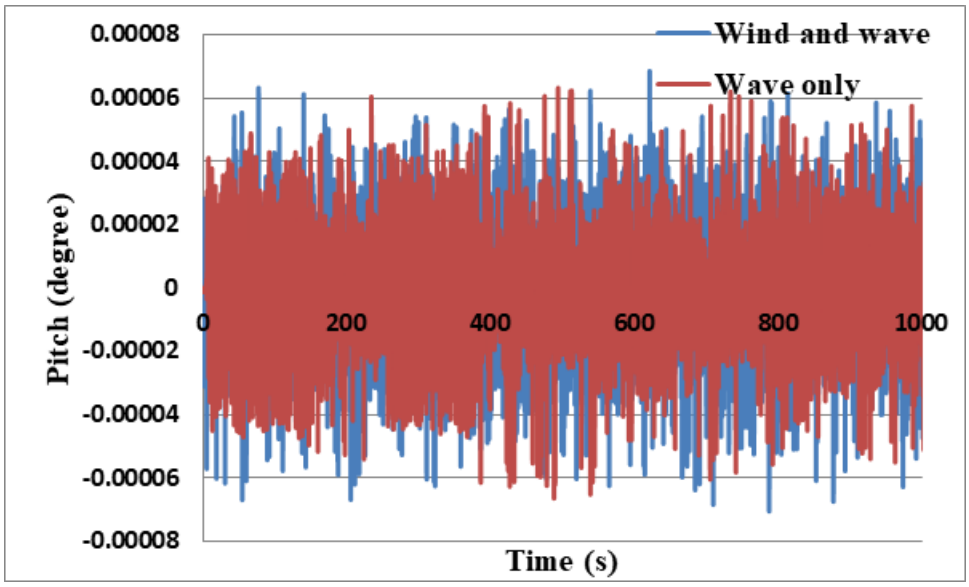

Fig. 6.23 Time history of Pitch of tower Load case3 (Hs=8.46m, Tp=10.13s, V=38.76m/s)

The time history of pitch response of leg for Load case 3 is compared for both the cases and shown in Fig.6.24. Due to the combined action of wind and wave, a shift in the mean position is observed, but the shift is lesser than the other load cases.

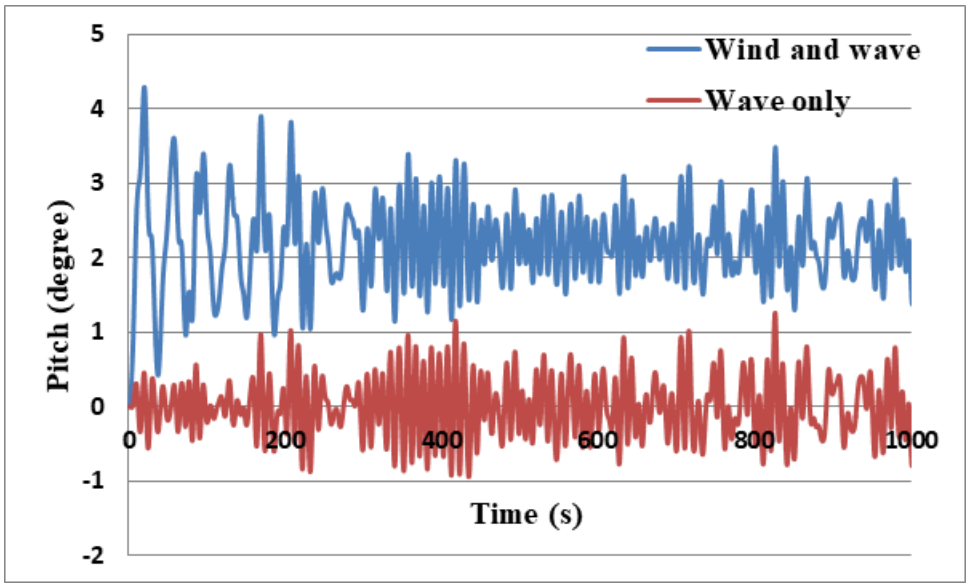

Fig. 6.24 Time history of Pitch of leg Load case3 (Hs=8.46m, Tp=10.13s, V=38.76m/s)

The power spectral density function of the pitch response of articulated leg for Load case 3 for both the cases is compared in Fig.6.25. It is shown that the presence of wind does not alter the energy content of the pitch power spectral density function. The peak occurs at 0.6 rad/s for both the cases. The peak value of PSD for the wave only case is 0.79 degree^{2}s (Fig.6.25a) and for the combined action of wind and wave the peak value is 0.8 degree^{2}s (Fig.6.25b).

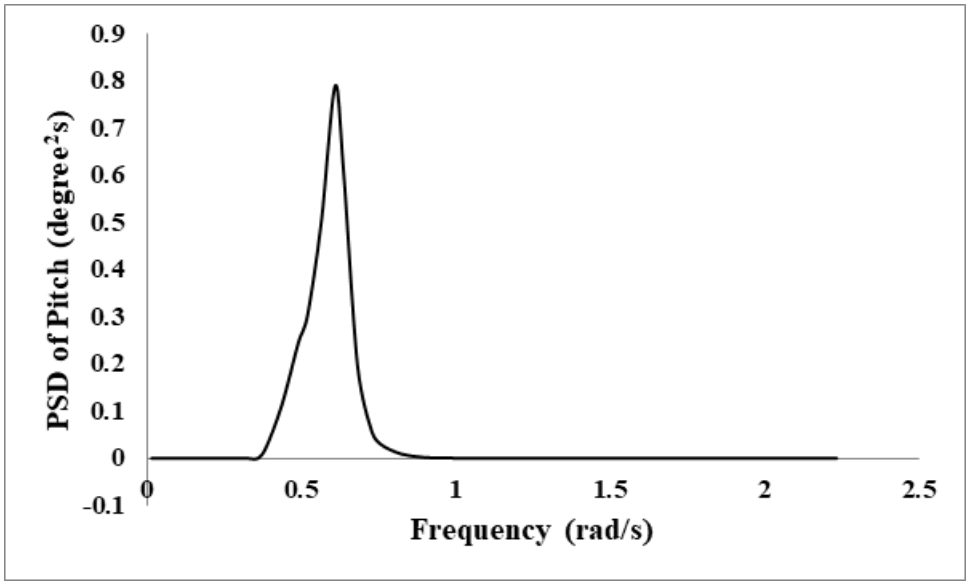

Fig. 6.25 (a) PSD of pitch motion of leg Load case3 (Hs=8.46m, Tp=10.13s, Wave only)

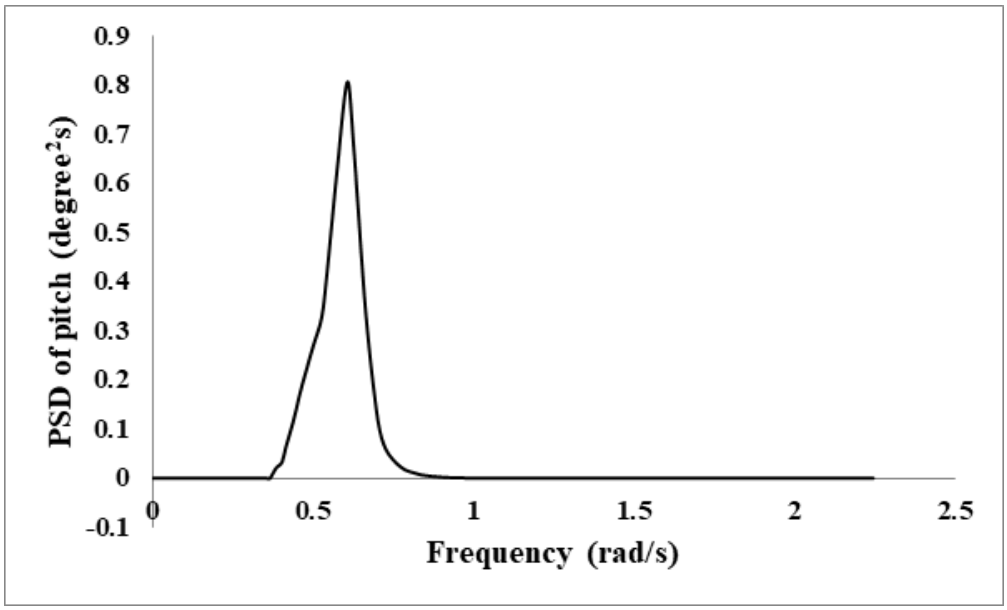

Fig. 6.25 (b) PSD of pitch motion of leg Load case3 (Hs=8.46m, Tp=10.13s, V=38.76m/s)

Time history of pitch response of articulated leg and tower for load case 3 is shown in Fig.6.26. Compared to the pitch response of articulated leg, the response of tower is very less in this load case also. This reduced response of tower, when compared to that of the legs shall be attributed to the presence of the articulated joints between the beams and the legs.

The statistical values of surge and pitch responses for all considered load cases are given in Table 6.5. Fig.6.27 depicts the surge motion of the tower when subjected to wave only and combined wind and wave cases.

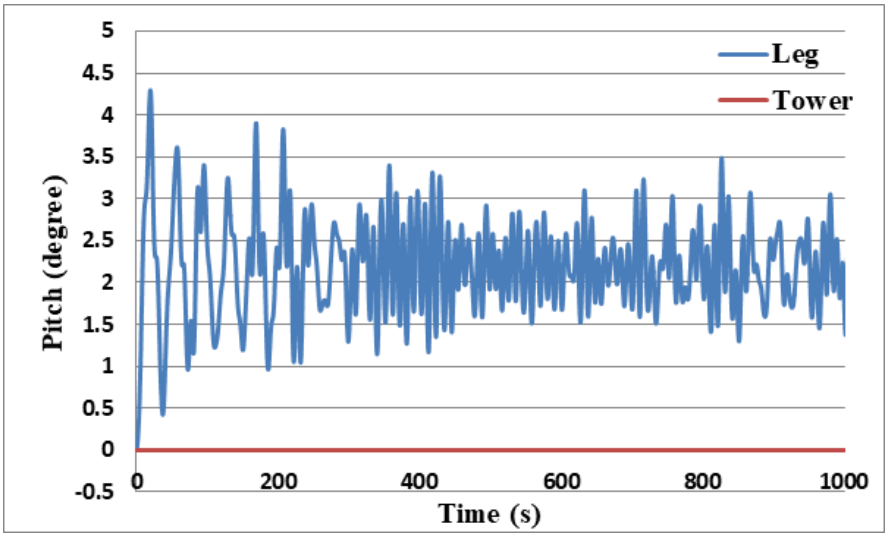

Fig. 6.26 Time history of Pitch of leg and tower Load case3 (Hs=8.46m, Tp=10.13s, V=38.76m/s)

Table 6.5 Statistical values of surge and pitch responses

Load Case	Statistics	Surge (m)		Pitch (degree)	
		Wave only	Wind and wave	Wave only	Wind and wave
Load case0	Maximum	0.02	2.42	8.9×10^{-6}	7.2×10^{-5}
	Minimum	-0.03	0.00	-9.1×10^{-6}	-7.2×10^{-5}
	Mean	0.00	1.22	1.4×10^{-8}	1.5×10^{-7}
	Standard Deviation	0.01	0.31	3.0×10^{-6}	1.9×10^{-5}
Load case1	Maximum	1.43	8.58	6.5×10^{-5}	7.3×10^{-5}
	Minimum	-1.28	0.00	-6.5×10^{-5}	-7.3×10^{-5}
	Mean	0.00	4.37	-9.4×10^{-9}	-5.9×10^{-7}
	Standard Deviation	0.39	0.69	1.6×10^{-5}	1.9×10^{-5}
Load case2	Maximum	2.94	5.81	6.3×10^{-5}	6.4×10^{-5}
	Minimum	-2.71	-0.16	-6.7×10^{-5}	-7.3×10^{-5}
	Mean	0.01	2.61	2.7×10^{-9}	-9.4×10^{-7}
	Standard Deviation	0.74	0.84	1.5×10^{-5}	1.9×10^{-5}
Load case3	Maximum	3.98	12.36	6.3×10^{-5}	7.1×10^{-5}
	Minimum	-2.88	0.00	-7.1×10^{-5}	-7.1×10^{-5}
	Mean	0.02	6.32	-8.3×10^{-9}	3.1×10^{-7}
	Standard Deviation	1.12	1.32	1.7×10^{-5}	1.8×10^{-5}

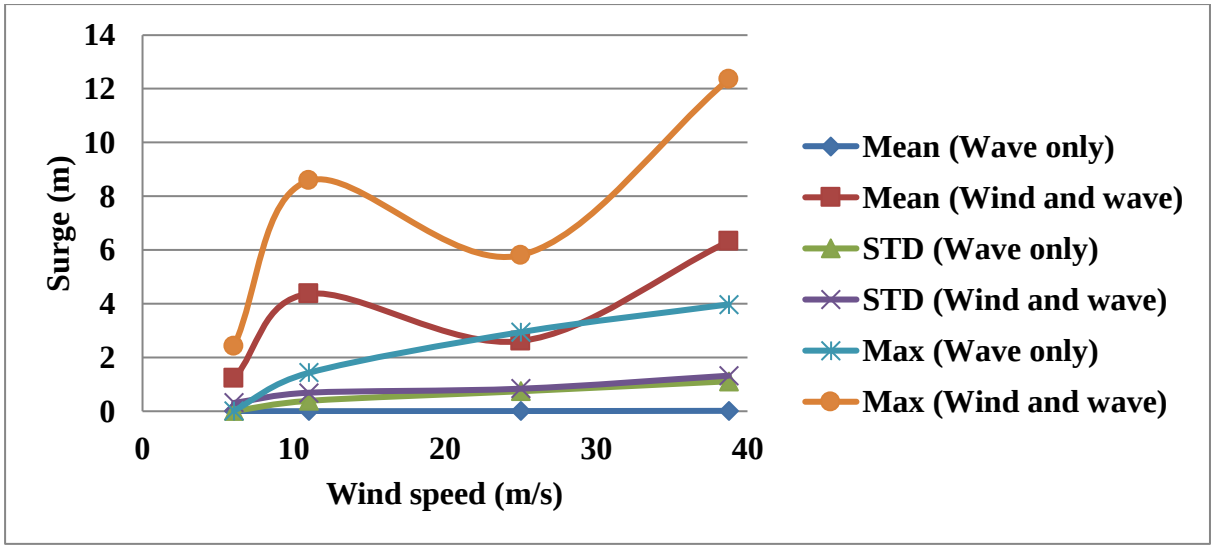

Fig. 6.27 Surge motion when subjected to wave only and combined wind and wave

The variation in mean value and maximum value are seen under the combined action of wind and wave. The mean value for wave only case is zero for all the load cases. There is not much variation in the value of standard deviation is seen under the combined action of wind and wave. These results indicate that the mean value of the responses is mainly wind induced, but the standard deviation is mainly wave induced. Though, the standard deviation of the response for the operational conditions is wind induced, the maximum of the responses under operational conditions is wind induced.

6.4.2 Dynamic response analysis under different sea states

In this section, the motion behaviour of articulated structure (prototype) in actual ocean environments for various sea states is investigated. Time history analyses are carried out in random waves alone and correlated wind and waves are investigated. In the absence of real offshore data for combined wind and wave, theoretical correlation is used. In this investigation, wave and wind are assumed to be correlated i.e. wind generated wave is assumed. The following formula is used to obtain significant wave height (H_s) and zero crossing periods (T_z) corresponding to each wind velocity (Sarpakaya and Isaacson, 1981 as cited in Zaheer and Islam, 2017).

$$u(z) = \sqrt{\frac{gH_s}{0.283}} \quad \text{.....6.6}$$

$$T_z = \sqrt{\frac{32\pi H_s}{g}} \quad \text{.....6.7}$$

Various sea states considered in the investigation are presented in Table 6.6. Each sea state is characterised by wind velocity, zero crossing period and significant wave height. Three cases of wind enabled wave environments are selected corresponding to wind velocities 10 m/s, 15 m/s and 25 m/s. Equations of $u(z)$ and T_z are used to simulate the various sea states. The resulting sea states are named as low (Hs=2.88 m, T_z=5.43 s), moderate (Hs=6.50 m, T_z = 8.15 s) and high (Hs =18.0 m, T_z =13.60 s), respectively.

Table 6.6 Sea state characteristics (Zaheer and Islam, 2017)

Wind velocity (m/s)	Significant wave height (m)	Zero crossing period (s)	Designation of sea state
10	2.88	5.43	low
15	6.50	8.15	moderate
25	18.00	13.60	high

The exact behaviour of the structure is obtained through analysis under random waves. Spectra models are used to represent random waves, which range from zero to infinite frequencies. A spectrum of wave describes the distribution of wave energy as a function of different wave frequencies which gives the total energy transmitted by a wave-field at a specific time. For the analysis of offshore platforms numerous spectral models are in use. In this work the random waves are represented by the most common and widely used spectra, Pierson–Moskowitz spectrum. It is assumed that wave attains the equilibrium state with wind (fully developed sea), if wind blows steadily for several days over a large area. The wave energy density in the Pierson–Moskowitz spectrum is given by

$$S(\omega) = 4\pi^3 \frac{{H_s}^2}{{T_z}^4} \frac{1}{\omega^5} exp\left(-\frac{16\pi^3}{{T_z}^4} \frac{1}{\omega^4}\right) \ldots\ldots\ldots\ldots\ldots\ldots 6.8$$

where, ω is frequency. Spectra plot for various sea states are presented in Fig.6.28. The plot shows a peak for unit frequency ratio. In the time domain analysis, using the above mentioned spectral model, ANSYS AQWA computes the variation of wave amplitude with time and the wave force is calculated. Wave and wind having the same direction are considered for the investigation.

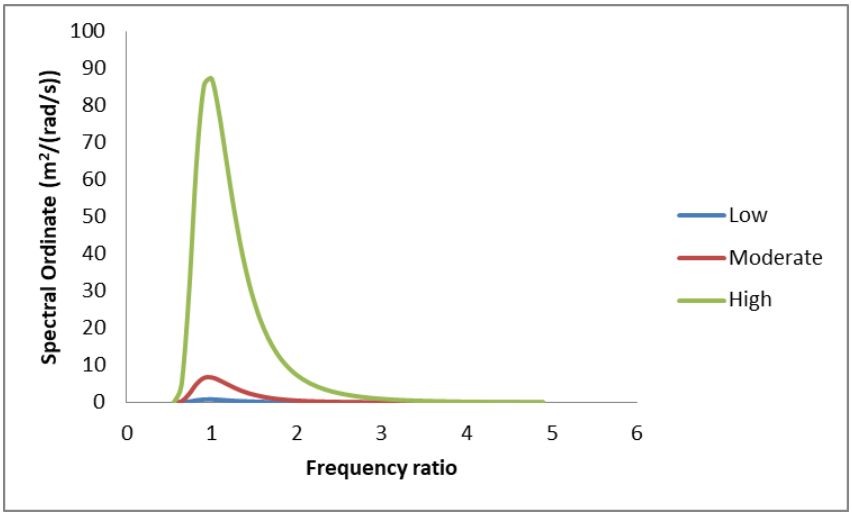

Fig. 6.28 Spectra plot for various sea states

For performing the combined wave and wind induced analysis, time-domain simulations are carried out in ANSYS AQWA on the prototype. The numerical simulations are conductd for investigating the dynamic response of the articulated wind tower caused by:

(i) Wave only

(ii) Combined action of wind and wave

The aerodynamic thrust generated by wind turbine for operating (blades in rotary motion and the control is active) and parked (blades feathered 90 degree and not rotating) cases are calculated and given as a point force at the top of the tower (Zang et al. 2013). In extreme environmental condition, wind turbines are parked. Time domain dynamic analysis is performed on the prototype for 144 m water depth. The time step of 0.1 s is used for the analysis in AQWA. At each time step the position of legs and tower is obtained by the integration of accelerations. For this predictor-corrector numerical integration technique is used by ANSYS AQWA. For obtaining the motion response of the tower and legs, the solution obtained at the end of each time step is used as the initial condition for the next time step. The direction of wave and wind is 0^0 as shown in Fig.6.29

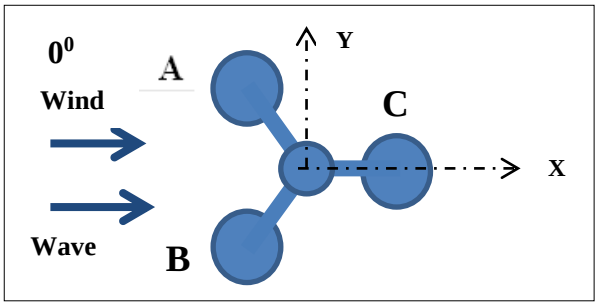

Fig. 6.29 Plan showing direction of wind and wave

6.4.2.1 Motion response of the tower under various sea states

Due to the action of wave and wind, significant responses are observed only in the surge and the responses are negligible in the other degrees of freedom. The statistical parameters of the surge and pitch response of tower at the nacelle under various sea states are presented in Table 6.7. The interesting qualitative and quantitative observations noted are discussed below.

Response under low sea state

In low sea state, under wave alone load case, the surge response is less about 0.44m. Further, the oscillations of the tower are very adjacent to its original position in the surge, which can be observed from the mean value of zero and the standard deviation of 0.131 m. Under the combined wind-wave load case, the total surge response is considerably increased. The effect of wind is found to be significant in this sea state. In this load case, the shift in the mean position is also seen and the value of standard deviation is increased by 4 times. The total pitch response of the tower is very less, 6.73×10^{-5}degrees. Also the addition of wind force does not affect the pitch response considerably in this sea state.

Table 6.7 Tower response under different sea states

Sea state	Statistics	Surge (m)		Pitch (degree)	
		Wave only	Wind and wave	Wave only	Wind and wave
low sea state	Maximum	0.44	6.39	6.73×10^{-5}	7.21×10^{-5}
	Minimum	-0.43	-4.76×10^{-7}	-6.60×10^{-5}	-7.41×10^{-5}
	Mean	0.00	3.35	2.68×10^{-7}	-3.50×10^{-7}
	Standard Deviation	0.13	0.52	1.14×10^{-5}	1.91×10^{-5}
moderate sea state	Maximum	3.66	8.64	6.41×10^{-5}	6.62×10^{-5}
	Minimum	-3.28	-4.76×10^{-7}	-6.50×10^{-5}	-7.10×10^{-5}
	Mean	0.01	4.38	-1.60×10^{-7}	-8.30×10^{-7}
	Standard Deviation	1.03	1.15	1.67×10^{-5}	1.85×10^{-5}
high sea state	Maximum	38.23	41.07	7.72×10^{-7}	7.65×10^{-5}
	Minimum	-22.39	-19.68	-7.00×10^{-5}	-7.50×10^{-5}
	Mean	0.40	3.03	4.82×10^{-7}	1.30×10^{-7}
	Standard Deviation	8.27	8.25	1.78×0^{-5}	1.79×10^{-5}

Response under moderate sea state

In moderate sea state, under wave alone load case, the surge response is 3.66 m. The oscillations of the tower are very adjacent to its original position in the surge in this sea state also, which can be observed from the mean value of 0.01. When the wind load is added along with the wave load, the total surge response is increased by 2.36 times. The shift in the mean surge response is seen and the value of standard deviation is increased by 11.5%. Even in the extreme condition of combined wind-wave load case, the pitch response of the tower is significantly low.

Response under high sea state

In high sea state, due to the combined wind-wave load case, total surge response is 41.07m and the shift in the mean value is also noted. The change in the value of standard deviation is less compared to the other two sea states (low and moderate) which show that the wave forces are mainly responsible for the variation of the responses. As compared to the response obtained under the wave only load case, the increase in surge response due to combined wind-wave load case is only 7%. In this sea state, the effect of wind is found to be significantly low when compared to other sea states. Under high sea state, and wave only load case, the total surge response is 86 times that of the response in low sea state and 10 times that of the response obtained in moderate sea state. At the same time, under the combined wind-wave load case, the surge response is increased by 6.4 times than in low sea state and 4.8 times than in moderate sea state. Therefore, it can be observed that the increased response of articulated tower due to combined wind-wave load case greatly depends upon the sea states. The pitch response of the tower is significantly low under the two load cases in all sea states.

6.4.2.2 Motion response of legs

The tower and the articulated legs act in an independent manner under the action of environmental loads as these structures connected by universal joints. Therefore investigation on the response of both the tower and articulated legs are required to understand the actual behaviour of the structure. With the aim of representing the total behaviour of structure under the combined action of wind and wave, the response of the articulated legs in high sea state are also studied. Only high sea state is selected for describing the motion response of articulated legs because significant responses are observed in the active degree of freedom

(surge) in high sea state compared to other sea states (Nagavinothini and Chandrasekaran, 2019). The statistical parameters of the surge and pitch responses are shown in Table 6.8. The position of the articulated legs is depicted in Fig.6.29.

The response of the articulated legs A, B and C remains the same for 0^0 direction of combined wind-wave loads. The increase in pitch response of articulated legs under combined wind and wave is lesser when compared with the wave only load case. Even though the legs show significant pitch response, it is observed that the pitch response of the tower remains negligible, confirming the effectiveness of articulated joints.

Table 6.8 Response of legs under high sea state

Articulated leg	Statistics	Surge (m)		Pitch (degree)	
		Wave only	Wind and wave	Wave only	Wind and wave
C	Maximum	10.98	11.80	13.40	14.41
	Minimum	-6.43	-5.65	-7.80	-6.85
	Mean	0.11	0.87	0.14	1.05
	Standard Deviation	2.37	2.37	2.87	2.87
A & B	Maximum	10.98	11.8	13.40	14.41
	Minimum	-6.43	-5.65	-7.80	-6.85
	Mean	0.11	0.87	0.14	1.05
	Standard Deviation	2.37	2.37	2.87	2.87

6.4.2.3 Joint shear under various sea states

Fatigue in articulated joints can occur due to the reversal of stresses, so joint shear is a significant parameter. The responses of joint shear in various sea states are evaluated here. The joint shear in both the top and bottom articulated joints in each leg under all load cases, i.e. wave only load and combined wind-wave load are evaluated. The statistical quantities of the joint shear under low, moderate and high sea states are presented in Table 6.9, 6.10, 6.11 respectively.

Time history of joint shear in top and bottom joint of leg C for wave only load under low sea state is compared in Fig.6.30. To understand the influence of wind on the joint shear, the time

history of joint shear in top and bottom joint of leg C for both wave only load and combined wind-wave load under low sea state are depicted in Fig.6.31 and Fig.6.32 respectively.

Table 6.9 Statistical values of joint shear (kN) under low sea state

Articulated leg	Statistics	Bottom Joint		Top Joint	
		Wave only	Wind and wave	Wave only	Wind and wave
C	Maximum	340	236	594	772
	Minimum	-335	-566	-595	-416
	Mean	0	-182	-2	179
	Standard Deviation	94	105	166	167
A & B	Maximum	163	142	361	641
	Minimum	-155	-681	-357	-108
	Mean	0	-269	1	270
	Standard Deviation	45	76	101	103

Table 6.10 Statistical values of joint shear (kN) under moderate sea state

Articulated leg	Statistics	Bottom Joint		Top Joint	
		Wave only	Wind and wave	Wave only	Wind and wave
C	Maximum	926	629	1305	1507
	Minimum	-960	-1123	-1558	-1379
	Mean	-1	-216	-16	196
	Standard Deviation	260	248	406	400
A & B	Maximum	573	217	1055	1467
	Minimum	-610	-1018	-927	-618
	Mean	-1	-365	8	369
	Standard Deviation	158	181	267	280

Table 6.11 Statistical values of joint shear (kN) under high sea state

Articulated leg	Statistics	Bottom Joint		Top Joint	
		Wave only	Wind and wave	Wave only	Wind and wave
C	Maximum	2285	1759	2282	2303
	Minimum	-3460	-3321	-3144	-2828
	Mean	23	-128	-144	-1
	Standard Deviation	734	644	734	690
A & B	Maximum	1320	1212	2959	3522
	Minimum	-3413	-4012	-1906	-1866
	Mean	-79	-291	72	278
	Standard Deviation	592	651	646	702

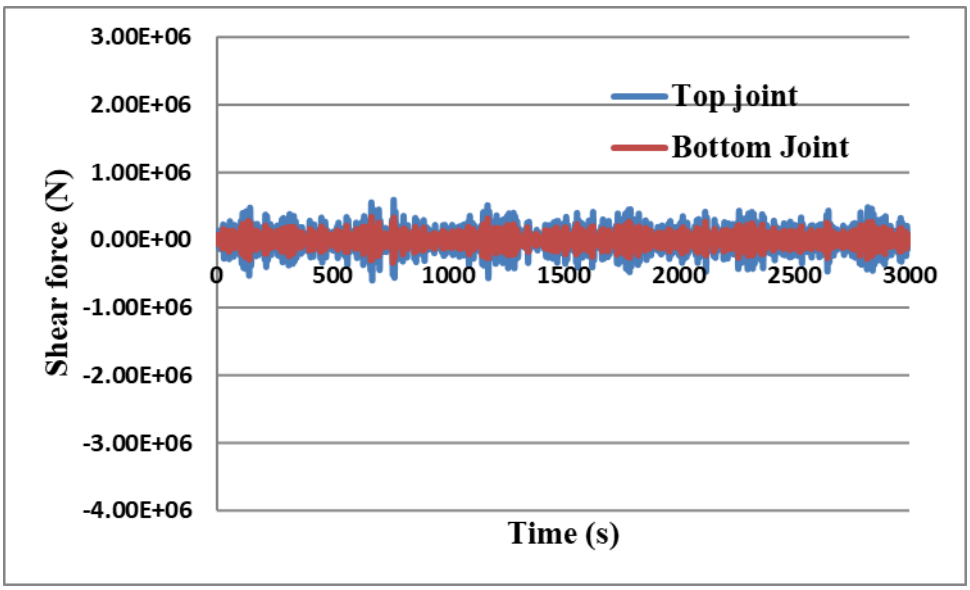

Fig. 6.30 Time history of joint shear in top and bottom joint of leg C for wave only load under low sea state

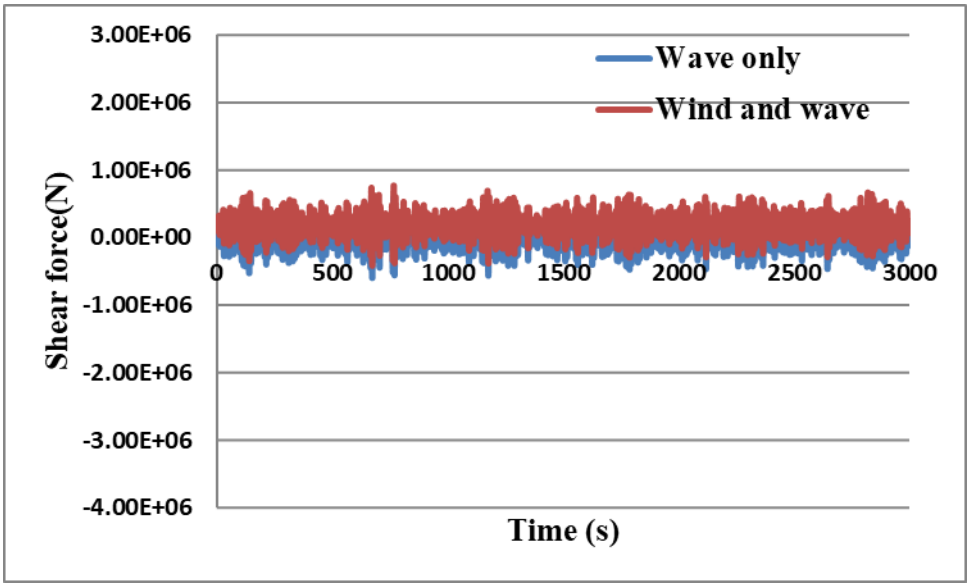

Fig. 6.31 Time history of joint shear in top joint of leg C under low sea state

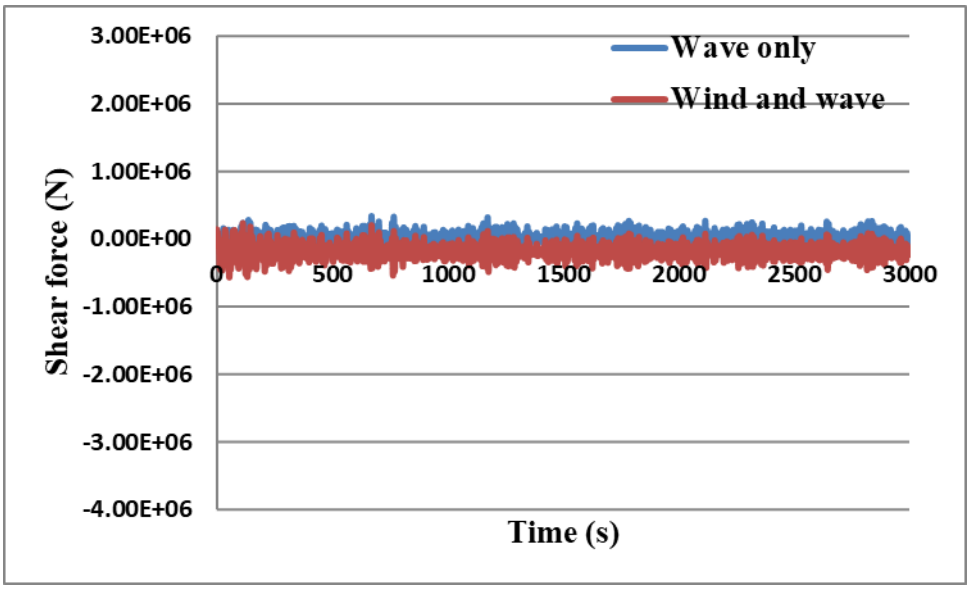

Fig. 6.32 Time history of joint shear in bottom joint of leg C under low sea state

Time history of joint shear in top and bottom joint of leg C for wave only load under moderate sea state is compared in Fig.6.33. To understand the influence of wind on the joint shear, the time history of joint shear in top and bottom joint of leg C for both wave only load and combined wind-wave load under moderate sea state are depicted in Fig.6.34 and Fig.6.35 respectively.

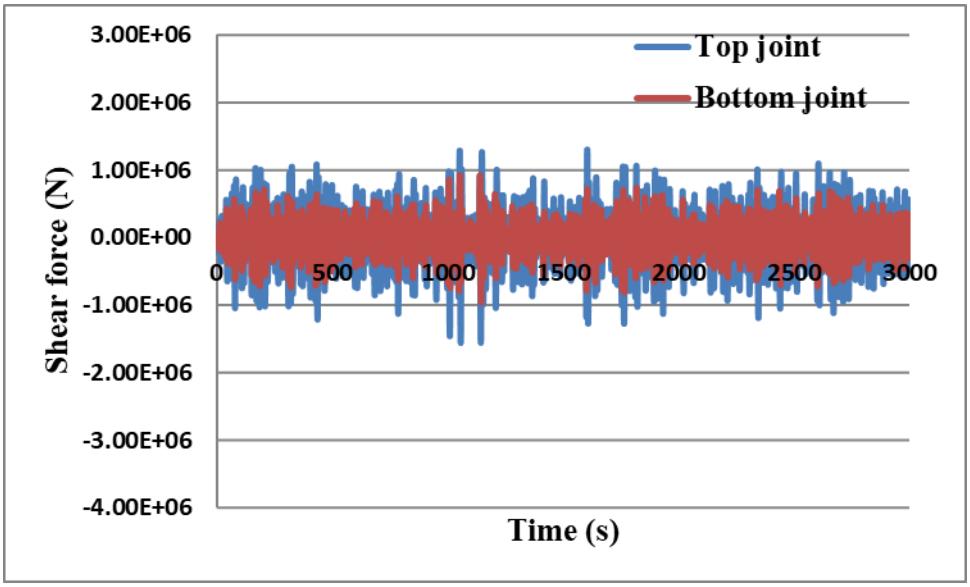

Fig. 6.33 Time history of joint shear in top and bottom joint of leg C for wave only load under moderate sea state

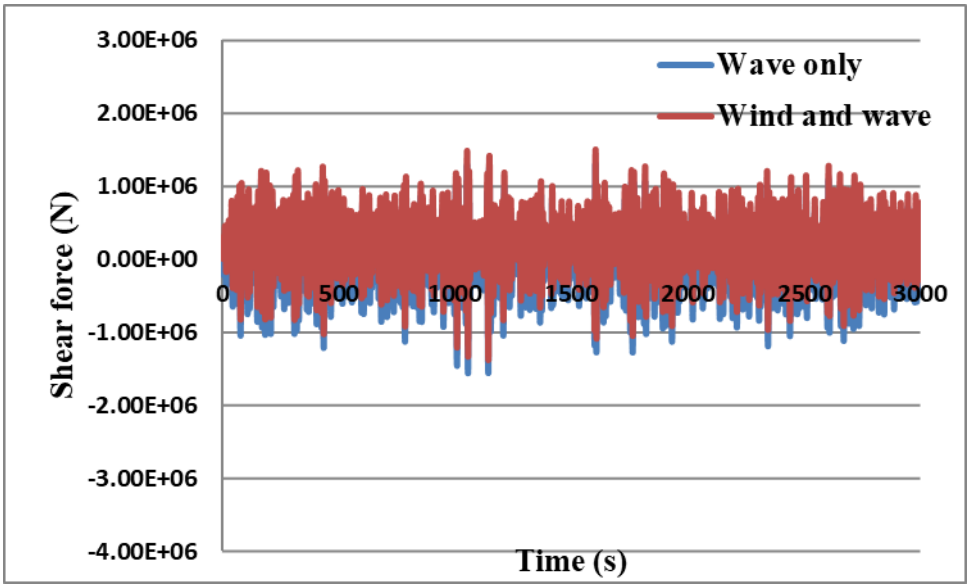

Fig. 6.34 Time history of joint shear in top joint of leg C under moderate sea state

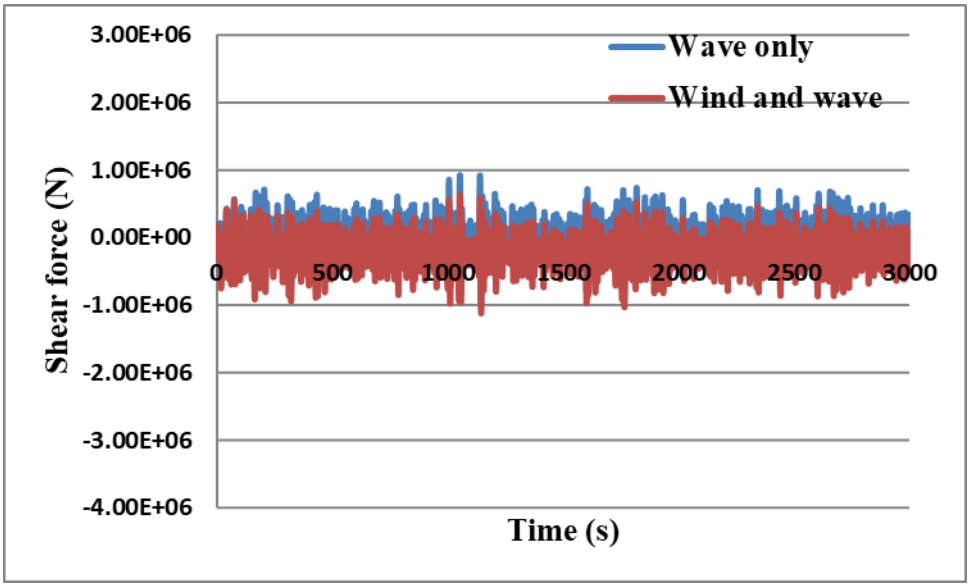

Fig. 6.35 Time history of joint shear in bottom joint of leg C under moderate sea state

Time history of joint shear in top and bottom joint of leg C for wave only load under high sea state is compared in Fig.6.36. To understand the influence of wind on the joint shear, the time history of joint shear in top and bottom joint of leg C for both wave only load and combined wind-wave load under high sea state are depicted in Fig.6.37 and Fig.6.38 respectively.

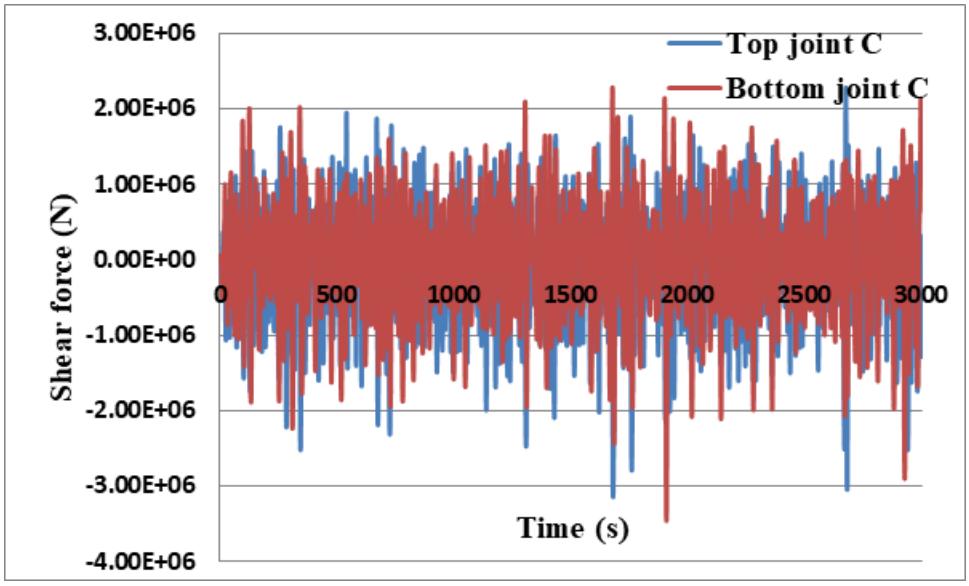

Fig. 6.36 Time history of joint shear in top and bottom joint of leg C for wave only load under high sea state

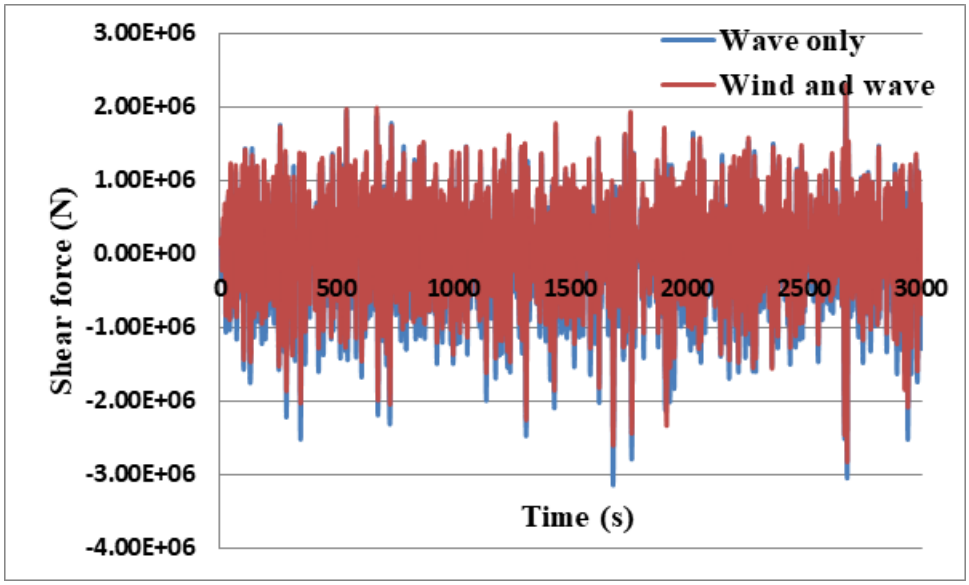

Fig. 6.37 Time history of joint shear in top joint of leg C under high sea state

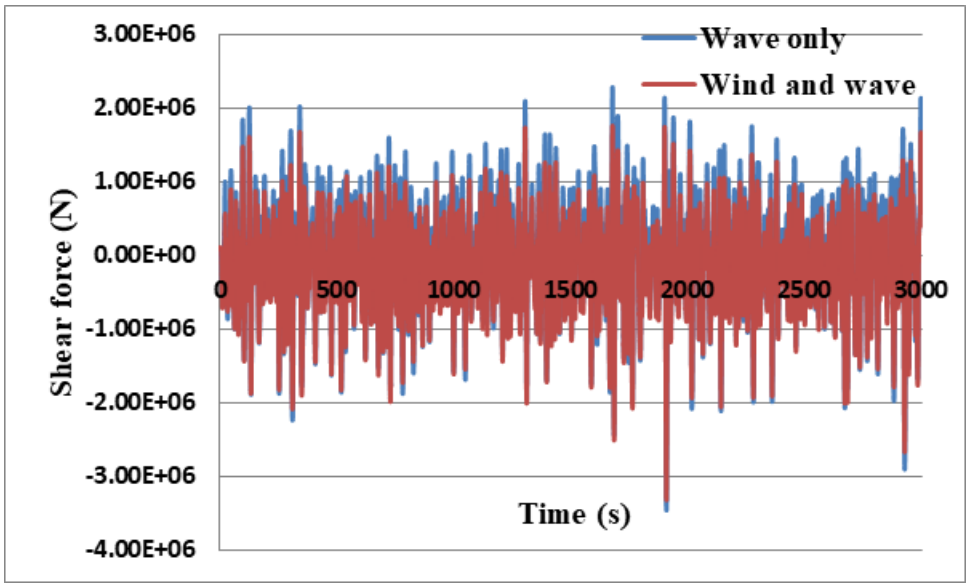

Fig. 6.38 Time history of joint shear in bottom joint of leg C under high sea state

When subjected to wave only environment shear forces at the top joint are higher than the bottom joint under low and moderate sea state. Under high sea state, shear forces are almost the same for both the joints when subjected to wave only environment. For all the sea states a decrease in maximum value and minimum value of shear in the bottom joint are observed which shows the drifting of the legs from its mean position under the combined action of wind and wave. In the top joint, for all the sea states an increase in maximum value and minimum value of shear are observed under the combined action of wind and wave. Shear force in the joints of articulated leg C is higher than in the legs A and B for all the sea states.

6.5 SUMMARY

In this chapter, details of numerical simulation of the prototype of three-legged articulated platform is presented. The numerical investigations are conducted on the prototype under regular waves and random waves, for wave induced as well as wind-wave induced cases to study the actual behaviour of the structure. Analyses are done for various sea states. The responses of the tower as well as legs and the shear forces in the joints are also evaluated for obtaining the complete behaviour of the designed platform. The results reveal that the proposed three-legged articulated wind tower is an appropriate one for supporting an offshore wind turbine.

CHAPTER 7

SUMMARY AND CONCLUSION

7.1 SUMMARY

The research work is conducted to design an innovative concept, a three-legged articulated support for an offshore wind turbine. The behaviour of the scaled physical model is investigated experimentally and numerically and comparisons made. Further, to study the complete behaviour of this compliant support system under the actual ocean environment, a numerical investigation on the dynamic response characteristics of the prototype under different sea states are evaluated for wave induced as well as wind-wave induced cases. The details of the study conducted are given below.

i. A three-legged articulated support is proposed and designed to support the NREL 5 MW reference turbine in a water depth of 144 m.
ii. A 1:60 scale model of a prototype is developed in compliance with the available water depth in the testing facility at the Department of Ocean Engineering, IIT Madras.
iii. The experimental investigations are conducted in the wave flume using the scale model of the three-legged articulated platform. The experiment is carried out for a wave period ranging from 1 s to 2.75 s at an interval of 0.25 s and for three wave heights 8 cm, 10 cm and 12 cm, for three orientations of the platform – 0^0, 90^0 and 180^0.
iv. The numerical model of the scale model of three-legged articulated tower is developed using ANSYS AQWA. The numerical simulation is performed for the same cases in ANSYS AQWA. The results obtained are validated with the experimental results.
v. Numerical investigations on the dynamic response of the prototype for the three-legged articulated platform under various environmental conditions is also conducted to test the suitability of the proposed structure.

7.2 CONCLUSIONS

Based on the investigations conducted to study the behavior of the designed three-legged articulated wind tower, the highlights and principal conclusions are:

- Free vibrations tests on the designed three-legged articulated platform revealed that the frequencies are away from the operational ocean wave periods. The free oscillation results from the numerical simulation compared well with the experiment. The surge and sway natural periods variations are within 12% and 9% respectively.

- It is found that the surge motion dominates the other motions. Sway and roll responses are negligibly small as expected. This assures that the nacelle axis is always horizontal. The universal joints provided at the top of the legs retain the top disc in a horizontal position while the structure is moving with the waves.

- The numerical simulations are validated against the experiments conducted and are demonstrated through favourable comparison of RAO in the predominant degree of freedom (surge). Deviation is found in pitch response of the tower as numerical model is not able to predict the frictional resistance offered by the articulated joint.

- From the numerical investigations on the prototype, the natural periods of surge, sway and yaw are found to be 37.4 s, 37.4 s and 34.1 s respectively. The natural periods for these modes do not fall in the range of typical wave periods (5 to 17 s).

- From the regular wave analysis on the prototype, it is shown that surge RAO reaches its peak at the corresponding natural frequency indicating less coupling with other modes.

- From the responses corresponding to different wave directions, it is concluded that orientation with respect to predominant wave direction during installation of the platform, is useful to reduce the response of the structure.

- From the numerical investigations on the prototype, it is found that due to the action of wave and wind, significant responses are only in the surge and the responses are negligible in the other degrees of freedom.

- The effect of wind is observed to be significant in the low sea state. Under the combined wind-wave load case, the total surge response is considerably increased.

- In moderate sea state, under wave alone load case, the oscillations of the tower are very close to its original position in surge but when the wind load is added along with the wave load, the shift in the mean value of surge response is seen and the value of standard deviation is increased.

- In high sea state, the effect of wind is observed to be significantly low when compared to other sea states. Under high sea state, wave alone load case, the total surge response is 86 times that of the response in low sea state and 10 times that of the response in moderate sea state. At the same time, under the combined wind-wave load case, the surge response is increased by 6.4 times than in low sea state and 4.8 times than in moderate sea state.

- The increase in the response of articulated tower due to combined wind-wave load case greatly depends upon the sea states.

- Even under the combined wind-wave load case, the pitch response of the tower is significantly low in all sea states.

- The tower shows a lesser rotational response compared to the legs due to the presence of the articulated joints between the tower and the legs in the design. These joints restrict the transfer of rotational responses from legs to the tower.

- When subjected to wave only environment shear forces at the top joint are greater than the bottom joint in low and moderate sea state. Under high sea state, shear forces are almost the same for both the joints when subjected to wave only environment.

- For all the sea states a decrease in maximum value and the minimum value of shear in the bottom joint are observed which shows the drifting of the centre of

gravity of the legs from its mean position due to the combined action of wind and wave.

- In the top joint, for all the sea states an increase in maximum value and minimum value of shear are observed.

- Shear force in the joints of articulated leg C is higher than in the legs A and B for all the sea states.

- The results show a stable dynamic behaviour of the structure which implies that the proposed three-legged articulated wind tower is a promising solution for offshore wind technology.

7.3 SCOPE FOR FUTURE WORK

The main recommendation for future work is to pursue experimental work in random waves by generating wind loads along with the wave loads using fans and a rotor to model gyroscopic effects. The numerical simulation of aero-hydro coupling on dynamic response of three-legged articulated tower during the operation of the wind turbine can also be investigated

LIST OF PUBLICATIONS

Publications:

Chinsu Mereena Joy, Anitha Joseph, Lalu Mangal, An Overview of Offshore Wind Energy Tower Designs, J. Inst. Eng. India Ser. C, The Institution of Engineers (India) 2019, (October 2019) 100(5): 841–850.

Paper presentation in Conferences:

Chinsu Mereena Joy, Anitha Joseph, Lalu Mangal, Experimental Investigation on the Dynamic Response of a Three legged Articulated Type Offshore Wind Tower, ASME 35th International Conference on Ocean, Offshore and Arctic Engineering OMAE2016, 19-06-2016 to 24-06-2016, Busan, Korea

Chinsu Mereena Joy, Anitha Joseph, Lalu Mangal, Numerical Analysis of Three Legged Articulated Tower Supporting 5MW Offshore Wind Turbine, International Conference on Innovative Trends in Civil Engineering for Sustainable Development (ITCSD - 2019), NIT Warangal, 13 - 15 September 2019

Vivek Philip, Anitha Joseph, Chinsu Mereena Joy, Three Legged Articulated Support for 5 MW Offshore Wind Turbine International Conference on Water Resources, Coastal and Ocean Engineering (ICWRCOE 2015), Elsevier Aquatic Procedia 4, (2015), 500-507

Deepak Vijay, Chinsu Mereena Joy, Anitha Joseph, Coupled Dynamic Analysis of 5mw Offshore Wind Turbine Supported on Three Legged Articulated Tower in Fast Under Regular Waves, Third International Conference on Modeling and Simulation in Civil Engineering, Dept. of Civil Engg, TKM College of Engineering, Kollam, Dec 9-11, 2015

REFERENCES

1. **Abhinav, K.A. and Saha, N.,** 2015. Coupled hydrodynamic and geotechnical analysis of jacket offshore wind turbine. Soil Dynamics and Earthquake Engineering, 73, pp.66-79.
2. **Adrezin, R., Bar-Avi, P. and Benaroya, H.,** 1996. Dynamic response of compliant offshore structures. Journal of aerospace engineering, 9(4), pp.114-131.
3. **Atreya, P., Islam, N., Alam, M. and Hasan, S.D.,** 2014. Dynamic Stability of Articulated Offshore Tower under Seismic Loading. International Journal of Engineering and Innovative Technology, 4(2), pp.137-147.
4. **Bachynski, E.E. and Moan, T.,** 2012. Design considerations for tension leg platform wind turbines. Marine Structures, 29(1), pp.89-114.
5. **Bae, Y.H. and Kim, M.H**., 2013. Rotor-floater-tether coupled dynamics including second-order sum–frequency wave loads for a mono-column-TLP-type FOWT (floating offshore wind turbine). Ocean Engineering, 61, pp.109-122.
6. **Bae, Y.H. and Kim, M.H.,** 2014. Coupled dynamic analysis of multiple wind turbines on a large single floater. Ocean Engineering, 92, pp.175-187.
7. **Bagbanci, H., Karmakar, D. and Guedes Soares, C.,** 2011. November. Dynamic analysis of spar-type floating offshore wind turbine. In 2nd Proceeding of Coastal and Maritime Mediterranean Conference, Tangier, Morocco, pp.407-412.
8. **Banik, A.K. and Datta, T.K.,** 2003. January. Stochastic response and stability analysis of single leg articulated tower. In International Conference on Offshore Mechanics and Arctic Engineering, Vol. 36827, pp.21-28.
9. **Banik, A.K. and Datta, T.K.,** 2008. Stability analysis of an articulated loading platform in regular sea. Journal of computational and nonlinear dynamics, 3(1): 011013
10. **Bar-Avi, P. and Benaroya, H.,** 1997. Stochastic response of a two DOF articulated tower. International journal of non-linear mechanics, 32(4), pp.639-655.
11. **Bulder, B.H., Van Hees, M.T., Henderson, A., Huijsmans, R.H.M., Pierik, J.T.G., Snijders, E.J.B., Wijnants, G.H. and Wolf, M.J.,** 2002. Study to feasibility of and boundary conditions for floating offshore wind turbines. ECN, MARIN, TNO, TUD, MSC, Lagerway the Windmaster, 26, pp.70-81.

12. **Butterfield, S., Musial, W., Jonkman, J. and Sclavounos, P**., 2007. Engineering challenges for floating offshore wind turbines (No. NREL/CP-500-38776). National Renewable Energy Lab.(NREL), Golden, CO (United States).
13. **Cermelli, C., Roddier, D. and Aubault, A.,** 2009. January. WindFloat: a floating foundation for offshore wind turbines—part II: hydrodynamics analysis. In International Conference on Offshore Mechanics and Arctic Engineering, Vol. 43444, pp.135-143.
14. **Chakrabarti, S. K.,** 1994. Offshore structure modeling World Scientific, Singapore (Vol. 9).
15. **Chandrasekaran S., Bhaskar K., Harilal L. and Brijith R.,** 2010. Dynamic Response Behaviour Of Multi -Legged Articulated Tower With & Without TMD, Proceedings of MARTEC 2010, The International Conference on Marine Technology, BUET, Dhaka, Bangladesh
16. **Chandrasekaran, S. and Madhuri, S.,** 2015. Dynamic response of offshore triceratops: numerical and experimental investigations. Ocean Engineering, 109, pp. 401-409.
17. **Cheema, A., Zhu, M., Chai, S., Chin, C.K.H. and Jin, Y.,** 2014. Motion response of a floating offshore wind turbine foundation. In 19th Australasian Fluid Mechanics Conference, pp.1-4.
18. **Collu, M., Kolios, A.J., Chahardehi, A. and Brennan, F.P.,** 2010. A comparison between the preliminary design studies of a fixed and a floating support structure for a 5 MW offshore wind turbine in the North Sea. RINA, Royal Institution of Naval Architects-Marine Renewable and Offshore Wind Energy-Papers, p.63.
19. **Council, G.W.E., 2018.** Global Wind Energy Report: Annual Market Update 2017. Global Wind Energy Council: Bruxelles, Belgium.
20. **Datta, T.K. and Jain, A.K.,** 1990. Response of articulated tower platforms to random wind and wave forces. Computers & structures, 34(1), pp.137-144.
21. **Duan, F., Hu, Z. and Niedzwecki, J.M.,** 2016. Model test investigation of a spar floating wind turbine. Marine Structures, 49, pp.76-96.
22. **Fulton, G.R., Malcolm, D.J., Elwany, H., Stewart, W., Moroz, E. and Dempster, H.,** 2007. Semi-Submersible platform and anchor foundation systems for wind turbine support: Agosto 30, 2004–Mayo 31, 2005. Proceedings of Concept Marine Associates Inc. Long Beach, California..

23. **Goupee, A.J., Koo, B.J., Kimball, R.W., Lambrakos, K.F. and Dagher, H.J.,** 2014. Experimental comparison of three floating wind turbine concepts. Journal of Offshore Mechanics and Arctic Engineering, 136(2).
24. **Guerrero-Lemus, R. and Martínez-Duart, J.M.,** 2013. Renewable Energy and CO_2: Current Status and Costs. In Renewable Energies and CO_2, Springer, London. pp.9-33.
25. **Gutierrez, J.E., Zamora, B., García, J. and Peyrau, M.R.,** 2013. Tool development based on FAST for performing design optimization of offshore wind turbines: FASTLognoter. Renewable energy, 55, pp.69-78.
26. **Hasan, S.D., Islam, N. and Moin, K.,** 2011. Multihinged articulated offshore tower under vertical ground excitation. Journal of Structural Engineering, 137(4), pp.469-480.
27. **Huang, Y. and Wan, D.,** 2020. Investigation of Interference Effects Between Wind Turbine and Spar-Type Floating Platform Under Combined Wind-Wave Excitation. Sustainability, 12(1), p.246.
28. **Iijima, K., Kim, J. and Fujikubo, M.,** 2010, January. Coupled aerodynamic and hydroelastic analysis of an offshore floating wind turbine system under wind and wave loads. In International Conference on Offshore Mechanics and Arctic Engineering, 49118, pp.241-248.
29. **Ishihara, T., Phuc, P.V., Sukegawa, H., Shimada, K. and Ohyama, T.,** 2007. July. A study on the dynamic response of a semi-submersible floating offshore wind turbine system Part 1: A water tank test. In Proceedings of the 12th International Conference on Wind Engineering, pp.2511-2518.
30. **Islam, N., Zaheer, M.M. and Ahmed, S.,** 2009. Double hinged articulated tower interaction with wind and waves. Journal of Wind Engineering and Industrial Aerodynamics, 97(5-6), pp.287-297.
31. **Jeon, S.H., Cho, Y.U., Seo, M.W., Cho, J.R. and Jeong, W.B.,** 2013. Dynamic response of floating substructure of spar-type offshore wind turbine with catenary mooring cables. Ocean Engineering, 72, pp.356-364.
32. **Jonkman, J. and Sclavounos, P.,** 2006. January. Development of fully coupled aeroelastic and hydrodynamic models for offshore wind turbines. In 44th AIAA Aerospace Sciences Meeting and Exhibit, p.995.
33. **Jonkman, J.M. and Buhl Jr, M.L.,** 2005. FAST user's guide. National Renewable Energy Laboratory, Golden, CO, Technical Report No. NREL/EL-500-38230.

34. **Jonkman, J.M. and Buhl Jr, M.L.,** 2007. Loads analysis of a floating offshore wind turbine using fully coupled simulation (No. NREL/CP-500-41714). National Renewable Energy Lab.(NREL), Golden, CO (United States).
35. **Jonkman, J.M.,** 2009. Dynamics of offshore floating wind turbines—model development and verification. Wind Energy: An International Journal for Progress and Applications in Wind Power Conversion Technology, 12(5), pp.459-492.
36. **Kaldellis, J.K. and Kapsali, M.,** 2013. Shifting towards offshore wind energy—Recent activity and future development. Energy policy, 53, pp.136-148.
37. **Karimirad M. and Michailides C.,** 2015. V-shaped semisubmersible offshore wind turbine: An alternative concept for offshore wind technology. Renewable Energy. 83, pp.126-143.
38. **Karimirad, M. and Moan, T.,** 2012. A simplified method for coupled analysis of floating offshore wind turbines, Marine Structures, 27 (1), pp.45-63.
39. **Karimirad, M. and Moan, T.,** 2012. Feasibility of the application of a spar-type wind turbine at a moderate water depth. Energy Procedia, 24, pp.340-350.
40. **Kausche, M., Adam, F., Dahlhaus, F. and Großmann, J.,** 2018. Floating offshore wind-Economic and ecological challenges of a TLP solution. Renewable Energy, 126, pp.270-280.
41. **Kirk, C.L. and Jain, R.K.,** 1978. Response of articulated towers to waves and current. Society of Petroleum Engineers Journal, 18(05), pp.283-290.
42. **Koo, B.J., Goupee, A.J., Kimball, R.W. and Lambrakos, K.F.**, 2014. Model tests for a floating wind turbine on three different floaters. Journal of Offshore Mechanics and Arctic Engineering, 136 (2), p.020907.
43. **Kota, S., Bayne, S.B. and Nimmagadda, S.,** 2015. Offshore wind energy: a comparative analysis of UK, USA and India. Renewable and Sustainable Energy Reviews, 41, pp.685-694.
44. **Le, C., Li, Y. and Ding, H.,** 2019. Study on the coupled dynamic responses of a submerged floating wind turbine under different mooring conditions. Energies, 12(3), p.418.
45. **Lee, J.H. and Kim, J.K.,** 2015. Dynamic response analysis of a floating offshore structure subjected to the hydrodynamic pressures induced from seaquakes. Ocean Engineering, 101, pp.25-39.
46. **Lee, K.H.,** 2005. Responses of floating wind turbines to wind and wave excitation Doctoral dissertation, Massachusetts Institute of Technology.

47. **Lefebvre, S. and Collu, M.,** 2012. Preliminary design of a floating support structure for a 5 MW offshore wind turbine. Ocean Engineering, 40, pp.15-26.
48. **Liu, Y., Xiao, Q., Incecik, A.,** 2017. Establishing a fully coupled CFD analysis tool for floating offshore wind turbines. Renewable Energy, 112, p. 280–301.
49. **Martin, H.R.**, 2011. Development of a scale model wind turbine for testing of offshore floating wind turbine systems, MSc. Thesis; University of Maine, Orono.
50. **Martin, H.R., Kimball, R.W., Viselli, A.M. and Goupee, A.J.,** 2014. Methodology for wind/wave basin testing of floating offshore wind turbines. Journal of Offshore Mechanics and Arctic Engineering, 136(2).
51. **Matha, D.,** 2010. Model development and loads analysis of an offshore wind turbine on a tension leg platform with a comparison to other floating turbine concepts: April 2009 (No. NREL/SR-500-45891), National Renewable Energy Lab (NREL), Golden, CO (United States).
52. **Matsukuma, H. and Utsunomiya, T.,** 2008. Motion analysis of a floating offshore wind turbine considering rotor-rotation, The IES Journal Part A: Civil & Structural Engineering, 1(4), pp.268-279.
53. **Moon III, W.L. and Nordstrom, C.J.,** 2010. February. Tension leg platform turbine: A unique integration of mature technologies. In Proceedings of the 16th offshore Symposium, Texas section of the society of Naval architects and marine engineers, pp. A25-A34.
54. **Mostafa, N., Murai, M., Nishimura, R., Fujita, O. and Nihei, Y.,** 2012. Study of motion of spar-type floating wind turbines in waves with effect of gyro moment at inclination. Journal of Naval Architecture and Marine Engineering, 9 (1), pp. 67-79.
55. **Moulas, D., Shafiee, M. and Mehmanparast, A.,** 2017. Damage analysis of ship collisions with offshore wind turbine foundations. Ocean Engineering, 143, pp.149-162.
56. **Murai, M. and Nishimura, R.,** 2010. May. A study on an experiment of behavior of a SPAR type offshore wind turbine considering rotation of wind turbine blades. In OCEANS'10 IEEE SYDNEY, pp. 1-8.
57. **Murtedjo, M., Djarmiko, E.B. and Sudjianto, H.,** 2005. The influence of buoyancy parameters on the dynamic behavior of articulated tower, Jurnal Mekanikal, 19 (1).
58. **Musial, W., Butterfield, S. and Boone, A.,** 2004. January. Feasibility of floating platform systems for wind turbines. In 42nd AIAA aerospace sciences meeting and exhibit p.1007.

59. **Myhr, A. and Nygaard, T.A.,** 2014**.** Experimental results for tension-leg-buoy offshore wind turbine platforms. Journal of Ocean and Wind Energy, ISOPE, 1(4), pp. 217-224.
60. **Myhr, A., Bjerkseter, C., Ågotnes, A. and Nygaard, T.A.,** 2014. Levelised cost of energy for offshore floating wind turbines in a life cycle perspective. Renewable energy, 66, pp.714-728.
61. **Nagamani, K. and Ganapathy, C.,** 2000. The dynamic response of a three-leg articulated tower, Ocean engineering, 27 (12), pp.1455-1471.
62. **Nagavinothini, R. and Chandrasekaran, S.,** 2019. Dynamic analyses of offshore triceratops in ultra-deep waters under wind, wave, and current. Structures, 20, pp.279–289.
63. National Offshore Wind Energy Policy, Government of India 2015. http://mnre.gov.in/file-manager/UserFiles/draft-national-policyfor-offshore-ind.pdf. Accessed Nov 2015
64. **Nejad, A.R., Bachynski, E.E., Kvittem, M.I., Luan, C., Gao, Z. and Moan, T.,** 2015. Stochastic dynamic load effect and fatigue damage analysis of drivetrains in land-based and TLP, spar and semi-submersible floating wind turbines. Marine Structures, 42, pp.137-153.
65. **Oguz, E., Clelland, D., Day, A.H., Incecik, A., López, J.A., Sánchez, G. and Almeria, G.G.,** 2018. Experimental and numerical analysis of a TLP floating offshore wind turbine. Ocean Engineering, 147, pp.591-605.
66. **Philippe, M., Babarit, A., Ferrant, P.,** 2013. Modes of response of an offshore wind turbine with directional wind and waves, Renewable Energy, 49, pp.151–155.
67. **Purohit, P. and Michaelowa, A.,** 2007. Potential of wind power projects under the Clean Development Mechanism in India. Carbon Balance and Management, 2(1), p.8.
68. **Roddier, D., Cermelli, C. and Weinstein, A.,** 2009. WindFloat: a floating foundation for offshore wind turbines—part I: design basis and qualification process. In ASME 2009 28th International Conference on Ocean, Offshore and Arctic Engineering, May, pp. 845-853.
69. **Ruzzo, C., Fiamma, V., Nava, V., Collu, M., Failla, G. and Arena, F.,** 2016. Progress on the experimental set-up for the testing of a floating offshore wind turbine scaled model in a field site. Wind Engineering, 40(5), pp.455-467.

70. **Sclavounos, P., Tracy, C. and Lee, S.,** 2007. Floating offshore wind turbines: Responses in a seastate pareto optimal designs and economic assessment. http://web.mit.edu/flowlab/pdf/Floating_Offshore_Wind_Turbines.pdf.
71. **Sclavounos, P.D., Lee, S., DiPietro, J., Potenza, G., Caramuscio, P. and De Michele, G.,** 2010. April. Floating offshore wind turbines: tension leg platform and taught leg buoy concepts supporting 3–5 MW wind turbines. In European wind energy conference EWEC, pp. 20-23.
72. **Sethuraman, L. and Venugopal, V.,** 2013. Hydrodynamic response of a stepped-spar floating wind turbine: Numerical modelling and tank testing. Renewable Energy, 52, pp.160-174.
73. **Shi, W., Han, J., Kim, C., Lee, D., Shin, H. and Park, H.,** 2015. Feasibility study of offshore wind turbine substructures for southwest offshore wind farm project in Korea. Renewable Energy, 74, pp.406-413.
74. **Shin, H., Dam, P.T., Jung, K.J., Rim, C. and Chung, T.,** 2013. Model test of new floating offshore wind turbine platforms. International Journal of Naval Architecture and Ocean Engineering, 5 (2), pp.199-209.
75. **Skaare, B., Hanson, T.D., Nielsen, F.G., Yttervik, R., Hansen, A.M., Thomsen, K. and Larsen, T.J.,** 2007. Integrated dynamic analysis of floating offshore wind turbines. In European Wind Energy Conference, Milan, Italy, May 7, pp.7-10
76. **Stewart, G., Lackner, M., Robertson, A., Jonkman, J. and Goupee, A.,** 2012. Calibration and validation of a FAST floating wind turbine model of the DeepCwind scaled tension-leg platform (No. NREL/CP-5000-54822). National Renewable Energy Lab.(NREL), Golden, CO (United States).
77. **Taylor, M.,** 2012. Renewable energy technologies: Cost analysis series, wind power. Renewable Energy, 1(5), pp.1-64.
78. **Tian, X.L., Xiao, J.R., Liu, H.X., Wen, B.R. and Peng, Z.K.,** 2020. A Novel Dynamics Analysis Method for Spar-Type Floating Offshore Wind Turbine. China Ocean Engineering, 34(1), pp.99-109.
79. **Tong, K.C.,** 1998. Technical and economic aspects of a floating offshore wind farm. Journal of Wind Engineering and Industrial Aerodynamics, 74, pp.399-410.
80. **Utsunomiya, T., Sato, T., Matsukuma, H. and Yago, K.,** 2009. May. Experimental validation for motion of a spar-type floating offshore wind turbine using 1/22.5 scale model. In ASME 2009 28th International Conference on Ocean, Offshore and Arctic Engineering, pp. 951-959.

81. Van Phuc, P. and Ishihara, T., 2007. A study on the dynamic response of a semi-submersible floating offshore wind turbine system Part 2: numerical simulation. ICWE12. Cairns, Australia, pp.959-966.

82. Viré, A., Xiang, J., Piggott, M., Cotter, C. and Pain, C., 2013. Towards the fully-coupled numerical modelling of floating wind turbines. Energy Procedia, 35, pp.43-51.

83. Wang, K., Ji, C., Xue, H. and Tang, W., 2017. Frequency domain approach for the coupled analysis of floating wind turbine system. Ships and Offshore Structures, 12(6), pp.767-774.

84. Weinzettel, J., Reenaas, M., Solli, C. and Hertwich, E.G., 2009. Life cycle assessment of a floating offshore wind turbine, Renewable Energy, 34 (3), pp.742-747.

85. Withee, J. E. 2006. "Fully coupled dynamics analysis of a floating wind turbine system", M.S.Thesis, Massachusetts Institute of Technology.

86. World Energy Resources—Wind 2016. https://www.worldenergy.org/wp-content/uploads/2017/03/WEResources_Wind_2016.pdf . Accessed July 2018

87. Yu, M., Hu, Z.Q. and Xiao, L.F., 2014. Wind-wave induced dynamic response analysis for motions and mooring loads of a spar-type offshore floating wind turbine, Journal of Hydrodynamics, 26 (6), pp.865-874.

88. Zaheer, M.M. and Islam, N., 2012. Stochastic response of a double hinged articulated leg platform under wind and waves, Journal of Wind Engineering and Industrial Aerodynamics, 111, pp.53-60.

89. Zaheer, M.M. and Islam, N., 2017. Dynamic response of articulated towers under correlated wind and waves, Ocean Engineering, 132, pp.114-125.

90. Zambrano, T., MacCready, T., Kiceniuk, T., Roddier, D.G. and Cermelli, C.A., 2006. Dynamic modeling of deepwater offshore wind turbine structures in Gulf of Mexico storm conditions. In 25th International conference on offshore mechanics and arctic engineering, 47462, pp.629-634.

91. Zhang, R., Tang, Y., Hu, J., Ruan, S. and Chen, C., 2013. Dynamic response in frequency and time domains of a floating foundation for offshore wind turbines, Ocean Engineering, 60, pp.115-123.